

The role of Kinesin-3 in regulating synaptic development in
Drosophila

Dissertation

zur Erlangung des Grades eines
Doktors der Naturwissenschaften

der Mathematisch-Naturwissenschaftlichen Fakultät

und
der Medizinischen Fakultät
der Eberhard-Karls-Universität Tübingen

vorgelegt
von

Yao Zhang
(張焱)
aus Cangzhou, China

April, 2012

Tag der mündlichen Prüfung: 15.06.2012

Dekan der Math.-Nat. Fakultät: Prof. Dr. W. Rosenstiel

Dekan der Medizinischen Fakultät: Prof. Dr. I. B. Autenrieth

1. Berichterstatter: Prof. Dr. H. Volkmer

2. Berichterstatter: Prof. Dr. R. Feil

Prüfungskommission: Prof. Dr. H. Herbert

Prof. Dr. O. Rieß

Prof. Dr. H. Volkmer

S. Di Giovanni MD. PhD.

I hereby declare that I have produced the work entitled: “the role of Kinesin-3 in regulating synaptic development in *Drosophila*”,

submitted for the award of a doctorate, on my own (without external help), have used only the sources and aids indicated and have marked passages included from other works, whether verbatim or in content, as such. I swear upon oath that these statements are true and that I have not concealed anything. I am aware that making a false declaration under oath is punishable by a term of imprisonment of up to three years or by a fine.

Tübingen, _____

Date

Signature

天行健，君子以自強不息。地勢坤，君子以厚德載物。
——《周易》



*As the universe's evolvement is ever vigorous,
a man should constantly strive for self-perfection.
As the earth's condition is receptive devotion,
a man should cultivate virtue to hold the outer world.*

--- 9 Ching

Dedicated to my family



Acknowledgements

Foremost I would like express my gratitude to my thesis committee members, Dr. Tobias Rasse, Prof. Dr. Hansjürgen Volkmer and Prof. Dr. Robert Feil for their constant support, valuable advice and guidance.

I want to express my special thanks to my supervisor Dr. Tobias Rasse. I am very grateful for all the supervision, guidance and help that he has provided during my PhD thesis. I also would like to thank Prof. Hermann Aberle, Dr. Catherine Collins and Prof. Aaron Diantonio for their comments on my projects and providing reagents.

Special thanks to Dr. Doychin Stanchev, Jeannine Kern, Junyi Zhu and Josef Lehner, with whom I have been collaborating. I also thank Baran Koç for helping with data analysis. Thanks to Junyi Zhu and Vrinda SKumar for transferring my flies and thanks to Jeannine Kern for watering my plants when I am not in the lab. Special thanks to Vrinda and her father for helping me buy medicines from India for my father's illness. Thanks to Dr. Natasha Veresceaghina, Dr. Bronwen Lasky, Dr. Karthik Tangavelou, Petra Föger, Josephine Ng, Shabab Hannan, Raphael Zinser, Stanley Dinesh, Kartharina Daub and Carola Schneider for being great colleagues. We have spent a lot of nice time together. I wish you all best of luck for the future. I believe there must still be people that I forget to mention here, but thank all of you who have helped me during my stay in Tübingen for my PhD.

I can never use enough words to express my gratitude to my family. If it were not for my father's insistence on supporting us to enjoy the best possible education, I could not have been who I am now. If it were not for my mother's unconditional love, I would not have got the strength to conquer so many obstacles and complete my study. My elder sister Hui is always my defender, teacher and friend. I feel so lucky to have an excellent sister. I also want to thank my brother-in-law who is tolerant and supports the family. And I thank my niece, who brings new hope for the family. I love you all so much.

I am deeply sorry for not being with the family when my father was diagnosed of lung cancer at the beginning of my PhD study. I am very proud of my family for their close mutual support to go through so many hardships and to keep optimistic. I am also deeply grateful for inheriting the family virtue passed down over generations of being kindhearted, righteous, and conscientious.

Table of contents

Common abbreviations.....	1
List of figures	7
1. Summary.....	8
2. Introduction.....	11
2.1 Structure, function and composition of chemical synapses.....	11
2.1.1 The presynaptic active zone.....	11
2.1.2 The postsynaptic density.....	14
2.2 Synaptic development.....	15
2.2.1 The general process of synaptic development.....	15
2.2.1.1 Initiation of synaptogenesis.....	15
2.2.1.2 Active zone assembly.....	16
2.2.1.3 Postsynaptic density formation.....	20
2.2.2 Signaling pathway regulating synaptic development	22
2.2.2.1 The Wnt pathway.....	22
2.2.2.2 The TGF- β pathway.....	24
2.2.2.3 The MAPK pathway.....	25
2.2.3 Molecular motors and synaptic development.....	27
2.2.3.1 Major molecular motors.....	27
2.2.3.2 Kinesin and synaptic development.....	29
2.3 The <i>Drosophila</i> neuromuscular junction.....	33
3. Material and Methods.....	35
4. Results.....	39
4.1 Characterization of the phenotype in <i>unc-104^{bris}</i> mutant.....	39
4.1.1 Brp mislocalization in <i>unc-104^{bris}</i> mutant is not downstream of insufficient Brp at the NMJ	39
4.1.2 Systemic AZ assembly defects at NMJ in <i>unc-104^{bris}</i> mutant larvae.....	41
4.1.3 The <i>unc-104^{bris}</i> mutation perturbs a mechanism regulating AZ assembly....	43
4.1.4 Impaired synaptic functions in <i>unc-104^{bris}</i> mutants.....	44
4.1.5 Defects in postsynaptic maturation in <i>unc-104^{bris}</i> mutants.....	46
4.1.6 Impaired axonal transport at the NMJ in <i>unc-104^{bris}</i> mutants.....	48
4.1.7 Overexpression of Rab3 ameliorate the AZ assembly phenotype in <i>unc-104^{bris}</i> mutants.....	51

4.1.8 Impaired synaptic activity contribute little to the AZ assembly phenotype in <i>unc-104^{bris}</i> mutants.....	53
4.2 Overactivation of the Wnd MAPK pathway leads to the synaptic development phenotypes in <i>unc-104^{bris}</i> mutant.....	56
4.2.1 Downregulation of a MAPK signaling pathway rescues NMJ overgrowth in <i>unc-104^{bris}</i> mutant.....	56
4.2.2 Downregulation of the Wnd MAPK pathway also rescued the AZ assembly phenotype in <i>unc-104^{bris}</i> mutants.....	58
4.2.3 No ameliorated axonal transport in <i>unc-104^{bris};wnd</i> double mutant larvae.....	61
4.2.4 The SSR underdevelopment phenotype in <i>unc-104^{bris}</i> mutants NMJs is also rescued by downregulation of MAPK pathway.....	63
4.2.5 The locomotion defects in <i>unc-104^{bris}</i> mutant larvae is not rescued by downregulation of MAPK pathway.....	63
4.2.6 Overactivation of the Wnd MAPK pathway is sufficient to cause AZ assembly phenotype resembling <i>unc-104^{bris}</i> mutants.....	66
4.2.7 Reduced Hiw level in <i>unc-104^{bris}</i> mutants.....	66
4.3 larval genotypes in each figure.....	69
5. Discussions.....	73
5.1 A neuronal kinesin regulating AZ assembly.....	73
5.2 An MAPK pathway regulating synaptic development.....	74
5.3 MAPK overactivation mediates the synaptic development abnormalities in <i>unc-104^{bris}</i> mutants.....	76
5.4 Kinesin-3/Unc-104 and synaptic function.....	81
5.5 No sign of synaptic retraction in <i>unc-104^{bris}</i> mutants.....	85
6. Conclusion.....	87
7. References.....	88
8. Curriculum Vitae.....	109

Common Abbreviations

AchR	acetylcholine receptor
AEL	after egg laying
ALS	amyotrophic lateral sclerosis
AMPA	2-amino-3-(5-methyl-3-oxo-1,2-oxazol-4-yl)propanoic acid
ANF	atrial natriuretic peptide
ANOVA	analysis of variance
ATP	adenosine-5'-triphosphate
AZ	active zone
BMP	bone morphogenetic protein
Brp	bruchpilot
Bsk	basket
Cac	cacophony
CAMKII	Ca ²⁺ /calmodulin-dependent protein kinase II
cAMP	cyclic adenosine monophosphate
CAST	cytomatrix at the active zone-associated structural protein
CCKLR	cholecystokinin like receptor
COS	CV-1 in origin, and carrying the simian virus 40 genetic material
CNS	central nervous system
CREB	cyclic adenosine monophosphate response element-binding
DCV	dense core vesicle

dgs	G protein α 60A
Dlg	disc large
DLK	dual leucine zipper kinase
DLIMK1	<i>Drosophila</i> lipophilic protein kinase1
DN	dominant negative
DNC-1	dynactin complex component-1
DRBP	<i>Drosophila</i> retinoid binding protein
DSK	drosulfakinin
DSyd-1	<i>Drosophila</i> synapse defective-1
DVGlut	<i>Drosophila</i> vesicular glutamate transporter
Dvl	dishevelled
EJP	excitatory junctional potential
EM	electron microscopy
ERC	ELKS/RAB6-interacting/CAST family member
ERK	extracellular regulated mitogen activated protein kinase
FHA	forkhead associated
Fz	Frizzled
GABA	γ -Aminobutyric acid
Gbb	glass bottom boat
GFP	green fluorescent protein
GluR	glutamate receptor
GlyR	glycine receptor

GKAP	guanylate kinase-associated protein
GPRC	G protein coupled receptor
GRIP1	glutamate receptor-interacting protein 1
GSK3 β	glycogen synthase kinase 3 β
HEPES	4-(2-hydroxyethyl)-1-piperazineethanesulfonic acid
Hiw	highwire
HL3	hemolymph-like solution 3
HRP	horseradish peroxidase
HSP	hereditary spastic paraplegia
5-HT	5-hydroxytryptamine
JIP	c-Jun N-terminal kinase interacting protein
JNK	c-Jun N-terminal kinase
JSAP-1	c-Jun N-terminal kinase/stress-activated protein kinase associated protein-1
KIF	kinesin super family protein
KHC	kinesin heavy chain
KLC	kinesin light chain
LIM	lipophilic protein
Liprin- α	protein tyrosine phosphatase receptor type f polypeptide-interacting protein- α
MAGUK	membrane-associated guanylate kinase
MAP1B	microtubule-associated protein 1B
MAPK	mitogen activated protein kinase
MAP2K/MKK	mitogen activated protein kinase kinase

MAP3K	mitogen activated protein kinase kinase kinase
mEJP	miniature excitatory junctional potential
MEK	mitogen activated protein kinase kinase or extracellular regulated mitogen activated protein kinase kinase
mGluR	metabotropic glutamate receptor
mRFP	monomeric red fluorescent protein
mRNA	messenger ribonucleic acid
MS	multiple sclerosis
MSPS	mini spindles
MuSK	muscle-specific kinase
nAChR	nicotinic acetylcholine receptor
NAB	neurabin
NCAM	neural cell adhesion molecule
Nlg	neuroligin
NMDA	N-methyl-D-aspartate
NMJ	neuromuscular junction
NR	N-methyl-D-aspartate receptor
OE	overexpression
PAK	p21-associated kinase
PI3K	phosphatidylinositol 3-kinases
PDZ	postsynaptic density-95/disc large/zonula occludens-1
PIX	pixie
PKA	protein kinase A

PSD	post synaptic density
PTV	Piccolo and Bassoon transport vesicle
RIM	rab-3-interacting molecule
Rpm-1	regulator of presynaptic morphology-1
RNAi	messenger ribonucleic acid interference
RSY-1	regulator of synaptogenesis-1
SAPAP	synapse-associated protein 90/ postsynaptic density-95-associated protein
SAX	saxophone
SEM	standard error of the mean
SMA	spinal muscular atrophy
SNAP-25	synaptosomal-associated protein 25
SNARE	soluble N-ethylmaleimide-sensitive factor attachment protein receptor
SSR	subs synaptic reticulum
SRPK79D	serine-arginine protein kinase at 79D
SV	synaptic vesicle
SV2	synaptic vesicle glycoprotein 2
SVP	synaptic vesicle precursor
SYD	synapse defective
SYG	synaptogenesis abnormal
SynCAM	synaptic cell adhesion molecule
synGAP	synaptic ras guanosine-5'-triphosphosase activating protein
TGF- β	transforming growth factor- β

Tkv	thickveins
TNT	tetanus toxin
UAS	upstream activation sequence
VNC	ventral nerve cord
Wit	wishful thinking
Wnd	wallenda
XMAP215	microtubule associated protein 215 kDa
YFP	yellow fluorescent protein
ZAC	zinc-activated ion channel

List of figures

Fig1. The *Drosophila* neuromuscular junction.

Fig2. Brp overexpression modifies the AZ assembly defect in *unc-104^{bris}* mutants.

Fig3. Systemic AZ assembly defects in *unc-104^{bris}* mutant NMJs.

Fig4. Impaired synaptic transmission in *unc-104^{bris}* mutant NMJs.

Fig5. Glutamate receptor composition in control and *unc-104^{bris}* mutants.

Fig6. Effect of the *unc-104^{bris}* mutation on the distribution of different synaptic protein and organelles at the NMJ.

Fig7. Rab3 overexpression partially rescues the AZ assembly defect in *unc-104^{bris}* mutants.

Fig8. Effect of blocking synaptic transmission on synaptic development.

Fig9. Downregulating MAPK pathway rescues the NMJ overgrowth phenotype in *unc-104^{bris}* mutants.

Fig10. Downregulating MAPK pathway inhibits the AZ assembly phenotype in *unc-104^{bris}* mutants.

Fig11. Mutations in *wnd* do not ameliorate axonal transport in *unc-104^{bris}* mutants.

Fig12. Mutations in *wnd* suppress SSR underdevelopment in *unc-104^{bris}* mutants, but do not affect SV localization at NMJ.

Fig13. Mutations in *wnd* do not rescue the locomotion impairments in *unc-104^{bris}* mutant larvae.

Fig14. Overactivation of MAPK pathway leads to AZ assembly phenotype reminiscent of *unc-104^{bris}* mutant.

Fig15. Reduced level of Hiw in the CNS of *unc-104^{bris}* mutant larvae.

Fig16. A schematic illustration of the functions of Unc-104 and MAPK pathway.

1. Summary

Synaptic development is a very complex and dynamic process. So far, mechanisms regulating synaptic development are still not well understood.

In this study, the *Drosophila* neuromuscular junction is used as a model to investigate mechanisms regulating synaptic development. An unbiased forward genetic screening identified *unc-104^{bris}*, which is a missense mutation of a conserved residual (R561H) in the forkhead associated (FHA) domain of the *Drosophila* kinesin-3 homolog *unc-104*. *unc-104^{bris}* mutant larvae are characterized by the distinct synaptic assembly phenotype that about 30% of the glutamatergic synapses at the neuromuscular junction (NMJ) are devoid of the presynaptic active zone (AZ) protein Bruchpilot (Brp), whereas in wildtype larvae less than 5% of the synapses which are nascent lack presynaptic Brp. What is more, *unc-104^{bris}* mutant NMJs have much smaller synaptic boutons, and the subsynaptic reticulum (SSR), an elaborate membranous structure formed by the muscle membrane which surrounds the NMJ, is not well developed. *unc-104^{bris}* mutant larvae die at late 3rd instar stage/early pupal stage and suffer from severe locomotion impairments.

The objective of this study is to systemically characterize the synaptic assembly phenotype and to identify the mechanisms underlining the impaired synaptic development in *unc-104^{bris}* mutants.

In the first set of experiments, I find that the level of total Brp at *unc-104^{bris}* mutant NMJs drops to half of that in wildtype. Excessive Brp deposit is found at the cell body region of the ventral nerve **code** (VNC) in *unc-104^{bris}* mutant larvae. However, the decreased Brp puncta formation at presynaptic active zone cannot be totally explained by decreased Brp level because overexpression of Brp restores the level of total Brp at the NMJ but only has limited effect on rescuing Brp puncta formation at the synapse. Furthermore, other major active zone components including the Ca²⁺ channel subunit protein Cacophony (Cac), the LAR protein-tyrosine phosphatase-interacting protein (Liprin- α) and serine-arginine protein kinase at 79D (SRPK79D) are also absent from the Brp(-) synapses in *unc-104^{bris}* mutants, suggesting that AZ assembly is abolished in these

synapses. Importantly, Cac and Liprin- α do not depend on Brp for their AZ localization, thus the concomitant absence of Cac, Liprin- α and Brp in a subset of *unc-104^{bris}* mutant synapses is not secondary of abortive Brp assembly at these synapses. Localization of synaptic vesicle (SV), SV associated proteins and peptide filled dense core vesicles (DCV) are severely reduced at *unc-104^{bris}* mutant NMJs as a result of reduced kinesin-3 function. Synaptic activity is also impaired at *unc-104^{bris}* mutant NMJs, which can be rescued by presynaptic reexpression of *unc-104* cDNA. Postsynaptically, recruitment of the inotropic glutamate receptor subunit GluRIIA, but not GluRIIB is selectively reduced at *unc-104^{bris}* mutant NMJs, implying that a transsynaptic signaling regulating receptor clustering is perturbed by mutation in this neuronal kinesin.

In the second set of experiments, the mechanism underlying the synaptic development phenotype in *unc-104^{bris}* mutant is investigated. *unc-104^{bris}* mutant NMJs have much smaller synaptic bouton, which is accompanied by doubled overall NMJ length. This closely resembles the NMJ overgrowth phenotype in larvae which have enhanced dual leucine zipper kinase (DLK, the Drosophila homolog of which is Wallenda (Wnd)) activity. Indeed, downregulating the Wnd MAPK pathway by loss of function mutation in *wnd*, or expression of dominant negative form of downstream signaling components similarly inhibited the NMJ overgrowth phenotype in *unc-104^{bris}* mutants. What is more, downregulation of the Wnd MAPK pathway also rescues the AZ assembly and SSR underdevelopment phenotype in *unc-104^{bris}* mutants. No ameliorated axonal transport is observed in *unc-104^{bris};wnd* double mutant larvae, suggesting that the rescuing effects of Wnd MAPK pathway downregulation is independent of axonal transport. An E3 ubiquitin ligase, Highwire (Hiw) has been shown to negatively regulate Wnd level and hence inhibit the Wnd MAPK pathway. Actually, loss of function mutation in *hiw* and Wnd overexpression both lead to AZ assembly phenotype reminiscent of *unc-104^{bris}* mutants without causing obvious axonal transport defects. Therefore, we propose that Wnd MAPK overactivation is underlining the synaptic development phenotype in *unc-104^{bris}* mutants. The level of Hiw is decreased in *unc-104^{bris}* mutants, which may lead to increased Wnd level and contribute to MAPK overactivation. Importantly, despite the ameliorated NMJ morphology, downregulating MAPK pathway in *unc-104^{bris}* mutants

rescues neither the locomotion impairment nor larval lethality, suggesting that other crucial MAPK independent functions of Unc-104 is important for normal larval activity and survival.

In summary, this work shows that Unc-104, the *Drosophila* kinesin-3, is an important regulator of synaptic development. A novel function of Hiw as well as the Wnd MAPK pathway in regulating active zone assembly is indentified. Unc-104 controls the level of Hiw, and further modulates Wnd MAPK pathway activity to promote normal synaptic development.

2. Introduction

Synapse is the structure which a neuron uses to communicate with other neurons or with cells of other kinds, e.g. muscle cells or gland cells. Two major types of synapses exist in the nervous system, electrical synapses and chemical synapses. In the beginning of the 20th century, there was heated debate about which synapse type was the major form in the mammalian central nervous system (CNS). Following the discovery of neuronal inhibition in the 1950th, chemical synapse became widely accepted to be the major synapse type responsible for the communication between CNS neurons (Brock et al., 1952).

2.1 Structure, function and composition of chemical synapses

Unlike electrical synapses which enable bidirectional signal transmission, chemical synapses generally only allow unidirectional signal propagation. The unsymmetrical structure of chemical synapses underlines the unidirectional nature of synaptic transmission.

2.1.1 The presynaptic active zone

The “presynaptic side” of a chemical synapse is where neurotransmitter is released. Neurotransmitters are stored at presynaptic compartment in the form of synaptic vesicles (SV). Active zone (AZ) is the highly specialized architecture at presynaptic compartment which enables tethering, docking, and fusion of SVs (Couteaux and Pecot-Dechavassine, 1970). Despite variation between organisms, the ultrastructural appearance of active zone is characterized by an electron-dense cytomatrix close to the plasma membrane, which is sometimes coupled with protrusions of various shapes and sizes extending into the cytoplasm. High density of synaptic vesicles forms a “halo” in close approximation with the electron dense structures.

Plasma membrane at the active zone

Several classes of proteins localize to the plasma membrane at the active zone. The first important class of proteins are the voltage gated Ca^{2+} channels, which enables Ca^{2+} influx upon the arrival of active potential, and further triggers synaptic vesicle fusion (Kawasaki et al., 2004; Kittel et al., 2006; Robitaille et al., 1990). The soluble N-ethylmaleimide-sensitive factor attachment protein receptor (SNARE) complex is crucial for mediating the membrane fusion between synaptic vesicle and plasma membrane during neurotransmitter release (Jahn et al., 2003; Rizo, 2003). Although not restricted to presynaptic membrane, t-SNARE proteins syntaxin and SNAP-25 has been shown to enrich at active zone (Kawasaki and Ordway, 2009; Schulze et al., 1995). Another class of proteins localizing to the presynaptic plasma membrane are adhesion molecules, including integrins (Chavis and Westbrook, 2001), cadherins (Shapiro and Colman, 1999; Yagi and Takeichi, 2000), Fasciclin II (Davis et al., 1997)/ NCAM (Rougon and Hobert, 2003), sidekicks (Yamagata et al., 2002), neuexins (Li et al., 2007; Ushkaryov et al., 1992), ephrinB (Dalva et al., 2000) and SynCAMs (Fogel et al., 2007), which associate with their corresponding post synaptic partners. These pairs of interactions enable the proper apposition between pre- and postsynaptic side, and also play important roles in synaptogenesis and modulation of synaptic activity (Ferreira and Paganoni, 2002; Kohsaka et al., 2007; Packard et al., 2003; Scheiffele, 2003).

Cytometrix at the active zone (CAZ)

The CAZ appears electron dense under electron microscopy (EM), suggesting its proteinaceous nature. Machineries facilitating the tethering and docking of synaptic vesicles are assembled here. Finer structure of the cytomatrix at the active zone in frog NMJ was revealed by an elegant study combining electron microscopy and tomography (Harlow et al., 2001). The cytomatrix in these synapses arranges in a net like structure, which presumably connects synaptic vesicles and calcium channels. The observed structure is consistent with the function of facilitating synaptic vesicle docking and regulating transmitter release.

Some type of synapses have more prominent electron-dense structures which protrude into the cytoplasm. These include the “T-bar” of the *Drosophila* neuromuscular synapses and CNS synapses (Fouquet et al., 2009; Yasuyama et al., 2002), the ribbon-like dense projection in the synapses between the rod photoreceptor and horizontal cell in rat visual system (Dick et al., 2003) and in frog inner ear hell cell (Lenzi and von Gersdorff, 2001). Synaptic vesicles are shown to be closely associated with these protrusions (Zhai and Bellen, 2004). Studies have shown that these protrusions have specific function of tethering synaptic vesicle to the active zone. Deletion of critical domains which mediate association between active zone proteins and synaptic vesicle abolishes the tethering of synaptic vesicle at the active zone, and leads to synaptic depression (Hallermann et al., 2010). Despite its role in tethering and clustering synaptic vesicles, these projections are not indispensable for neurotransmitter release. In mice where formation of synaptic ribbons is severely impaired in retinas, ribbon like structures float in the cytoplasm and have synaptic vesicles attached to them. Retina of such mice has normal response to low-intensity light, but shows very severely reduced reaction of high-intensity light (Dick et al., 2003).

Intense study in recent years have identified numerous proteins localizing to the CAZ, which plays different roles in maintaining different aspects of the functional integrity of synapses. These include the RIM1/unc-10 (Wang et al., 1997; Weimer et al., 2006), Munc13/unc-13 (Weimer et al., 2006), Bassoon (tom Dieck et al., 1998), Piccolo/Aczonin (Fenster et al., 2000), CAST/ERC/Brp (Fouquet et al., 2009; Ohtsuka et al., 2002), Liprin- α /Syd-2 (Fouquet et al., 2009), Dsyd-1/ RhoGAP100F (Owald et al., 2010), RIM-binding proteins (Hibino et al., 2002; Liu et al., 2011), etc. These proteins exhibit complex interactions with one another, forming sophisticated tertiary structures to facilitate proper synaptic function (Takao-Rikitsu et al., 2004). During synaptogenesis, these proteins assemble at a defined temporal and spatial order, although the mechanisms regulating the formation of CAZ are still not very well understood (Fouquet et al., 2009; Oswald et al., 2010).

2.1.2 The postsynaptic density

The “postsynaptic” side of a synapse is where the receptors of neurotransmitters are anchored. Ultrastructurally, it is characterized by an electron dense region closely aligned with the presynaptic active zone, and thus normally called the postsynaptic density (PSD). Apart from adhesion molecules which associate with their presynaptic partners, the most important proteins at the plasma membrane of PSDs are neurotransmitter receptors and voltage-gated ion channels. Depending on synapse types, various neurotransmitter receptors localize to the plasma membrane at the PSD (Gong and Lippa, 2010). Neurotransmitter receptors can be classified into the following two major categories.

Ionotropic neurotransmitter receptors, which open or close upon binding with their ligands and thus change their permeability to certain ions, can directly trigger either excitative or inhibitory postsynaptic response. These receptors fall into the superfamily of ligand gated ion-channels. Major ionotropic receptors include the NMDA, AMPA and Kainate types of glutamate receptors (GluNs, GluAs and GluKs), GABA_A receptors, Glycine receptors (GlyRs), serotonin receptors (5-HT₃), nicotinic acetylcholine receptors (nAChRs), Zinc-activated ion channel (ZAC) and ATP-gated channels (Collingridge et al., 2009).

The second major type of neurotransmitter receptors is the metabotropic receptors, which fall into the G-protein coupled receptor (GPCRs) superfamily. Rather than directly altering postsynaptic membrane potentials, they are coupled with secondary messengers and responsible for modulating synaptic strength. Major metabotropic receptors include dopamine receptors (D₁-D₅), Serotonin receptors (5-HT_{1, 2, 4, 6}), metabotropic glutamate receptors (mGluRs), neuropeptide receptors, muscarinic acetylcholine receptors (mAChRs) and GABA_B receptors (Chen et al., 2005; Eglen, 2006; Pin and Acher, 2002).

Underneath the postsynaptic plasma membrane, important signaling molecules including Ca²⁺/Calmodulin-dependent protein kinases II (CAMKII) and SynGAPs exist which have important role in modulating synaptic strength including LTP induction, and are involved

in memory formation (Gardoni et al., 2001; Rumbaugh et al., 2006; Strack et al., 1997). Scaffold proteins including PSD-95/Dlg, Shanks and SAPAP/GKAP play important role in organizing the PSD structure (Kim and Sheng, 2004; Sala et al., 2001). These scaffold proteins mostly contain the PSD95/Dlg/Zo-1 (PDZ) domain, which associates with receptors, adhesion molecules, cytoskeletons and signaling molecules (Kim and Sheng, 2004).

2.2 Synaptic development

2.2.1 The general process of synaptic development

After the process of a neuron navigates to the surface of its target cell, synaptic connection starts to be established. The process of synaptic formation is referred to as synaptogenesis, which is a complex and highly dynamic process (Jin, 2005; Waites et al., 2005).

2.2.1.1 Initiation of synaptogenesis

Interaction between presynaptic and postsynaptic adhesion molecules has been established to be the priming step for synaptogenesis (Akins and Biederer, 2006). The cell adhesion protein Cadherin has been implicated in the initial establishment synaptic contacts (Waites et al., 2005). Cadherins localizes at innate axon-dendrite contacts (Benson and Tanaka, 1998; Fannon and Colman, 1996); blocking Cadherin function has been shown to delay synaptic formation, leading to reduced synapse size, abnormal synaptic maturation and perturbed synaptic function (Bozdagi et al., 2004). However, Cadherin function does not seem to be indispensable for synaptic formation. In cultured hippocampal neurons at 10 days *in vitro*, blocking Cadherin function does not affect synaptic formation (Bozdagi et al., 2004). In developing chick optic tectum, introduction of antibody blocking N-cadherin causes excessive filopodia formation from retinal ganglion cell axons but does not abolish synapse formation (Inoue and Sanes,

1997). Absence of N-cadherin in *Drosophila* ommatidium leads to axon mistargeting but synaptic formation is preserved (Lee et al., 2001).

Protocadherins are also involved in the induction of synaptic specification. Protocadherins localize to synapses (Phillips et al., 2003), and loss of function studies in mouse and fly both suggest that protocadherin mainly functions to facilitate the establishment of proper synaptic contact but not essential for downstream synapse formation (Lee et al., 2003; Wang et al., 2002).

Study in *C. elegans* demonstrated that the interaction between SYG-1 in HSN neurons and SYG-2 in vulval epithelial cells is important for the establishment of proper synaptic connects controlling egg-laying. The epithelial cells serve as guideposts to lead growth cone extension and define the sites for presynaptic assembly (Shen and Bargmann, 2003; Shen et al., 2004). Concentration of SYG-1 at the nascent synaptic contact is crucial for recruiting active zone proteins to the HSNL synapses and thus for initiating synaptic assembly (Patel et al., 2006). There are homologs of the *syg-1* and *syg-2* gene in flies and vertebrates as well, but it is not yet clear to what extent their function is conserved across species.

2.2.1.2 Active zone assembly

Assembly of synaptic machinery closely follows initial establishment of synaptic contact. Mechanisms regulating presynaptic active zone assembly are so far best characterized in *Drosophila* neuromuscular synapses and in *C. elegans*.

Interaction between presynaptic neurexins and postsynaptic neuroligins across the synaptic cleft has been shown to be crucial for recruiting synaptic proteins to start synaptic assembly (Akins and Biederer, 2006; Sudhof, 2008). Expression of Neuroligin in non-neuronal cells can trigger synapse formation in contacting axons. This effect is mediated via the interaction of Neuroligin with axonal Neurexin; the synaptogenetic effect of ectopically expressed Neuroligin is blocked by the addition of a soluble form of Neurexin into the medium (Scheiffele et al., 2000).

The C-terminus of Neurexin extends into the cytoplasm. It contains a sequence for binding to the class-II PDZ domain of a membrane associated guanylate kinase (MAGUK) CASK, and a binding site for protein 4.1 which promotes actin/spectrin microfilaments formation (Biederer and Sudhof, 2001; Hata et al., 1996). Through its interaction with CASK and protein 4.1, cytoskeleton scaffold necessary for assembling the active zone structure is formed and tethered to nascent active zone via Neurexin (Biederer and Sudhof, 2001). Establish of actin filaments at nascent active zone has been recently proved important for continued active zone maturation in *C. elegans*. The adaptor protein neurabin (NAB-1) has been shown to form ternary complexes with the active zone protein SYD-1 and SYD-2/Liprin- α . Through its association with the F-actin network at immature active zones, NAB-1 recruits SYD-1 and SYD-2 to the active zone (Chia et al., 2012).

Downstream of adhesion molecules

SYD-1 and SYD-2/ Liprin- α seem to be the major organizers of active zone maturation acting downstream of adhesion molecules. Localization of several active zone proteins has been shown to be dependent on SYD-1. Mutation in *syd-1* leads to mislocalization of several active zone proteins at the HSNL synapses in *C. elegans*, including SYD-2/ Liprin- α , ELKS-1/ERC and UNC-10/RIM (Dai et al., 2006; Hallam et al., 2002; Patel et al., 2006). SYD-1 functions at the active zone at least partially through SYD-2, as SYD-2 gain-of-function allele can suppress the synaptic assembly defects in HSN neurons in *syd-1* mutants (Dai et al., 2006; Taru and Jin, 2011).

SYD-2/Liprin- α mutant *C. elegans* shows lengthened but less condensed synaptic structures, as well as more diffused distribution of synaptic proteins (Zhen and Jin, 1999). In flies, mutations in SYD-2/Liprin- α and SYD-1 lead to similarly enlarged active zone (Fouquet et al., 2009; Kaufmann et al., 2002; Oswald et al., 2010). Superresolution microscopy study revealed that in *Drosophila* neuromuscular junction both SYD-2/Liprin- α and SYD-1 form discrete puncta at the lateral border of active zone. In both

SYD-2/Liprin- α and SYD-1 mutants, assembly of Brp at the active zone is disorganized and the segregation between neighboring synapses is seemingly compromised (Fouquet et al., 2009; Oswald et al., 2010). This is consistent with the notion that SYD-2/Liprin- α and SYD-1 may function to delineate the active zone boundary and to maintain the constricted active zone conformation.

However, in many cases it is hard to clearly define an upstream-downstream relationship between AZ proteins during synaptic assembly; synaptic proteins frequently show a synergistic interaction to straighten each other's assembly at the active zone. Although SYD-1 has been shown to be important for proper synaptic localization of SYD-2/Liprin- α in *C. elegans* and flies (Oswald et al., 2010; Patel et al., 2006), a gain-of-function allele of *syd-2* can restore the normal localization of SYD-1 in *syg-1* mutant of *C. elegans*. Synaptic localization of the ERC/CAST homolog ELKS-1 is severely impaired in *syd-2* mutant *C. elegans*, indicating the dependence of ELKS-1 on SYD-2 for its proper localization (Patel et al., 2006). Yeast two-hybrid experiment revealed that SYD-2/Liprin- α directly associates with ERC/CAST in rat hippocampal neurons (Ko et al., 2003). This interaction is also important for the active zone localization of SYD-2/Liprin- α as coexpression of ERC with SYD-2/Liprin- α has the effect of recruiting the latter to synaptic sites (Ko et al., 2003).

There are evidences supporting the notion that at least some of the active zone components are already "preassembled" before arriving at their final destination and integrate into the active zone as a "module". In vertebrates, Piccolo and Bassoon transport vesicles (PTVs) which contain several important active zone proteins are believed to be active zone precursor vesicles (Shapira et al., 2003; Sorra et al., 2006; Zhai et al., 2001). Synaptic content of Piccolo, Bassoon and RIM conforms nicely to a unitary model of integration (Shapira et al., 2003). Furthermore, morphology study showed that in rat primary hippocampal neuron culture Bassoon is recruited to and immobilized at functional active zones in the form of particles rather than from a diffuse pool (Bresler et al., 2004).

Anchoring Ca²⁺ channel to the active zone

In vertebrates, localization of Ca²⁺ to the active zone has been shown to depend on its interaction with the PDZ domain of RIM (Coppola et al., 2001; Han et al., 2011; Kaeser et al., 2011). Primary neuron culture of RIM knockout mice shows dramatically decreased Ca²⁺ channel localization to the active zone and reduced Ca²⁺ transient. Interestingly, reexpression of the C-terminus PDZ domain of RIM is sufficient to restore Ca²⁺ channel localization and Ca²⁺ influx, whereas the N-terminus is important for synaptic vesicle priming (Kaeser et al., 2011). Rim interacts both with t-SNARE protein SNAP-25 and n-SNARE synaptotagmin, which may mediate its function in priming synaptic vesicles to the release-ready pool (Coppola et al., 2001). In *C. elegans*, mutation of *unc-10/rim* and *syd-2/liprin-α* leads to similar disassociation of synaptic vesicles with dense projections at the active zone (Stigloher et al., 2011).

In *Drosophila* neuromuscular synapses, the ERC/ELKS/CAST homolog Bruchpilot (Brp) was shown to be the major constituting component of the electron-dense projections (the “T-bar”), which was believed to be the ribbon involved in synaptic vesicle tethering as well as mediating the close coupling of Ca²⁺ influx with synaptic vesicle fusion (Fouquet et al., 2009; Hallermann et al., 2010; Kittel et al., 2006). *brp* mutants show reduced Ca²⁺ channel abundance at neuromuscular synapses, impaired evoked response and the conspicuous T-bar structure at the active is missing (Fouquet et al., 2009; Kittel et al., 2006; Wagh et al., 2006). Brp puncta formation at the active zone is clearly several hours after the initial assembly of the active zone, and is suggested to be a sign of structural maturation of synapses (Fouquet et al., 2009; Rasse et al., 2005).

Orchestration of counteracting signals

The dynamics of active zone assembly seems to be the result of the crosstalk between pro-assembly and counter-assembly factors. In *C. elegans*, regulator of synaptogenesis-1 (RSY-1) has been shown to be a negative regulator of presynaptic assembly. Lose of RSY-1 function leads to enhanced synaptic formation and

recruitment of excessive synaptic proteins to the active zone (Patel and Shen, 2009). In *Drosophila*, mutation of a serine–arginine protein kinase (SRPK79D) leads to the formation of Brp-containing electron-dense puncta along the axon, which resemble the T-bar structure at the active zone of neuromuscular synapses. Synapse vesicles are also shown to be tethered to these electron dense structures in the axon. Overexpression of SRPK79D in an otherwise wildtype background reduces the size of Brp puncta at the active zone. These suggest that SRPK79D functions as a negative regulator of active zone assembly, which is important for inhibiting “premature assembly” of active zone components before integrating into the active zone machinery (Johnson et al., 2009; Nieratschker et al., 2009). At *Drosophila* neuromuscular junction, Rab3 seems to merit a pro-assembly mechanism at the active zone. About 30% of synapses at *rab3* mutant NMJs form extra-large active zones; crucial presynaptic proteins are absent from the rest of synapses, although postsynaptic differentiation is grossly normal. Reexpression of Rab3 at late developmental stages can rapidly restore the formation of active zone at the previously active zone-free synapses, revealing a function of Rab3 in facilitating active zone assembly (Graf et al., 2009).

2.2.1.3 Postsynaptic density formation

Expression of the presynaptic cell adhesion molecule Neurexin in COS cells has been shown to be sufficient to induce postsynaptic assembly in contacting cocultured hippocampal primary neurons, and this synaptogenetic effect of Neurexin is shown to be mediated by the interaction between Neuroligin and Neurexin (Graf et al., 2004; Nam and Chen, 2005). In *Drosophila nlg1* mutants, synapses at the neuromuscular junction have presynaptic active zones but some lack postsynaptic specifications (Banovic et al., 2010).

Neuroligins have been shown to be important upstream regulator of structural and functional maturation of PSDs. In mice there are four variants of Nlgs (Nlg1-4). It was shown that Nlg1 only localizes to glutamatergic synapses, and Nlg2 only to GABAergic synapse, and this differential localization underlines their regulation of synaptic

development and function at specific cell types (Budreck and Scheiffele, 2007; Chubykin et al., 2007; Graf et al., 2004; Song et al., 1999; Varoqueaux et al., 2004).

The intracellular domain of Neuroligin binds with class-I PDZ domain containing proteins, including PSD95/Dlg which is a postsynaptic MAGUK protein (Irie et al., 1997). Furthermore, PSD95/Dlg also interacts with GKAP, which forms complex with Shanks (Naisbitt et al., 1999). Synaptic localization of Shank is inhibited by a splicing variant of GKAP that lacks the Shank binding sequence (Naisbitt et al., 1999).

Other cell adhesion molecules also have been shown to be involved in the early stage of PSD formation. At *Drosophila* neuromuscular junction, Fasciclin II (FasII), an immunoglobulin-related cell adhesion protein has been shown to localize to synaptic contact site soon after nerve arrival. A mutant allele of *fasII* abolishes Dlg localization to the PSD, and also reduces glutamate receptor incorporation (Kohsaka et al., 2007). Interactions between cell adhesion molecules and synaptic organizing proteins are important for recruitment of other proteins to the PSD which contribute to further PSD assembly leading to functional maturation (Lardi-Studler and Fritschy, 2007; Scheiffele, 2003; Sudhof, 2008).

The NR2 subunits of NMDA type glutamate receptors show specific interaction with the first two PDZ domains at the C-terminus of PSD95/Dlg (Niethammer et al., 1996), which has been shown to be crucial for recruiting NMDA receptors to the postsynaptic membrane (Kim and Sheng, 2004). Also through its first two PDZ domains, PSD95/Dlg directly associates with the Shaker-type K⁺ channel and facilitates its anchoring to the postsynaptic membrane (Kim et al., 1995).

Through the interaction between the C-terminal leucine zipper domain of Shank and the PDZ domain binding motif of PIX, Shank, PIX and associated signaling molecule p21-associated kinase (PAK) form a ternary complex (Park et al., 2003). PIX is a guanine nucleotide exchange factor for the Rac1 and Cdc42 small GTPases (Bagrodia et al., 1998; Manser et al., 1998), and PAK is a downstream effector of Rac1/Cdc21 (Bagrodia and Cerione, 1999). Overexpression of Shank leads to increased PAK and PIX localization to the dendritic spines in cultured rat hippocampal neurons (Park et al.,

2003). Thus along with promoting the functional coupling of Rac1/Cdc42 and PAK, Shank also anchors these proteins to the PSD. Shank also has been shown to associate with Homers, another class of postsynaptic scaffold proteins (Tu et al., 1999). A constitutively expressed isoform of Homer oligomerizes and forms complexes with group-I mGluRs (Xiao et al., 1998). The PSD-enrichment of Homer-mGluR complexes is also mediated by their interaction with Shank (Tu et al., 1999; Tu et al., 1998).

To sum up, synaptogenesis and maturation is a which involves the interplay between many intracellular and intercellular signals. The resultant synaptic structure is highly dynamic and plastic, which is up to strengthening or elimination under physiological or pathological conditions. Intensive studies have revealed several important signaling pathways regulating synaptic development, some of which is going to be discussed below.

2.2.2 Signaling pathway regulating synaptic development

2.2.2.1 The Wnt pathway

Wnt signaling has been implicated in controlling vast aspects of development, including cell proliferation, tissue polarity establishment, cell migration and cell fate determination (van Amerongen and Nusse, 2009). Studies also establish a role of Wnt signaling pathway in regulating synaptic development in the nervous system (Budnik and Salinas, 2011).

In the canonical Wnt pathway, Wnt binds to its receptor Frizzled (Fz), leading to activation of the downstream effector Dishevelled (Dvl). Dvl in turn inhibits phosphorylation of β -catenin by GSK-3 β , which normally directs β -catenin for degradation. Increased β -catenin level in the cytoplasm enhances its nuclear translocation, which enables β -catenin to bind transcription factors and to regulate gene expression (van Amerongen and Nusse, 2009). However, due to the many variants of

Wnts, as well as the discovery of many non-canonical Wnt receptors, Wnt signaling has been found to function in an increasing complex network (Budnik and Salinas, 2011).

The role of Wnt pathway in regulating synaptic development was first described in mice, where secreted Wnt7a from the granule cell guide the mossy fiber axons to form the characteristic synaptic pattern (Hall et al., 2000). Blocking Wnt7a activity impairs the normal patterning of mossy fiber, and also inhibits synapse formation in the cerebellum. Wnt7a regulates axonal terminal remodeling through stabilization of microtubule cytoskeleton. This effect is achieved by inhibiting GSK-3 β , which leads to decreased phosphorylation of microtubule associated protein 1B (MAP1B) and thus increased microtubule stability (Lucas et al., 1998).

The function of Wnt signaling in controlling microtubule stability is also implicated in growth cone dynamics as well as formation of synaptic boutons in *Drosophila* neuromuscular junction (Dent et al., 1999; Roos et al., 2000). Blocking *Drosophila* Wnt1 secretion inhibits synaptic bouton formation and disrupts microtubule structure at the NMJ; synaptic development is severely disturbed, leading to formation of “ghost boutons” lacking both presynaptic active zone and postsynaptic differentiation, apparently leaving only the neuronal membrane at the NMJ (Packard et al., 2002).

In vertebrates, Wnt7a overexpression has been shown to enhance presynaptic assembly. Frizzled-5 (Fz5) and Dvl1 seem to be the downstream effectors mediating this effect. Inhibition of Fz5 activity strongly affects presynaptic assembly in rat hippocampal neurons (Ahmad-Annuar et al., 2006; Sahores et al., 2010).

The function of non-canonical Wnt ligand Wnt5a seems to be mainly postsynaptic. In rat hippocampal neurons, Wnt5a recruits PSD95 to dendritic spines from cytoplasmic pool without affecting its expression. This effect involves activation of postsynaptic JNK pathway rather than changing β -catenin levels (Farias et al., 2009). Wnt11r has been implicated in regulating the pre patterning of AchRs in muscles during vertebrate neuromuscular synaptogenesis. Wnt11r activates the tyrosine kinase receptor MuSK, which triggers downstream signaling cascade mediating AChR clustering (Jing et al.,

2009; Luo et al., 2002). Consistently, *dvl1* knockout mouse also shows disturbed AchR pre-patterning (Henriquez et al., 2008).

Apart from the pro-synaptic effect of Wnt pathway, study in *C. elegans* showed that Wnt can also merit inhibitory information during synaptogenesis. The DA9 motor neuron form *en passant* synapses with muscles along the dorsal ventral axis. Interaction between the Fz/LIN-17 at the asynaptic segment of the DA9 motor neuron axon and the Wnt/LIN-44 expressed by the cells near the tail inhibits synaptic formation at this region. Worms carrying the *lin-17* mutant and *lin-44* mutant both display ectopic synapse formation (Klassen and Shen, 2007).

2.2.2.2 The TGF- β pathway

The transform growth factor- β (TGF- β) signaling has been implicated in controlling various events during development and disease (Derynck et al., 2001; Massague and Wotton, 2000). In the canonical TGF- β pathway, TGF- β ligand activates the type-II and type-I serine/threonine kinase receptors, and further induces Smad dependent transcription events (Moustakas et al., 2001). The non-Smad pathway is not dependent on Smad induced transcription, and instead is mainly mediated by activation of MAPK and PI3K pathways (ten Dijke et al., 2000). The TGF- β superfamily can be further divided into TGF- β , bone morphogenic proteins (BMPs) and activins which bind with their distinct receptors and trigger different downstream events (Moustakas et al., 2001).

The role of TGF- β pathway in regulating synaptic development is best characterized in the NMJs (Bayat et al., 2011; Wu et al., 2010). In *Drosophila*, mutation in the homolog of type-II BMP receptor wishful thinking (Wit) leads to significantly reduced NMJ size and severely impaired synaptic function (Aberle et al., 2002; Marques et al., 2002). Wit expression is restricted to neurons, and reexpression of Wit in motor neuron is sufficient to rescue the NMJ phenotypes, suggesting a specific presynaptic function. Loss of function mutations in other TGF- β signaling molecules, including the BMP ligand homolog glass bottom boat (Gbb), the type-I receptor homologs saxophone (Sax) and

thickveins (Tkv), as well as the Smad homologs Mad and Medea cause similar synaptic growth and functional defects at *Drosophila* NMJ (McCabe et al., 2004; McCabe et al., 2003; Rawson et al., 2003). These evidences establish TGF- β pathway as a retrograde signaling controlling synaptic development.

TGF- β pathway is also implicated in synapse stabilization. Disruption of TGF- β pathway in *Drosophila* leads to formation of distinct synaptic “footprints”: in some part of the NMJ the postsynaptic specification persists, however presynaptic structures are retracted. In parallel with activating Mad regulated transcriptions, the function of TGF- β pathway in synapse stabilization is also partially mediated by LIM kinase1 (DLIMK1). It was shown that Wit directly associates with DLIMK1, and neuronal overexpression of DLIMK1 rescues both the synaptic retraction as well as the functional impairment in *wit* mutants (Eaton and Davis, 2005). Misregulated TGF- β pathway is also implicated in the pathogenesis of neurodegenerative diseases including hereditary spastic paraplegia (HSP), amyotrophic lateral sclerosis (ALS), spinal muscular atrophy (SMA), multiple sclerosis (MS) and Huntington’s disease (Bayat et al., 2011; Wang et al., 2007).

2.2.2.3 The mitogen-activated protein kinase (MAPK) pathway

The MAPK pathway is a highly complex signal cascade connecting extracellular signaling with intracellular responses. Three major subgroups of MAPKs have been well characterized, including the extracellular signal-related kinases (ERKs), p38 MAPKs and c-jun N-terminal kinases (JNKs). MAPKs are activated by specific MAP2Ks: MEK1/2 for ERKs, MKK3/6 for p38 MAPKs and MKK4/7 for JNKs (Chang and Karin, 2001). MAP2Ks are further regulated by MAP3Ks, which are activated by various stimulus including growth factors, peptide hormones, cytokines, cell stress and others. Expression of many MAPK regulators and components has been shown to be enriched in the nervous system, and MAPK signaling has been shown to be involved in neural development and neurological diseases (Impey et al., 1999; Jover-Mengual et al., 2007).

In *Drosophila*, loss of function mutation in the serine threonine kinase *unc-51* leads to accumulation of active zone components along the axon, impaired presynaptic active zone formation, decreased synapse number as well as reduced synaptic function at the NMJ (Wairkar et al., 2009). Mechanistic study reveals that Unc-51 inhibits the activity of the ERK MAPK pathway to promote synaptic development. Mutation in the *Drosophila* ERK homolog *rolled* rescues the synaptic development phenotype as well the impaired synaptic activity in *unc-51* mutants (Wairkar et al., 2009). Consistently, overexpression of Ras and Raf which are the upstream activators of the MAPK pathway, as well as gain of function allele of *rolled* leads to overgrowth of NMJ in *Drosophila* (Fischer et al., 2009; Koh et al., 2002). This function of regulating synaptic growth is mediated by the adhesion molecule FasII (Koh et al., 2002).

The postsynaptic effect of Wnt5a in recruiting the synaptic scaffold protein PSD95 to the dendritic spine is also through a non-canonical Wnt signaling pathway involving JNK activation (Farias et al., 2009).

A series of studies delineate a conserved MAPK pathway in regulating synaptic development, axonal regeneration and plasticity. Mutations in a *Drosophila* E3 ubiquitin ligase highwire (*Hiw*) lead to extremely lengthened neuromuscular junction, reduced synaptic bouton size as well as severely impaired synaptic function (Wan et al., 2000). Further study revealed that *Hiw* inhibits the level of a dual-leucine zipper kinase (DLK) to restrict NMJ development (Collins et al., 2006). Loss of function mutations in a DLK homolog *wallenda* (*wnd*) as well as expression of dominant negative forms of the JNK homolog basket (*Bsk*) or dominant negative forms of the transcription factor Fos can rescue the NMJ development phenotype of *hiw* mutants. In *C. elegans*, the *Hiw* homolog regulator of presynaptic morphology-1 (*Rpm-1*) localizes to the presynaptic terminal. Loss of function mutant of *rpm-1* leads to vast synaptic development abnormalities. Some *rpm-1* mutant synapses have multiple active zones, whereas many others have none; motor neurons also show disturbed axonal branching (Nakata et al., 2005; Schaefer et al., 2000; Zhen et al., 2000). The function of *Rpm-1* in regulating synaptic development is also dependent on its role in controlling the signal strength of the DLK as well as p38 MAPK pathway in the nematode (Nakata et al., 2005).

Interestingly, the Wnd MAPK signaling cascade also has been shown to regulate axonal regeneration after injury, which is also a conserved function between flies, worms and vertebrate (Miller et al., 2009; Xiong et al., 2010; Yan et al., 2009).

In the present study, I am going to show that the Wnd MAPK pathway also regulates synaptic assembly. Overactivated Wnd MAPK pathway is involved in the synaptic development defects caused by of a hypomorph allele of Kinesin-3 homolog in *Drosophila*.

Apart from the signaling pathways discussed above, some other signal cascades also have been shown to regulate synaptic development (Wu et al., 2010). Interaction between neuron and glia also plays important role during synaptic establishment and maturation. These mechanisms work together to regulate synaptic formation ensure the accurate wiring of neural network.

2.2.3 Molecular motors and synaptic development

Synapses normally form at the tips of neuronal processes, which can be extremely distant from neuronal cell body at a cellular scale. For instance, in humans the somatic motor neurons controlling toe movement extend axons of more than one meter long to establish synaptic connection with appropriate muscle. Synaptic proteins, synaptic vesicles, mitochondria, etc have to be transported to the synaptic site, and proteins to be degraded have to be transported back to the cell body. Very efficient and tightly controlled intracellular transport is of vital importance both for the establishment of the synaptic structure as well as maintenance of synaptic function (Cai and Sheng, 2009).

2.2.3.1 Major molecular motors

Motor proteins responsible for intracellular transport belong to three major groups: kinesins, dyneins and myosins. Both kinesins and dyneins are microtubule associated motors which travel along microtubule tracks (Vale, 2003). In vitro analysis

demonstrates that most kinesins are plus-end directed motors, whereas dyneins are minus-end directed. Because microtubules in axons arrange uniformly, having plus-end pointing to the axonal terminal and minus-end pointing to the cell body, kinesins are believed to be the major anterograde motor transporting cargos to the synapses while dyneins are mainly responsible for retrograde transport to carry cargos back to the cell body. In proximal region of dendrites, there is a mixed microtubule polarity, but at distal region the microtubule bundles are also unidirectional, having the plus-ends pointing to the tips.

Microtubule tracks normally extend till some distance away from the plasma membrane and are continued by actin filaments (F-actins) based cytoskeletons. Unconventional myosins are actin associated motors which is responsible for transporting cargoes along actin filaments. Although so far less well understood than microtubule based transports, local transport of cargoes along actin filaments is of crucial importance as this is always the immediate step before cargoes arrive at their final destination or the priming step for microtubule based transport (Bridgman, 2004). Here we focus on the function of kinesin based intracellular transport.

Systematic study identifies 45 Kinesin super family proteins (KIFs) in mouse genomes, 38 of which are expressed in the brain (Miki et al., 2001). All KIFs share a highly conserved “head domain”, which contains an ATP binding motif and microtubule binding motif. The head domain hydrolyzes ATP, which causes conformational change to the head domain and leads to processability (Hirokawa and Noda, 2008). Apart from the head domain, kinesins also contain a “stalk” region and “tail” region, which are both highly variable. The stalk region contains coiled-coil domains which enable formation of functional kinesin dimers. The tail regions are important for cargo recognition. The conventional kinesins (KIF5s in vertebrate) are also coupled with kinesin light chains (KLCs) to facilitate cargo binding (Gyoeva et al., 2004), thus KIF5s are also called kinesin heavy chains (KHCs). Many adaptor proteins also have been identified, which modulate kinesin-cargo interaction (Hakimi et al., 2002; Kamm et al., 2004; McGuire et al., 2006). Due to the various cargo binding specificities, activity regulation mechanisms

and expression profile, kinesin based transport is involved in regulating various aspects of synaptic development.

2.2.3.2 Kinesin and synaptic development

Anterograde transport of t-SNARE proteins including SNAP-25 and syntaxin, which localized to the presynaptic plasma membrane, seems to be mainly carried out by Kinesin-1/KIF5s. SNAP-25 has been predicted to associated with the Kinesin-1/KIF5/KHC, and its direct interaction with the cargo-binding domain of the human KHC was proved by yeast two-hybrid experiments (Diefenbach et al., 2002). Syntaxin transport has been shown to be regulated by the microtubule associated protein syntabulin (Su et al., 2004). Because syntabulin is associated with the Kinesin-1 family member KIF5B and acts as an adaptor protein to mediate cargo binding, the tight Syntaxin-Syntabulin association strongly suggests the synaptic delivery of Syntaxin is also Kinesin-1 based (Cai et al., 2007).

Several lines of evidence suggest that at least some presynaptic active zone proteins are transported by Kinesin-1/KIF5s. Immunoisolation experiments show that in rat brains KIF5B is associated with Bassoon containing membranous organelles. These organelles are presumably active zone precursors because they also contain other active zone proteins including Piccolo, N-Cadherin, Syntaxin as well SNAP-25 (Cai et al., 2007). In primary hippocampal neurons, knockdown of the KIF5 adaptor protein Syntabulin and disrupting its association with KIF5 or Syntaxin both strongly inhibit axonal transport of these Bassoon containing active zone precursor vesicles, leading to accumulation of Bassoon containing vesicles in neuronal cell bodies (Cai et al., 2007). Furthermore, this Syntabulin dependent transport of active zone precursor vesicles is crucial for activity dependent structural plasticity, as formation of new synapse after stimulation is strongly inhibited by Syntabulin knockdown, whereas Syntabulin overexpression enhances this process (Cai et al., 2007).

The Kinesin-3/Unc-104 family is a class of motors with major neuronal functions. Structurally the Kinesin-3 motors contain a distinct forkhead –associated (FHA) domain, which is important for regulating motor dimerization, microtubule affinity and processability (Lee et al., 2004). Members of the kinesin-3 family have been shown to be the major transporters of synaptic vesicle precursors (SVPs), and they have important role in regulating synaptic development. Unc-104 in *C. elegans* is the first identified member of the kinesin-3 family. *unc-104* mutant worms have few synaptic vesicles in the axon terminals, forming less synapses which are also smaller. At the same time, synaptic vesicles like aggregates are found in motor neuron cell body (Hall and Hedgecock, 1991). In the mouse genome there are three subtypes of Kinesin-3 motors, KIF1A, KIF1B and KIF1C (Miki et al., 2001). Both *kif1A* knockout and *kif1B* knockout mice show similar severely reduced synaptic vesicle density at nerve terminals as well as decreased synapse number (Yonekawa et al., 1998; Zhao et al., 2001). *In vitro* assay also proved a direct association of KIF1B β , one of the KIF1B variants, with synaptic vesicle precursors marked by Synaptotagmin, Synaptophysin and SV2 (Zhao et al., 2001). In *Drosophila*, loss of function mutations in the kinesin-3 homolog *unc-104/imac* lead to embryonic lethality (Pack-Chung et al., 2007). In *unc-104* mutant fly embryos, transport of synaptic vesicle precursors as well as peptide filled dense core vesicles (DCVs) is severely impaired, motor neuron terminals fail to transform into synaptic boutons, and few neuromuscular synapses form (Pack-Chung et al., 2007). Another two hypomorphic alleles of *Drosophila unc-104* lead to lethality at late larval stage or pupal stage, but leading to similar impairment of SVP and DCV transport (Barkus et al., 2008).

Mitochondria at the synaptic terminals are crucial for synaptic development as well for generating energy for proper synaptic activity (Morris and Hollenbeck, 1993; Shepherd and Harris, 1998). What is more, mitochondria also have been shown to be involved in Ca²⁺ buffering mechanism in some forms of synaptic plasticity (Tang and Zucker, 1997). Kinesin-1/KIF5s have been shown to be the major anterograde mitochondria transporters (Cai et al., 2005; Glater et al., 2006; Stowers et al., 2002). Cell from the *kif5B* knockout mouse shows prominent perinuclear localization of mitochondria, which

can be rescued by exogenous *kif5B* expression. Subcellular fractionation experiment also shows that mitochondria associate with KIF5B (Tanaka et al., 1998).

Mitochondria do not seem to depend on kinesin light chain (KLC) for binding with KIF5s. Instead, several other adaptor proteins have been implicated in mediating motor-cargo binding and KIF5 recruitment during mitochondria transport. Miro proteins are Ras GTPases localizing to mitochondria membrane (Fransson et al., 2003). Miro binds to Milton, an adaptor protein associated with KIF5/KHC and forms a complex mediating mitochondria transport (MacAskill et al., 2009; Stowers et al., 2002; Wang and Schwarz, 2009). Importantly, Miro mediates a Ca^{2+} dependent regulation of mitochondria transport. In vertebrates, Ca^{2+} binding to the EF hand calcium binding domain of Miro leads to dissociation of the mitochondria-Miro-Milton complex with KHC, while in *Drosophila* Ca^{2+} binding to Miro cause KHC detachment from microtubule (MacAskill et al., 2009; Wang and Schwarz, 2009). In both cases, Ca^{2+} binding negatively regulate mitochondria transport.

Syntabulin is another adaptor protein regulating KIF5/Khc based mitochondria transport. Syntabulin is targeted to mitochondria via its C-terminal sequence. In primary neuron cultures, Syntabulin is co-transported with mitochondria along neuronal processes. Interfering Syntabulin interaction with KHC and knockdown of Syntabulin both strongly inhibit mitochondria localization in neurites, and also reduce mitochondria anterograde transport (Cai et al., 2005).

Other kinesin associated proteins also have been implicated in regulating kinesin based transport. The presynaptic active zone component Liprin- α has been shown to associate with KHC in *Drosophila* (Miller et al., 2005). While Liprin- α association with kinesin is probably important for its synaptic delivery, Liprin- α also seems to play a role in regulating the behavior of motor proteins. In the axons of *liprin- α* mutant larvae, there is excessive synaptic vesicle deposit, which is accompanied by decreased anterograde axonal transport and increased retrograde transport of Synaptobrevin-GFP labeled vesicles. Through direct and indirect interactions, Liprin- α may function to regulate the activity of multiple motors and thus coordinate proper axonal transport (Miller et al.,

2005). In *C. elegans*, where Liprin- α is shown to bind the Kinesin-3 homolog Unc-104, Liprin- α seems to be important for facilitating the association of Unc-104 with synaptic vesicles as well as enhancing Unc-104 processability (Wagner et al., 2009). In mouse primary hippocampal neurons, the GluR2 interaction protein GRIP1 is able to recruit KHC to the somatodendritic region, whereas the kinesin binding domain of JNK/SAPK-associated protein-1 (JSAP-1) leads to KHC accumulation at the somatoaxon area (Setou et al., 2002).

Although less well understood than presynaptic functions, some important roles of kinesin in regulating postsynaptic differentiation also have been revealed. KIF17 is a brain enriched kinesin which is implicated in NMDA receptor subunit transport in dendrites. In mouse neurons the NR2B subunit of NMDA receptor forms protein complex containing mLin-10/Mint11/X11, mLin-2/CASK and mLin-7/MALS. KIF17 is shown to directly bind to the PDZ domain of mLin-10 and transport NR2B containing complex *in vitro* (Setou et al., 2000). In primary mouse hippocampal neuron cultures, YFP tagged KIF17 colocalized with NR2B subunits along dendrites; knockdown of KIF17 or blocking motor function by expression of a truncated form of KIF17 reduces synaptic localization of NR2B and leads to its accumulation in neuronal cell body (Guillaud et al., 2003). Transport of the AMPA receptor subunit GluR2 in mouse neurons is found to be Kinesin-1 dependent. The GluR2 interaction protein GRIP1 has been shown to directly bind KHC, and recruit it for GluR2 transport in the dendrites. Blocking KHC function impaired dendritic localization of both GRIP1 and GluR2 (Setou et al., 2002).

Recent study also reveals that transport of mRNA to the synapses to enable local translation is important for structural plasticity. In sensory neurons, treatment with Serotonin leads to synapse specific long term facilitation which can last for more than 72 hours (Casadio et al., 1999). Maintenance, but not induction of this long term facilitation is dependent on the expression and axonal transport of the *Aplysia* eukaryotic translation elongation factor 1 α as well as its mRNA (Giustetto et al., 2003).

2.3 The *Drosophila* neuromuscular junction

The fruit fly, *Drosophila melanogaster* has been established as a valuable model organism for biological sciences. The fly genome has been among the first ones to be fully sequenced; many proteins as well as important biological processes are conserved between *Drosophila* and vertebrates (Adams et al., 2000). The genetic background of *Drosophila* is well characterized, and powerful genetic tools have been established. The widely used UAS-Gal4 system enables efficient spatial and temporal control of gene expression (Brand and Perrimon, 1993). Transposon based mutagenesis as well as transgenic technique enable convenient and low-cost generation of transgenic animals. *Drosophila* is easy to maintain, with relatively short life cycle, making it a favorable organisms for performing large scale mutagenesis and unbiased screening (Bellen et al., 2004; Medina et al., 2006).

The *Drosophila* neuromuscular junction is a well established model system for studying synaptic development and for modeling neurological disorders. The arrangement of larval neuromuscular system is very well characterized. Each segmental unit of the larval body wall musculature contains 30 muscles, which are innervated by 32 motor neurons in the ventral nerve cord. The arrangement of muscles and arborization of motor neuron terminals are both stereotyped, making it possible to reliably identify and compare the neuromuscular junctions of interest.

The *Drosophila* neuromuscular junctions are glutamatergic, which resembles the excitatory synapses in vertebrate central nervous system. A neuromuscular junction normally comprises up to 20-50 synaptic boutons, which are connected by neuronal membrane. Within each synaptic bouton, there are about 10 single synapses. During development, along with the growth of muscles, new synaptic boutons are added into NMJs and new synapses can form within preexisting as well as new boutons.

Various experimental techniques are easily applicable to NMJs, including electrophysiology, immunohistochemistry as well as electron microscopy. Especially thanking to the transparent nature of the larval cuticle and availability of various fluorescently tagged proteins, non-invasive live imaging of protein and organelle

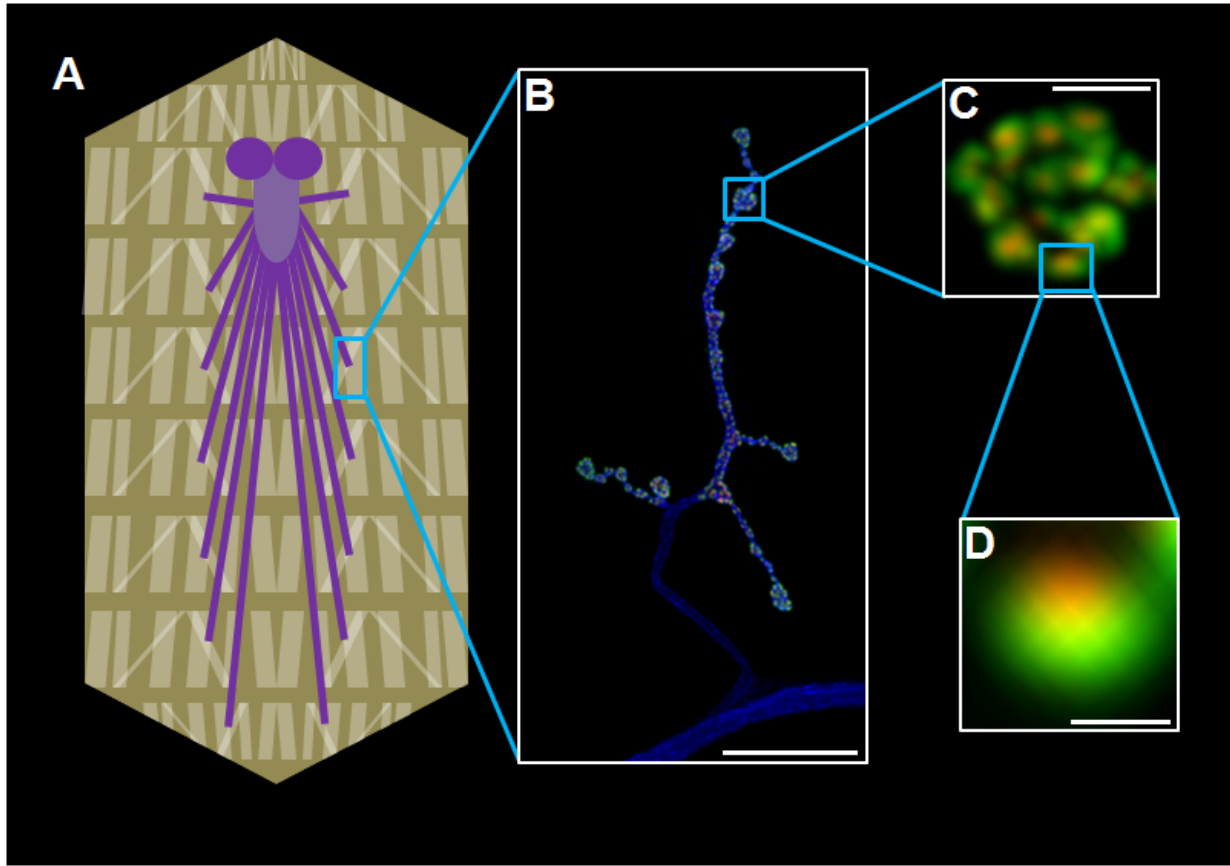


Fig1. The *Drosophila* neuromuscular junction. (A), illustration of the musculature of a filleted *Drosophila* larva opened along dorsal longitudinal axis of the body. Segmental nerves extend from the ventral nerve cord and innervate defined muscles. (B), (C) and (D), sample neuromuscular junction (B), synaptic bouton (C) and glutamatergic synapse (D), respectively. In (B-D), Larvae were stained with the neural membrane marker HRP (blue), presynaptic active zone marker Brp (red) and postsynaptic density marker GluRIIC (green). Scale bars, in (B), 20 μ m; in (C), 2 μ m; in (D), 500nm.

dynamics has provided important new insight for understanding neural development at native setting (Fuger et al., 2007; Rasse et al., 2005).

In this thesis, *Drosophila* is used as a model organism to study the mechanisms regulating synapse development and maintenance of neuronal function. The synaptic phenotype caused by a hypomorph allele of the *Drosophila* kinesin-3 homolog, *unc-104^{bris}* is to be investigated and the underlying mechanism causing the observed structural and functional abnormalities is to be explored. With these efforts, this work will hopefully help to gain new insight in understanding how various signals orchestra to enable normal synaptic development, and further to shed light in the pathogenesis of related neurological disorders.

3. Materials and methods

The electrophysiology experiments and most of the data analysis pertaining to electrophysiology were performed by Dr. Doychin Stanchev. These data are included with his permission.

Fly Stocks

Flies were cultured on standard soft media seeded with live yeast at 25°C if not otherwise indicated. *w¹¹¹⁸*, UAS-*fos^{DN}*, UAS-*bsk^{DN}*, *elav-Gal4*, *unc-104^{d11024}*, UAS-*cac-gfp* were from Bloomington Stock Center. *unc-104^{bris}* was from Jay E. Brenman (Medina et al., 2006). UAS-*mito-gfp*, D42-Gal4, and UAS-*anf-gfp*, D42-Gal4 recombination stocks were from William Saxton (Barkus et al., 2008). GluRIIA-mRFP and GluRIIB-GFP with native promoters and UAS-*brp* and UAS-*brp-RNAi* (C8) were gifts from Stephan Sigrist (Rasse et al., 2005; Wagh et al., 2006). UAS-*srpk79d-gfp* was from Erich Buchner (Nieratschker et al., 2009). *hiw^{ΔN}*, UAS-*wnd*, UAS-*hiw-gfp*, *wnd1* and *wnd3* stocks were from Aaron DiAntonio (Collins et al., 2006).

Immunohistochemistry

Larvae were dissected in Ca²⁺-free HL3 solution and fixed in 4% formaldehyde in PBS for 3 minutes (staining with native fluorescent proteins) or for 10 minutes (for staining with only immunofluorescent labeling). Mid third instar stage larvae were used for dissection if not otherwise indicated. Primary antibodies incubation was done overnight at 4°C in PBS with 0.05% Triton-X and 5% normal goat serum. Fillets were then washed and incubated with fluorescent-conjugated secondary antibodies at room temperature for 2 hours. Larval fillets were mounted on a glass slide in mounting media (Vectashield, Vector). Primary antibodies used were: mouse monoclonal anti-Dlg (4F3) at 1:50 and mouse monoclonal anti-Brp (NC82) at 1:100 (Developmental Studies Hybridoma Bank), rabbit anti-GluRIIC at 1:2000 (Stephan Sigrist), rabbit anti-DVGlut at 1:1000 (Hermann

Aberle), rabbit anti-Rab3 at 1:1000 (Graf et al., 2009). Fluorescent-conjugated secondary antibodies used were: goat anti-mouse Alexa 488 or Alexa 568 and goat anti-rabbit Alexa 488 or Alexa 568 (Molecular Probes); goat anti-mouse Atto 647 (Sigma). Goat anti-HRP conjugated with Cy3 (Dianova) was added together with secondary antibodies. All used at 1: 500.

Images were captured using a Zeiss LSM 710 confocal microscope, with a 40x plan apochromat 1.3 N.A. oil objective and the ZEN software. Pixel size of $0.1\mu\text{m}\times 0.1\mu\text{m}$ and $0.5\mu\text{m}$ interval between frames were constantly kept during imaging. Pinhole was kept 1 or 1.5 during imaging. ImageJ 1.43 (NIH) was used for image processing and subsequent data analysis.

Quantifications of Brp puncta/PSD Size and Intensity

Image processing and quantification were essentially performed as previously described (Fuger et al., 2007). Larvae to be compared are dissected on the same day, stained in the same tube, mounted on the same slice, and imaged using the same settings. On the original image stack, “Gaussian blur” filter with a radius of one was applied (Process/filters/Gaussian blur). Subsequently, a maximum projection of the image stack was made and scaled by two (Image/scale). A threshold was set to create a binary mask so that the less than 5% of the smallest synapses are lost and most of the structure of interest are preserved with appropriate size (Image/adjust/threshold). The mask was then projected to the original image (Process/image calculator/operation “Min”) to create a new image in which only the intensity and shape of structure of interest are preserved and the background has a value of zero. Manual segmentation was done on the resulted picture using the pencil tool with line thickness of two pixels and “color picker” value of zero. Area and average intensity of discrete structures in the segmented picture were analyzed (Analyze/ Analyze particles). To Measure the intensity and area of structures within the NMJ (DVGlut, Mito-GFP, Rab3, ANF-GFP, etc.), a region of interest was defined by applying a mask generated from the corresponding HRP channel.

Electrophysiology

Current clamp intracellular recordings were performed on muscle 6 segment A2 of third instar stage larvae. The larvae were pinned and stretched in a Sylgard-coated perfusion chamber and visualized on Olympus BX51WI microscope. "Bee-stinger" sharp electrodes (10-15 M Ω), made of borosilicate glass (outer diameter 1.5 mm) were filled with 3 M KCl. Only cells with resting potential between -55 and -80 mV and input resistance higher than 4 M Ω were included in the analysis. Recordings were performed in HL3 Stewart saline (Stewart et al., 1994) containing (in mM): 70 NaCl, 5 KCl, 20 MgCl₂, 10 NaHCO₃, 5 trehalose, 115 sucrose, and 5 HEPES; the concentration of calcium was 1, pH adjusted to 7.2. All experiments were performed at 18°C. Stimulation of the segmental nerve was executed by pulling the cut end of the nerve into a self-made suction electrode (5-6 μ m in diameter) filled with HL3 and passing a brief (0.3 ms) bi-polarizing pulse across the nerve. Stimulation was accomplished with a ISO-STIM 01D stimulus isolation unit (NPI electronics GmbH, Tamm, Germany). The signal was acquired with an Axoclamp 900A amplifier (Axon Instruments), digitized with a Digidata 1440A analog to digital board, recorded with a PC used pClamp 10.3 (Axon Instrument) and analyzed with AxoGraph X software. The amplitudes of the EJPs were corrected for nonlinear summation (Kim et al., 2009; McLachlan and Martin, 1981). To be specific, the following equation was used:

$$EJP_a = EJP_m / [1 - f(EJP_m/D)]$$

in which EJP_a is the adjusted EJP after correction for non-linear summation; EJP_m is the measured amplitude of active potential; D is the driving force, which equals to (resting potential-reversal potential), and the reversal potential for *Drosophila* NMJ is assumed to be 0mV; f is the membrane capacitance factor, whose value at *Drosophila* NMJ is 0.55. Only EJPs which are higher than 15% of the resting potential are corrected for non-linear summation using the above equation. The quantal content was calculated by dividing the average of corrected EJP by the average mEJP amplitude.

Larval locomotion assay

Larvae between the ages of about 36 hours AEL and 84 hours AEL were combined and recovered from the media by dispersing briefly in 15% sucrose solution followed by rinsing with tap water. Subsequently, larvae were kept at 25°C with 70% humidity for 45 minutes, before being transferred to a 15×15 agar plate for 10 minutes filming. Locomotion speed and larval size (area) were analyzed with custom-built software (AnimalTracer, Rasse et al., unpublished results). Larval length was calculated from the measured size assuming that the ratio between the length and width of larva is 3.5. Larvae were grouped according to their length and the average locomotion speed of larvae in the same length group was calculated.

Statistics

Statistical tests were performed following the procedure below. Data sets were first tested for normality. According to the result of normality test and number of groups in the data set, statistical test were done in one of the four following ways. 1) For data sets with two groups which were both normally distributed, student's t test was used. 2) For data sets with two groups, and at least one of which was not normally distributed, Mann Whitney test was used. 3) For data set with three groups or more which were all normally distributed, one way ANOVA was used followed by Tukey's multiple comparison test. 4) For data set with three groups or more, and at least one of which were not normally distributed, Kruskal-Wallis test were used followed by Dunn's multiple comparison test. In every case, $P > 0.05$ was regarded not significantly different and indicated by "n.s." in charts; $P < 0.05$, $P < 0.01$ and $P < 0.001$ were indicated by "*", "**", and "***" in charts, respectively.

4. Results

The electrophysiology experiments and most of electrophysiology related data analysis were performed by Dr. Doychin Stanchev. Data was included with his permission.

The ratio data analysis in section 4.1.5 was performed with the help of Baran Koç.

4.1 Characterization of the phenotype in *unc-104^{bris}* mutant

Using forward genetics screening we have previously identified a mutant allele of the *Drosophila kinesin-3* homolog, *unc-104^{bris}*, which leads to three major synaptic development defects. Firstly, *unc-104^{bris}* NMJs shows impaired presynaptic AZ assembly. Whereas in wild type larvae only less than 5% of the synapses at the neuromuscular junction are negative for the presynaptic AZ organizing protein Brp, about 30% of the *unc-104^{bris}* mutant synapses are found unopposed by Brp (Kern et al., unpublished observations). Secondly, *unc-104^{bris}* NMJs are much more elongated, which is accompanied by significantly reduced size of synaptic boutons. Thirdly, development of the subsynaptic reticulum (SSR), a postsynaptic membranous system surrounding synaptic boutons, is greatly reduced.

4.1.1 Brp mislocalization in *unc-104^{bris}* mutant is not downstream of insufficient Brp at the NMJ

A null allele of *Drosophila unc-104* leads to severe reduction of Brp at motor neuron terminals at late embryonic stage (Pack-Chung et al., 2007). It is also shown that Brp abnormally accumulated in the neuronal cell bodies in the ventral ganglion of *unc-104^{bris}* mutant larvae (Kern et al., unpublished observations). Comparing the total amount of Brp per NMJ between control and *unc-104^{bris}* mutant revealed that the quantity of Brp at *unc-104^{bris}* mutant NMJs dropped to only half of that in control (Fig. 2 A, B). The size of presynaptic Brp puncta in *unc-104^{bris}* mutant also reduced by half (Fig. 2 A, C).

One possible explanation of the observed Brp mislocalization at *unc-104^{bris}* mutant neuromuscular synapses is that it is a result of insufficient supply of Brp to the NMJ. In

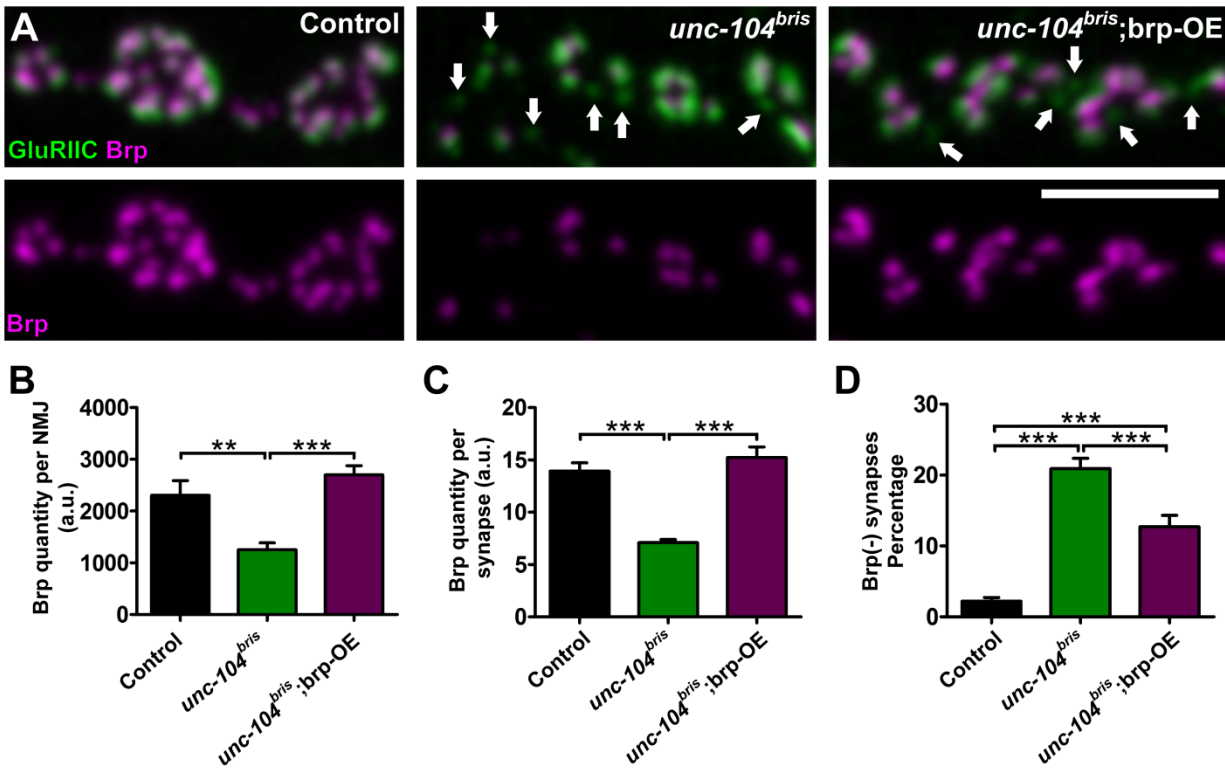


Fig2. Brp overexpression modifies the AZ assembly defect in *unc-104^{bris}* mutants. (A) Confocal images of neuromuscular synapses immunostained with Brp (magenta) and GluRIIC (Green) in control, *unc-104^{bris}* and *unc-104^{bris};brp-OE* larvae. Arrows indicate synapses devoid of presynaptic Brp puncta. Bar, 5µm. (B-D) Quantification of the amount of Brp per NMJ, Brp quantity at single punctum (Area × Intensity), as well as the percentage of synapses devoid of Brp in groups stated in (A). (B) The amount of Brp per NMJ in *unc-104^{bris}* mutants was about half of wildtype control. Pan-neural overexpression of Brp cDNA induced by elavX-Gal4 in an otherwise *unc-104^{bris}* background at 29°C doubled Brp quantity at the NMJ, to a similar level with controls (control: 2306 ± 283.0 a.u.; *unc-104^{bris}*: 1252 ± 133.3 a.u.; *unc-104^{bris};brp-OE*: 2697 ± 180.9 a.u.. control vs. *unc-104^{bris}*: P<0.01; *unc-104^{bris}* vs. *unc-104^{bris};brp-OE*: P<0.001; control vs. *unc-104^{bris};brp-OE*: P>0.05). (C) Size of presynaptic Brp punctum in *unc-104^{bris}* mutant NMJs was also about of half wildtype control. Brp overexpression in the *unc-104^{bris}* background doubled Brp puncta size to a similar level with wildtype control (control: 1.392 ± 0.081 a.u.; *unc-104^{bris}*: 0.709 ± 0.030 a.u.; *unc-104^{bris};brp-OE*: 1.522 ± 0.102 a.u.. control vs. *unc-104^{bris}*: P<0.001; *unc-104^{bris}* vs. *unc-104^{bris};brp-OE*: P<0.001; control vs. *unc-104^{bris};brp-OE*: P>0.05). (D) The percentage of synapses devoid of presynaptic Brp puncta in *unc-104^{bris}* NMJs was over 8 folds higher than wildtype control. Brp overexpression partially rescued the percentage of Brp(-) synapses in *unc-104^{bris}* mutants, but it was still 5 times higher than wildtype (control: 2.21 ± 0.54%; *unc-104^{bris}*: 20.92 ± 1.46%; *unc-104^{bris};brp-OE*: 12.70 ± 1.61%. control vs. *unc-104^{bris}*: P<0.001; *unc-104^{bris}* vs. *unc-104^{bris};brp-OE*: P<0.001; control vs. *unc-104^{bris};brp-OE*: P<0.001). Number of NMJs quantified in (B-D): control: N=9; *unc-104^{bris}*: N=8; *unc-104^{bris};brp-OE*: N=8. Experiments performed at 29 °C. Statistical test: One-way ANOVA followed by Tukey's Multiple Comparison Test. **, P<0.01; ***P<0.001. Error bars indicate the SEM.

order to test this hypothesis, Brp was overexpressed at the NMJs in an otherwise *unc-104^{bris}* mutant background. Pan-neural overexpression of Brp using the *elav-Gal4* driver at 29°C doubled Brp level in *unc-104^{bris}* mutant NMJs, to a similar level with wildtype control (Fig.2 A, B). Concurrently, Brp overexpression also brought the presynaptic Brp puncta size in *unc-104^{bris}*;Brp-OE group back to a level similar with wildtype (Fig.2 A, C). Brp overexpression also significantly reduced the percentage of synapses devoid of presynaptic Brp puncta (thereafter **Brp(-) synapse**) in *unc-104^{bris}* mutants. However, despite the full rescue of Brp quantity at the NMJ, the percentage of Brp(-) synapses in the *unc-104^{bris}*;Brp-OE NMJs was still 5 times higher than wild type control (Fig.2 A, D). Importantly, Brp overexpression also failed to rescue the other phenotypes including larval lethality, NMJ overgrowth (unpublished observation). Therefore, our result shows that it is not likely that the reduced Brp assembly at active zone in *unc-104^{bris}* mutant synapses is secondary of reduced Brp availability at the NMJ. Instead, the above result speaks for a reduced ability of clustering Brp at the presynaptic compartment of these Brp(-) synapses.

4.1.2 Systemic AZ assembly defects at NMJ in *unc-104^{bris}* mutant larvae.

Apart from Brp, recent studies have identified several other AZ proteins in *Drosophila*. These include the voltage gated Ca^{2+} channel subunit Cac, Syd-2/Liprin- α , the SR protein kinase SRPK79D, the multidomain RhoGAP-like protein DSyd-1 and most recently the RIM binding protein DRBP (Fouquet et al., 2009; Johnson et al., 2009; Kittel et al., 2006; Liu et al., 2011; Nieratschker et al., 2009; Oswald et al., 2010). These AZ proteins are involved in maintaining various aspects of the structural and functional integrity of synapses. During synaptic development, these proteins are incorporated into the AZ at defined temporal sequence (Fouquet et al., 2009; Oswald et al., 2010; Oswald and Sigrist, 2009).

In order to detail the AZ assembly phenotype caused by the *unc-104^{bris}* mutation, GFP-tagged AZ proteins were expressed in *unc-104^{bris}* mutant larvae and their localization at

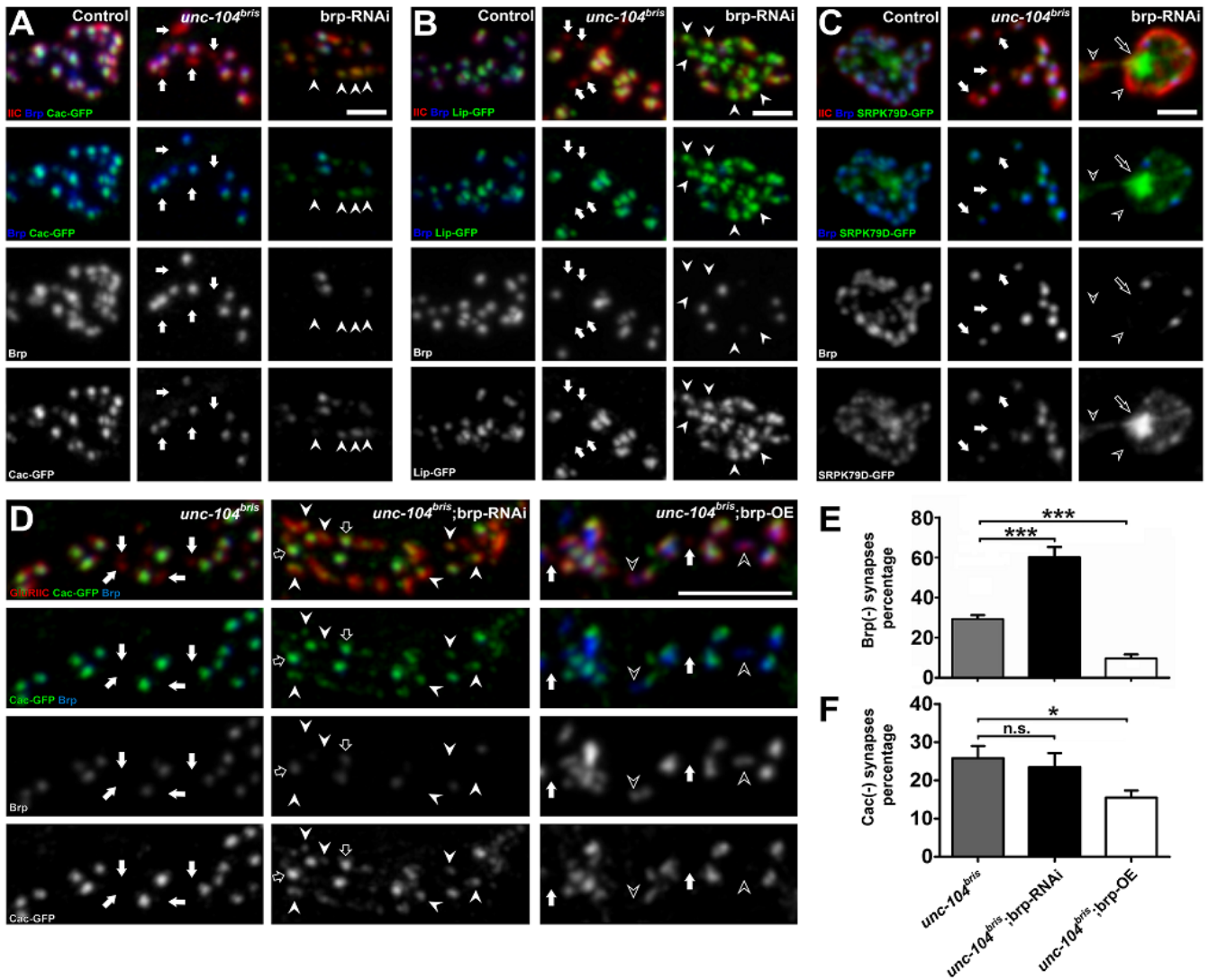


Fig3. Systemic AZ assembly defects in *unc-104^{bris}* mutant NMJs. (A-C) Confocal images of *Drosophila* NMJs immunostained with synaptic proteins. Synapses were marked by GluRIIC staining (Red), shown in the first row of each group. (A) Cac^{2+} channel clustering at AZs in wildtype control, *unc-104^{bris}* and *brp-RNAi* larvae expressing Cac-GFP. Brp(-) synapses in *unc-104^{bris}* animals are also devoid of Cac^{2+} channel (arrows). In contrast, Brp(-) synapses in Brp-RNAi animals are mostly Cac-GFP positive (arrowheads). (B) Liprin- α clustering at AZs in wildtype control, *unc-104^{bris}* and *brp-RNAi* larvae expressing Liprin- α -GFP. Liprin- α -GFP does not localize to Brp(-) synapses in *unc-104^{bris}* animals (arrows), whereas in *brp-RNAi* animals Liprin- α -GFP is evident at Brp(-) synapses (arrowheads). (C) SRPK79D localization at AZs in wildtype control, *unc-104^{bris}* and *brp-RNAi* larvae expressing SRPK79D-GFP. SRPK79D did not concentrate at Brp(-) synapses in *unc-104^{bris}* group (arrows). At *brp-RNAi* NMJs, SRPK79D also failed to concentrate at Brp(-) synapses (open arrowheads); large aggregation of SRPK79D-GFP is evident in the bouton (open arrows). Bar, 2 μ m. (D) Confocal images of *Drosophila* NMJs immunostained with GluRIIC (red) and Brp (blue & grey) in *unc-104^{bris}*, *unc-104^{bris};brp-RNAi* and *unc-104^{bris};brp-OE* larvae expressing Cac-GFP. Arrows: [Brp(-), Cac(-)] synapses; open arrows: [Brp(-), Cac(+)] synapses; arrowheads: [Brp(-), Cac(+)] synapses; open arrowheads: [Brp(+), Cac(-)] synapses. (E) Quantification of Brp(-) synapses and Cac(-) synapses in groups stated in (D). Brp-RNAi doubled the percentage of Brp(-) synapses in *unc-104^{bris}* mutant NMJs, while *brp-OE* decreased it by half (*unc-104^{bris}* vs. *unc-104^{bris};brp-RNAi*: $P < 0.001$; *unc-104^{bris}* vs. *unc-104^{bris};brp-OE*: $P < 0.001$). Brp-RNAi did not change the percentage of Cac(-) synapses in *unc-104^{bris}* mutant NMJs, while *brp-OE* decreased it mildly (*unc-104^{bris}* vs. *unc-104^{bris};brp-RNAi*: $P > 0.05$; *unc-104^{bris}* vs. *unc-104^{bris};brp-OE*: $P < 0.05$). Number of NMJs quantified in (E): *unc-104^{bris}*: N=8; *unc-104^{bris};brp-RNAi*: N=7; *unc-104^{bris};brp-OE*: N=8. Experiments performed at 29 °C. Statistical test: One-way ANOVA followed by Dunnett's Multiple Comparison Test. *, $P < 0.05$; *** $P < 0.001$; n.s., $P > 0.05$. Error bars indicate the SEM.

synapses was examined. Mid third instar stage larvae were co-stained with GluRIIC as marker for PSD and the presynaptic AZ marker Brp. The examined AZ proteins colocalized tightly with Brp in *unc-104^{bris}* mutant NMJs (Fig. 3 A-C). Brp(-) synapses at *unc-104^{bris}* mutant NMJs were also negative for Cac, Liprin- α and SRPK79D (Fig. 3 A-C, arrows), and Brp(+) synapses were positive for the examined AZ proteins. Thus the Brp(-) synapses at *unc-104^{bris}* mutant NMJs virtually did not contain any of the examined, essential AZ components. These results reveal that AZ assembly is abolished at a subset of synapses in *unc-104^{bris}* mutant larvae.

4.1.3 The *unc-104^{bris}* mutation perturbs a mechanism regulating AZ assembly

Brp has been proposed to play a central role in AZ assembly in *Drosophila* neuromuscular synapses (Fouquet et al., 2009). Cac shows very tight colocalization with Brp in Rab3 mutant larvae where the distribution of presynaptic Brp puncta at the neuromuscular synapses is limited to a small subset of synapses (Graf et al., 2009). It is not known yet how Brp affects the localization of Liprin- α and SRPK79D. The systemic AZ assembly defect in *unc-104^{bris}* mutant synapses is possibly secondary of altered Brp localization or rather consequence of the perturbation of a mechanism regulating the clustering of all examined proteins at the AZ.

In order to elucidate how Brp affect the localization of other AZ proteins, we decreased the level of Brp at *Drosophila* NMJs by pan-neural expression of a *brp*-RNAi construct driven by the *elav*-Gal4 driver in larvae coexpressing GFP-tagged AZ proteins. Brp knockdown resulted in large population of synapses unapposed by Brp (solid arrowheads in Fig. 3 A, B, and open arrowheads in Fig. 3 C). Unlike *unc-104^{bris}* mutants, the Brp(-) synapses in *brp*-RNAi larvae are clearly positive for Cac and Liprin- α (Fig. 3 A, B, arrowheads). These results show that localization of Cac and Liprin- α to AZ is not dependent on Brp, thus it is unlikely that the coincidental absence of Cac and Liprin- α with Brp at a subpopulation of *unc-104^{bris}* mutant synapses is secondary of the absence of Brp at these synapses.

In *brp*-RNAi larvae, SRPK79D-GFP signal was still present across the bouton and concentrated at Brp(+) synapses, but it showed poor enrichment at Brp(-) synapses (Fig. 3 C, open arrowheads). Large cloud of SRPK79D-GFP with strong signal was evident in the bouton (Fig. 3 C, open arrows), possibly a sign of self-aggregation due to the absence of AZ localizing signal. These results suggest that the association with Brp is instrumental for SRPK79D's AZ localization.

To further examine the nature of coincidental Brp and Cac localization at *unc-104^{bris}* mutant synapses, we modulated Brp quantity in *unc-104^{bris}* mutant larvae expressing Cac-GFP. Decreasing Brp quantity by a *brp*-RNAi construct doubled the percentage of Brp(-) synapses in *unc-104^{bris}* mutant NMJs, resulting ~ 60% of synapses unapposed by presynaptic Brp puncta (Fig. 3 E); however no change in the percentage of Cac(-) synapses between *unc-104^{bris}* and *unc-104^{bris}*;Brp-RNAi larvae was observed (Fig. 3 F). Actually in *unc-104^{bris}*;Brp-RNAi larvae there were large number of synapses having Cac but devoid of Brp (Fig. 3 D, arrowheads). However, it is noteworthy that the size of these Cac puncta at Brp(-) synapses were significantly smaller than those at Brp(+) synapses (open arrows), suggesting that Brp plays a role in maintaining the normal quantity, but not the presence of Cac at the AZ. Brp overexpression in *unc-104^{bris}* larvae decreased the percentage of Brp(-) synapses (Fig. 3 E); There was also a decrease in Cac(-) synapses upon Brp overexpression (Fig. 3 F), which might be due to an increase in overall activity upon Brp-OE. Brp(+), Cac(-) synapses are evident in *unc-104^{bris}*;brp-OE NMJs (Fig. 3 D, open arrowheads).

Taken together, the absence of AZ proteins at a subset of synapses in *unc-104^{bris}* mutants is not secondary of Brp mislocalization. A mechanism controlling the assembly of synaptic proteins at AZ is disrupted by the *unc-104^{bris}* mutation.

4.1.4 Impaired synaptic functions in the *unc-104^{bris}* mutant

To assess the effect of the *unc-104^{bris}* mutation on synaptic function, current clamp recording on mid third-instar stage larval NMJ was performed. Evoked excitatory

junctional potentials (EJPs) were severely impaired in *unc-104^{bris}* mutants compared with controls (Fig. 4 A, B). These were fully rescued by pan-neural expression of wild type *unc-104* cDNA driven by the elav-Gal4 driver.

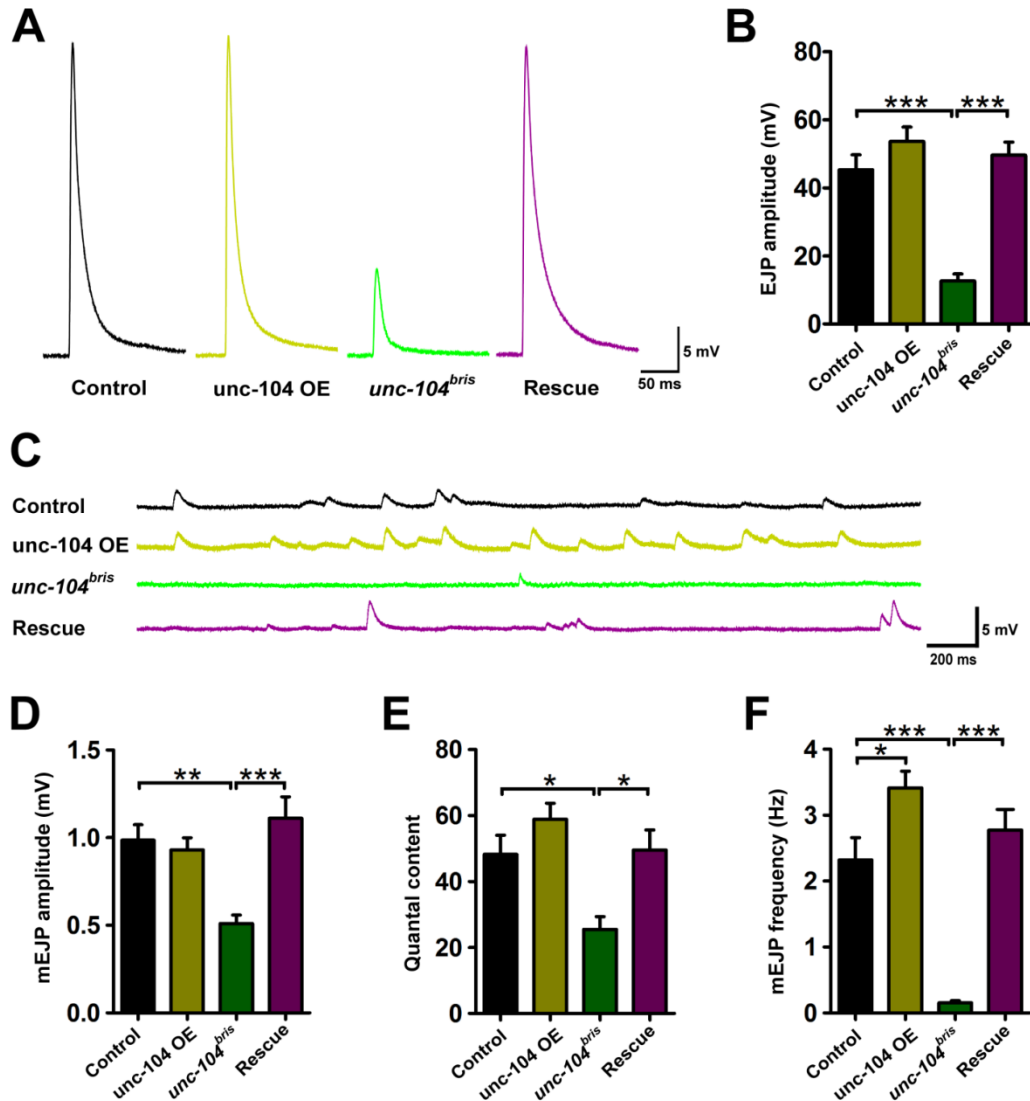


Fig4. Impaired synaptic transmission in *unc-104^{bris}* mutant NMJs. (A) and (C), Representative traces of evoked release and spontaneous release recorded from wildtype control, Unc-104-OE, *unc-104^{bris}* and *unc-104^{bris}*-Rescue group. (B) and (D-F) Quantification of average EJP amplitude, mEJP amplitude, quantal content and mEJP frequency in the same groups. *unc-104^{bris}* mutant NMJs showed significant reduction in all of the four quantified parameters, and these were rescued by pan-neural expression of *unc-104*-mcherry induced by the elav-gal4 driver. Neural overexpression of *unc-104* in an otherwise wildtype background increased mEJP frequency compared with wildtype NMJs. 6-11 NMJs were quantified for each group. Martin's correction for nonlinear summation (see material and methods) was applied for EJPs shown in (B) and for calculating quantal content. Statistical test: One-way ANOVA followed by Tukey's Multiple Comparison Test. *, P<0.05; **, P<0.01; ***P<0.001; n.s., P>0.05. Error bars indicate the SEM.

Spontaneous activity was also assessed by measuring the amplitude and frequency of miniature excitatory junctional potentials (mEJPs). Compared with controls, mEJP frequency was dramatically decreased in *unc-104^{bris}* mutant NMJs (Fig. 4 C, F); mEJP amplitudes were also significantly reduced in *unc-104^{bris}* mutants (Fig. 4 C, D). Both the decrease in mEJP frequency and mEJP amplitude were restored by pan-neural expression of *unc-104* cDNA. Interestingly, *unc-104* overexpression in an otherwise wildtype background led to higher mEJP frequency than wildtype (Fig. 4 C, F).

We also calculated quantal content, which is an estimation of synaptic vesicles released at evoked release event. Quantal content of *unc-104^{bris}* mutant NMJs decreased by half compared with control, implying significantly less synaptic vesicles being released at evoked event. Quantal content reduction in *unc-104^{bris}* mutant was also rescued by pan-neural reexpression of *unc-104* cDNA (Fig. 4 E). Taken together, *unc-104^{bris}* mutation caused significant reduction in both spontaneous and evoked synaptic activity, leading to severe impairment of synaptic function at *Drosophila* NMJs.

4.1.5 Defects in postsynaptic maturation in the *unc-104^{bris}* mutant

Crosstalk between pre- and postsynaptic compartments is essential in coordinating synaptic function. Presynaptic abnormality is almost inevitably associated with postsynaptic changes (Graf et al., 2009; Oswald et al., 2010), which may either reflect a reaction to lesion or a complimentary response to maintain synaptic transmission. Observing the distinct AZ assembly phenotype and change in synaptic activity in *unc-104^{bris}* mutants, it is interesting to know if there are also postsynaptic abnormalities caused by this mutation. Two types of ionotropic glutamate receptors have been identified at the *Drosophila* neuromuscular synapses, the IIA-type and the IIB-type, which differ in their subunit composition. Apart from the three compulsory subunits (GluRIIC, GluRIID and GluRIIE), they either contain GluRIIA or GluRIIB as a fourth subunit to form a functional heterotetrameric receptor. The IIA- and IIB-type glutamate

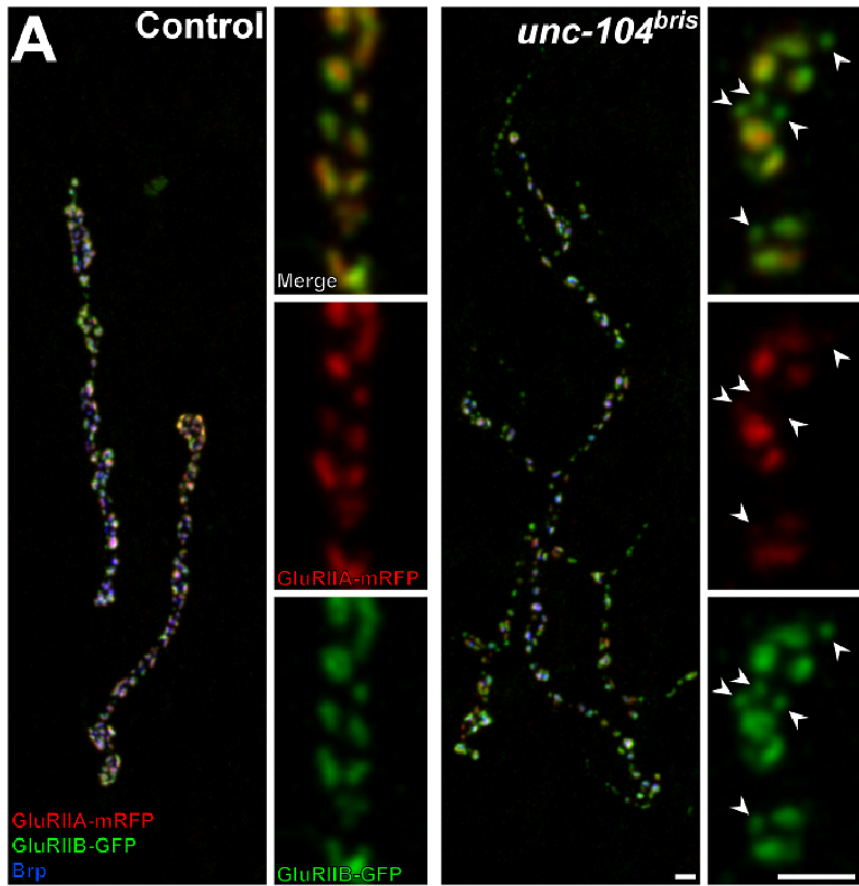
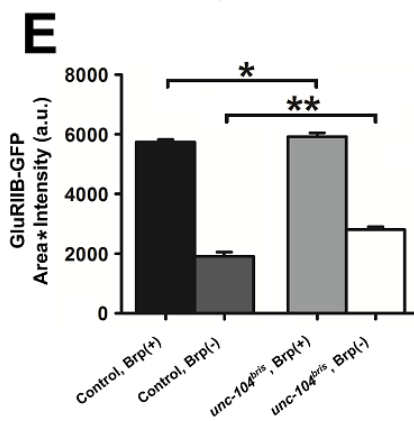
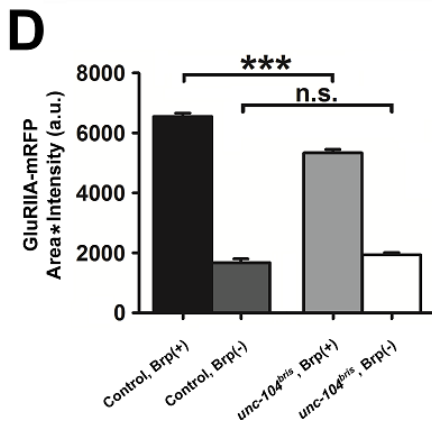
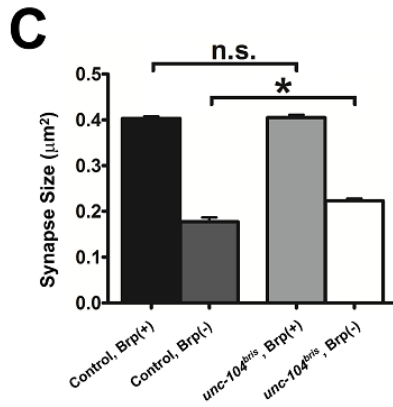
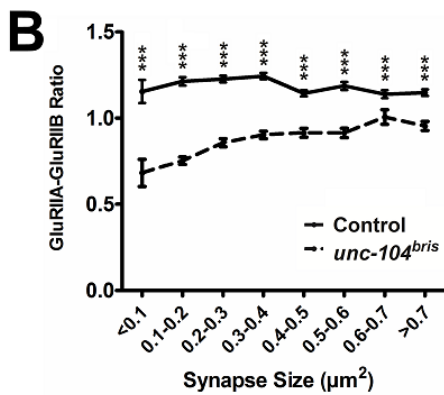


Fig5. Glutamate receptor composition in control and *unc-104^{bris}* mutant animals. (A) Confocal images of neuromuscular synapses stained with Brp (blue) in control and *unc-104^{bris}* mutant larvae expressing GluRIIA-mRFP (red) and GluRIIB-GFP (green). GluRIIA was reduced in *unc-104^{bris}* mutant synapses (arrowheads). Bars, 2 μ m. **(B-D)** Quantification of GluRIIA-mRFP intensity, GluRIIB-GFP intensity and GluRIIA/ GluRIIB ratio at PSDs in control and *unc-104^{bris}* mutant NMJs, grouped by synapse size. **(B)** GluRIIA-mRFP intensity in *unc-104^{bris}* was significantly lower than control in all size groups. **(C)** In contrast, GluRIIB intensity in control and *unc-104^{bris}* mutants PSDs were very similar. Synapses in the 0.2-0.3 μ m², 0.3-0.4 μ m² and 0.5-0.6 μ m² groups at *unc-104^{bris}* mutant NMJs showed slightly higher GluRIIB-GFP intensity than control in corresponding groups. **(D)** As a result, *unc-104^{bris}* mutant PSDs showed lower GluRIIA/ GluRIIB ratio in all size groups. For (B-D), Number of synapses analyzed: N \geq 48 for all size groups. **(E)** PSD size of Brp(+) and Brp(-) synapses in control and *unc-104^{bris}* mutants. The average PSD size of Brp(-) synapses in *unc-104^{bris}* mutants was greater than that of Brp(-) synapses in control (control: 0.177 \pm 0.009 μ m² [n=118]; *unc-104^{bris}*: 0.223 \pm 0.005 μ m² [n=766]. P<0.01); no significant difference was observed in Brp(+) synapses between control and *unc-104^{bris}* mutants (control: 0.403 \pm 0.005 μ m² [n=2310]; *unc-104^{bris}*: 0.405 \pm 0.006 μ m² [n=1091]. P>0.05). Statistical test: Mann-Whitney test. *, P<0.05; **, P<0.01; ***P<0.001; n.s., P>0.05. Error bars indicate the SEM.



receptors exhibit very distinct electrophysiological properties (DiAntonio et al., 1999; Marrus et al., 2004; Petersen et al., 1997; Qin et al., 2005). Every neuromuscular synapse contains a mixture of IIA- and IIB-type glutamate receptors.

We expressed mRFP-tagged GluRIIA and GFP-tagged GluRIIB together in control and *unc-104^{bris}* mutant larvae and investigated their localization at neuromuscular synapses. GluRIIA localization at *unc-104^{bris}* mutant synapses was severely impaired-- there was a significant reduction of GluRIIA-mRFP intensity in *unc-104^{bris}* mutant synapses compared with wildtype control, which was especially pronounced in small synapses (Fig. 5 A, arrowheads and B). The localization of GluRIIB appeared grossly normal in *unc-104^{bris}* mutants (Fig. 5 A, arrowheads and C).

It is reported that the receptor composition changes during the development of *Drosophila* neuromuscular synapse: immature synapses are typically rich in IIA-type receptors, whereas the two types of receptors are balanced as synapses mature (Schmid et al., 2008). We quantified the IIA/IIB ratio and found that consistent with reported, the small synapses in control group appeared slightly “IIA-rich” compared with mature ones which had more balanced GluRs (Fig. 5 D). Synapses in *unc-104^{bris}* mutants lost the normal IIA/IIB ratio, and became overall IIB-rich. Small synapses in the *unc-104^{bris}* mutant larvae showed the strongest deviation from the normal IIA/IIB ratio; bigger synapses demonstrated higher IIA/IIB ratio, yet still being significantly lower than synapses of the same size in control (Fig. 5, D).

The change in GluR composition in *unc-104^{bris}* mutant synapses is consistent with the reduction in mEJP amplitude, as the IIA-type receptors has higher single channel conductance than IIB-type ones (DiAntonio et al., 1999). Because properly controlled GluR receptor composition at synapse is important for normal synaptic function, the altered GluR incorporation in *unc-104^{bris}* mutant synapses demonstrates a previously unknown role of Kinesin/Unc-104 in regulating PSD maturation.

4.1.6 Impaired axonal transport at the NMJ in *unc-104^{bris}* mutant

Kinesin-3/Unc-104 is a very important neuronal motor protein. Previous studies have shown that *unc-104* null mutants have severe defect in dense core vesicles (DCV) and SVs transport (Pack-Chung et al., 2007). Two unmapped hypomorphic alleles of *unc-104* lead to larval lethality at late larval or pupal stage, showing similar impairment in DCV transport but with no obvious abnormality in mitochondria localization (Barkus et al., 2008). In rat primary hippocampus neuron cultures, shRNA knockdown of *kif1a* leads to very similar axonal transport abnormality with *unc-104* hypomorphs in flies (Lo et al., 2011). Interaction between the FHA domain and CC2 domain of Unc-104/KIF1A has been shown to be important for the regulation of its monomer-to-dimer transition, microtubule binding as well as processability (Lee et al., 2004). It is interesting to know how the disruption of FHA domain by the *unc-104^{bris}* mutation affects the transport of cargoes to NMJs.

Localization of SV and SV associated protein Rab3 at the NMJ were first examined. Mid third instar larvae were stained with the *Drosophila* vesicular glutamate transporter (DVGlut) antiserum as a marker for SV (Daniels et al., 2004). HRP staining was used to mark neuronal membrane. In control NMJs, intense DVGlut signal marked SVs filling entire synaptic boutons (Fig. 6 A); distribution of Rab3 is very similar with SV (Fig. 6 C). In *unc-104^{bris}* mutants which there were much thinner NMJ branches and smaller boutons, DVGlut staining became very low and was almost undetectable at some distal segments where the NMJ was particularly thin and boutons scarcely formed (Fig. 6 A, arrows and B). The same sharp reduction also held true for Rab3 immunoreactivity in *unc-104^{bris}* mutant NMJs (Fig. 6 C arrows and D). The above results proved that the *unc-104^{bris}* mutation disrupted the function of Unc-104 in maintaining the normal localization of SV and SV associated proteins at the NMJ. Notably, the reduction in SV as well as Rab3, which is implicated in SV recycling, is also consistent with reduced quantal content in evoked release (Fig. 4 E).

We next examined the localization of DCV and mitochondria to the NMJs. ANF-GFP and Mito-GFP have been shown to mark neuropeptide containing DCVs and mitochondria respectively (Rao et al., 2001); these constructs were driven by the D42-

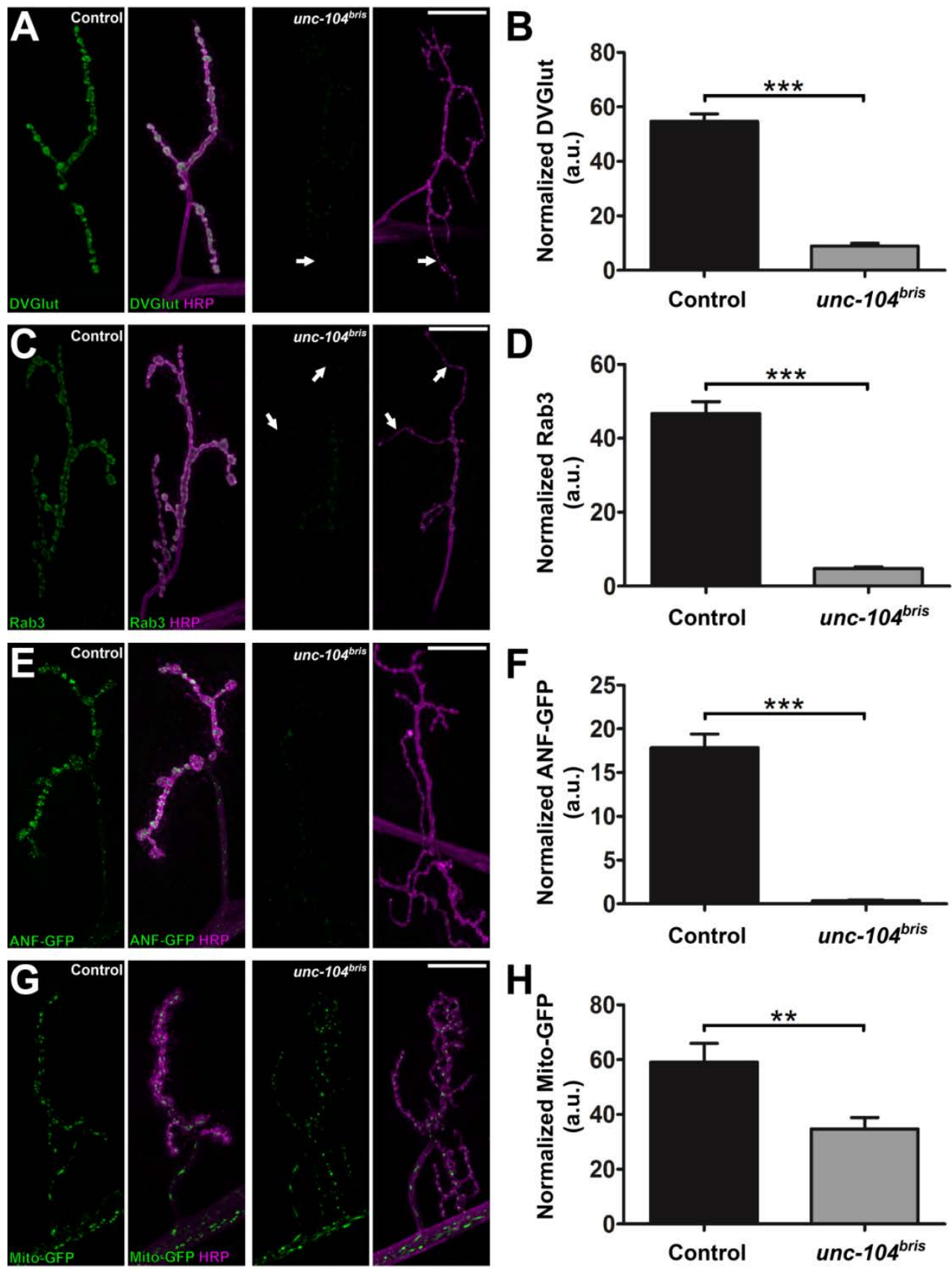


Fig6. Effect of the *unc-104^{bris}* mutation on the localization of different synaptic protein and organelles at the NMJ. (A) Confocal images of NMJs stained with DVGlut as a marker for SVs in wildtype control and *unc-104^{bris}* mutants. Neuronal membrane was labeled by HRP (magenta). The number and density of SVs reduced dramatically at *unc-104^{bris}* mutant NMJs. **(B)** Quantification of DVGlut at the NMJs shown in (A), normalized by HRP area (control: 54.70 ± 2.75 a.u.; *unc-104^{bris}*: 8.92 ± 1.04 a.u.. $P < 0.001$). **(C)** Similar with (A), Rab3 (green) quantity also dropped very significantly at *unc-104^{bris}* mutant NMJs. **(D)** Quantification of Rab3 at the NMJs shown in (C), normalized by HRP area (control: 46.69 ± 3.25 a.u.; *unc-104^{bris}*: 4.77 ± 0.46 a.u.. $P < 0.001$). **(E)** and **(G)**, confocal images of NMJs in control and *unc-104^{bris}* mutant larvae expressing ANF-GFP (Green, in E) or Mito-GFP (Green, in G) induced by the D42-Gal4 driver. ANF-GFP was barely present in *unc-104^{bris}* mutant NMJs, in contrast with its affluent abundance in control NMJs. Mito-GFP localization was only mildly affected in *unc-104^{bris}* mutant NMJs. **(F)** and **(H)**, quantification of ANF-GFP and Mito-GFP at the NMJ as shown in (E) and (G), normalized by HRP area. ANF-GFP in *unc-104^{bris}* mutant NMJs dropped to only 2% of that in control (control: 17.84 ± 1.56 a.u.; *unc-104^{bris}*: 0.34 ± 0.10 a.u.. $P < 0.001$); Mito-GFP affluence in *unc-104^{bris}* mutant NMJs also decreased, but to a far lesser extent (control: 59.09 ± 6.84 a.u.; *unc-104^{bris}*: 34.77 ± 4.13 a.u.. $P < 0.01$). $N = 9-13$ NMJs in each group. Statistical test: Student's t test. **, $P < 0.01$; ***, $P < 0.001$. Error bars indicate the SEM.

Gal4 driver which predominantly expresses in motor neurons. Mid third instar stage larvae were stained with HRP as neuronal membrane marker, and subjected to confocal imaging. ANF-GFP positive DCVs were abundant in wildtype NMJs, while in *unc-104^{bris}* mutant NMJs the signal was extremely compromised, dropped to merely about 2% of wildtype (Fig. 6 E, F). Mitochondria quantity normalized by HRP area at *unc-104^{bris}* mutant NMJs also dropped by about 40% when compared with wildtype (Fig. 6 G, H). All in all, the *unc-104^{bris}* mutation in the FHA domain severely disrupted the normal function of the Kinesin-3 and led to drastic reduction in the delivery of multiple important cargos to the NMJ.

4.1.7 Overexpression of Rab3 ameliorate the AZ assembly phenotype in *unc-104^{bris}* mutants

Rab3 has been shown to regulate presynaptic AZ assembly in *Drosophila* neuromuscular synapses; *rab3* mutant and *unc-104^{bris}* mutant NMJs share the similarity that AZs formation is impaired in a subset of synapses (Graf et al., 2009). As Rab3 localization at the NMJs was severely reduced in *unc-104^{bris}* mutant (Fig. 6 C, D), it is possible that the reduced Rab3 is involved in the AZ assembly phenotype in the *unc-104^{bris}* mutant. In order to test this possibility, *rab3* cDNA was expressed using the pan-neuronal driver *elav-Gal4* in *unc-104^{bris}* mutant larvae (Fig. 7).

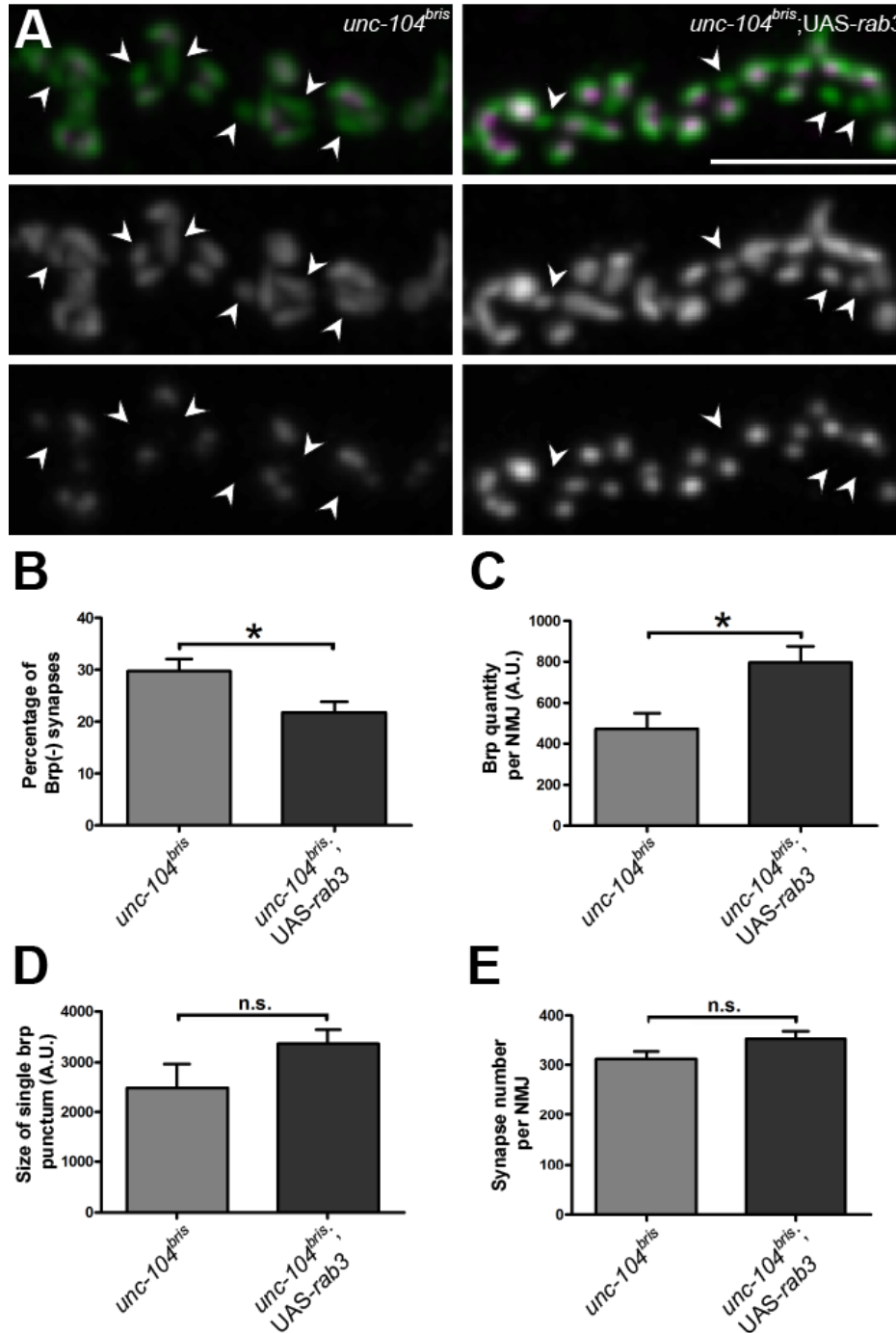


Fig7. Rab3 overexpression partially rescues the AZ assembly defect in *unc-104^{bris}* mutants. (A) Confocal images of neuromuscular junctions immunostained with presynaptic active zone protein Brp and PSD marker GluRIIC in *unc-104^{bris}* and *unc-104^{bris};UAS-rab3* larvae. Expression was induced by the pan-neural driver elav-Gal4. Arrows indicate synapses devoid of presynaptic Brp puncta. Bar, 5 μ m. (B-E) Quantification of the percentage Brp(-) synapses (B), total Brp quantity per NMJ (C), average presynaptic punctum Brp size (Area \times Intensity) (D), as well as synapse number per NMJ (E) in groups demonstrated in (A). Number of NMJs quantified in (B-E): N = 8. Statistical test: student's t test. *, P < 0.05; n.s., P > 0.05. Error bars indicate the SEM.

Rab3 overexpression in the *unc-104^{bris}* mutant background reduced the percentage of Brp(-) synapses by about 30% percent (Fig. 7, A, B). It is proposed that Rab3 regulate AZ assembly by increasing the probability that Brp clusters at the AZ. In *rab3* mutant NMJs, the quantity of overall Brp is not different compared with wildtype, however Brp concentrates at a subset of synapses, forming “super AZs” at these site while leaving the other presynaptic site apparently empty (Graf et al., 2009). The effect of Rab3 overexpression in reducing the abundance of Brp(-) synapses at *unc-104^{bris}* mutant NMJ could also possibly be the result of a similar effect, i.e. by redistributing the available Brp at the NMJ more among more synapses but leaving the total Brp quantity at the NMJ unaltered. Surprisingly, Rab3 overexpression strongly increased the total Brp quantity at *unc-104^{bris}* mutant NMJs by almost 70% (Fig. 7, C). Rab3 reexpression in *rab3* mutant NMJs leads to disperse of “super AZs” and even redistribution of Brp among presynaptic sites, and hence reduces average AZs size (Graf et al., 2009). However, no detectable change in AZ size was found in *unc-104^{bris}* mutants with Rab3 overexpression; actually there was even a mild trend of increasing Brp puncta size by Rab3 overexpression, but it was not statistically significant (Fig. 7).

Taken together, these results show that Rab3 overexpression ameliorates the AZ assembly phenotype in *unc-104^{bris}* mutants. Rab3 overexpression strongly increased overall Brp quantity at *unc-104^{bris}* mutant NMJs, while had little effect on AZ size.

4.1.8 Impaired synaptic activity contribute little to the AZ assembly phenotype in *unc-104^{bris}* mutants

Synaptic activity has been shown to play a role both in modifying synaptic strength in mature synapses as well as in regulating synaptic development (Ataman et al., 2008; Rebola et al., 2010; Samson and Pare, 2005). As there was severe impairment of synaptic activity in *unc-104^{bris}* mutant NMJs (Fig. 4), we also sought to test if the decreased synaptic activity played a role in leading to the AZ assembly phenotype.

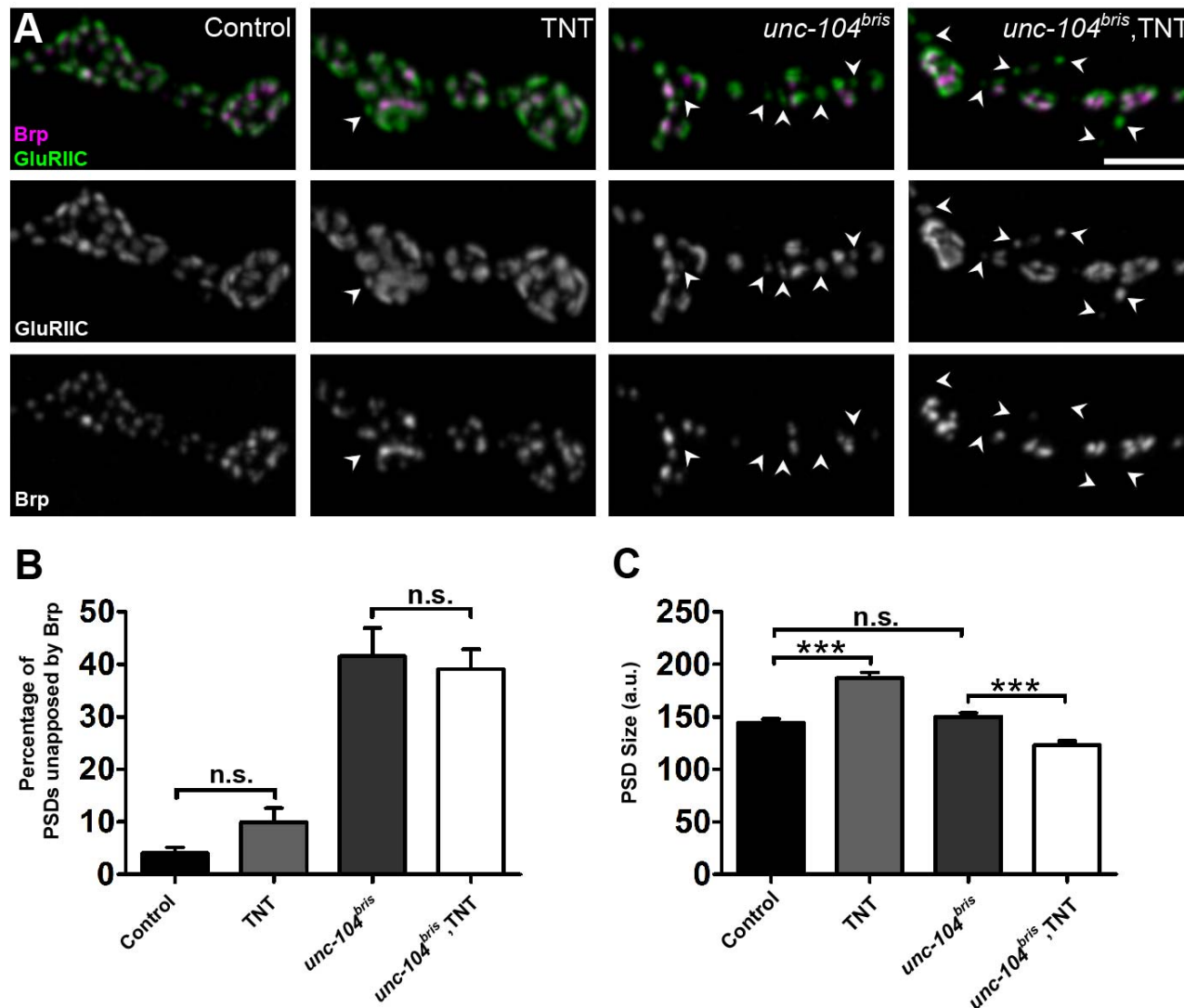


Fig8. Effect of blocking synaptic transmission on synaptic development. (A) Confocal images of neuromuscular junctions immunostained with presynaptic active zone protein Brp and PSD marker GluRIIC in larvae of the following four groups: control, TNT, *unc-104^{bris}* and *unc-104^{bris},TNT*. Expression was induced by the motor neuron specific driver OK319-Gal4. Arrows indicate synapses devoid of presynaptic Brp puncta. Bar, 5 μ m. (B-C) Quantification of the percentage of PSDs unapposed by presynaptic Brp (B) and average PSD size in terms of GluRIIC area in groups demonstrated in (A). Number of NMJs quantified in B: N=4 for all groups. Number of PSDs quantified in C: N>650 for all groups. Statistical test: For B, One-way ANOVA followed by Tukey's multiple comparison test. For C, Kruskal-Wallis test followed by Dunn's multiple comparison test. ***, P<0.001; n.s., P>0.05. Error bars indicate the SEM.

Tetanus toxin (TNT) cleaves Synaptobrevin and blocks synaptic vesicle fusion. In *Drosophila*, neuronal expression of tetanus toxin has been used as a tool to effectively block synaptic transmission (Schmid et al., 2008).

Using the motor neuron specific driver OK319-Gal4, TNT was expressed in an otherwise wildtype or *unc-104^{bris}* mutant background. At 25°C, expressing TNT in wildtype larvae led to strikingly reduced locomotion speed and lethality at late larval stage. However, despite the severely impaired behavior, NMJ development was grossly normal in TNT expressing larvae (Fig. 8 A, B). There was a mild tendency of increased abundance of Brp(-) synapses in TNT expressing larvae, however it was not statistically significant (Fig. 8 B).

Interestingly, an increase in PSD size was observed in TNT expressing NMJs. Expressing TNT in *unc-104^{bris}* mutant larvae further worsened the already impaired larval movement. TNT expression in the *unc-104^{bris}* mutant background also did not alter the abundance of Brp(-) synapses. Unlike the case of TNT expression at wildtype background, TNT expression at *unc-104^{bris}* mutant background led to reduced PSD size (Fig. 8 C), implying that the postsynaptic compensatory mechanism of increasing PSD size upon blocking synaptic vesicle release is abolished in *unc-104^{bris}* mutants. Actually the average PSD size between wildtype control and *unc-104^{bris}* mutant were also not different, despite the difference in synaptic activity (Fig. 8 C).

Taken together, blocking synaptic transmission does not have an obvious effect of affecting AZ assembly. TNT expression at neither wildtype background nor *unc-104^{bris}* mutant background leads to worsened active zone assembly, thus synaptic activity likely contribute little to the presynaptic AZ assembly phenotype at *unc-104^{bris}* mutant NMJs.

4.2 Overactivation of the Wnd MAPK pathway leads to the synaptic development phenotypes in *unc-104^{bris}* mutant

A series of work identified an MAPK signaling cascade which controls NMJ growth in *Drosophila* (Collins et al., 2006; Tian et al., 2011; Wan et al., 2000; Xiong et al., 2010). Highwire (Hiw), which is an E3 ubiquitin ligase, has been shown to be a negative regulator of this MAPK pathway (Collins et al., 2006). Mutation in the *hiw* gene leads to very similar NMJ morphology with *unc-104^{bris}* mutants including elongated NMJ and much smaller synaptic bouton (Wan et al., 2000). Hiw inhibits MAPK pathway through downregulating the level of a dual leucine zipper kinase (DLK) homolog, Wallenda (Wnd). Loss of function mutation in *wnd*, expression of a dominant negative form of JNK homolog Basket (Bsk^{DN}), as well expression of a dominant negative form of a downstream JNK effector Fos (Fos^{DN}) have similar effect of inhibiting the NMJ overgrowth phenotype in *hiw* mutants (Collins et al., 2006). We sought to investigate if this MAPK pathway also plays a role in the *unc-104^{bris}* mutant phenotype.

4.2.1 Downregulation of a MAPK signaling pathway rescues NMJ overgrowth in *unc-104^{bris}* mutant

We first investigated the effect of *wnd* mutation on the NMJ overgrowth phenotype in *unc-104^{bris}* mutants. Loss of function mutations in *wnd* were combined with *unc-104^{bris}* mutation and NMJ morphology was assessed in double mutant larvae. Compared with *unc-104^{bris}* mutant larvae, NMJ length was dramatically reduced in *unc-104^{bris};wnd* double mutant larvae (fig. 9 A, B). Importantly, compared with wildtype control, *wnd* mutation itself did not show an effect of limiting NMJ growth (fig. 9 A, B, compare “Control” with “*wnd*”), thus the inhibition of NMJ overgrowth in *unc-104^{bris}* by *wnd* mutation is due a specific inhibition rather than a general effect.

Next, the effect of disrupting JNK and Fos function on the NMJ overgrowth phenotype of *unc-104^{bris}* mutants was tested. In the *Drosophila* genome, there is a single JNK gene, *basket* (*bsk*). A T181A mutation in *bsk* produces a nonphosphorylatable dominant

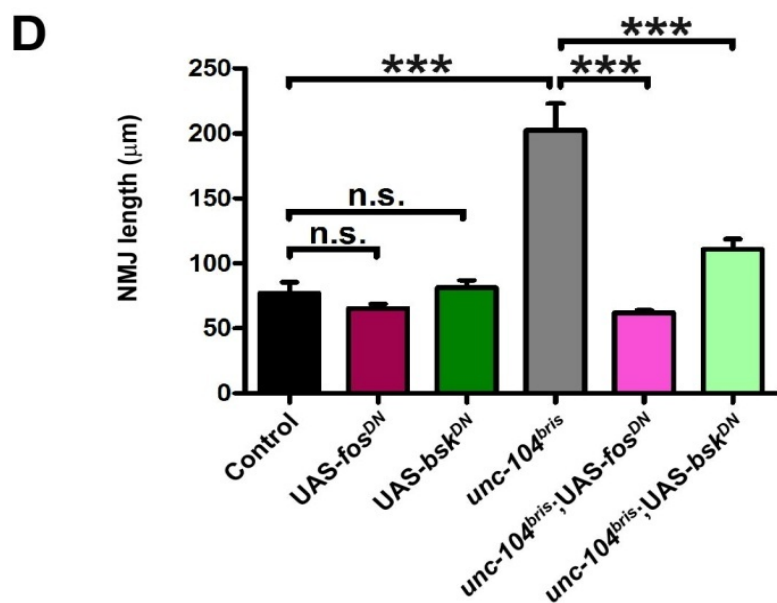
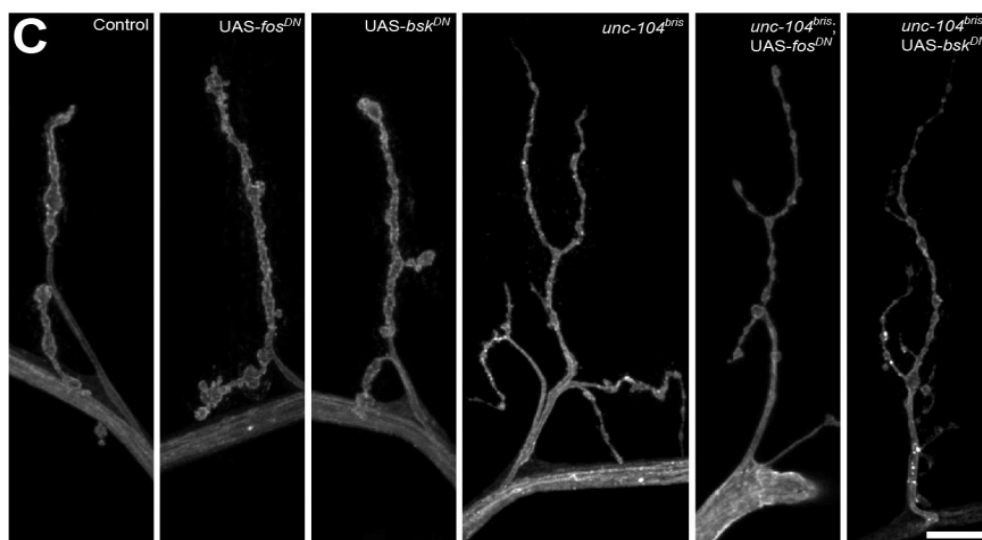
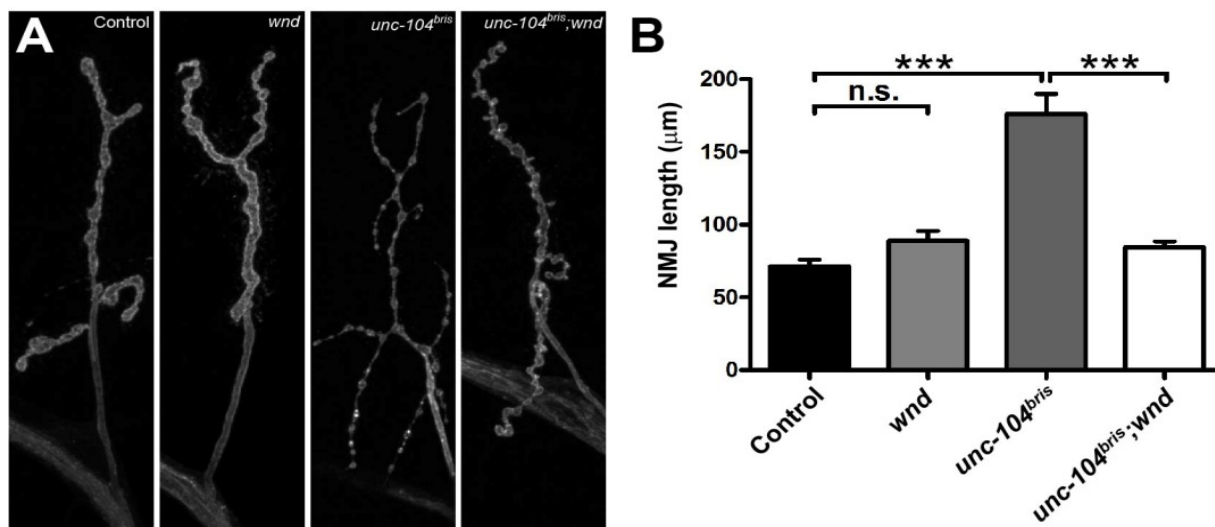


Fig9. **Downregulating MAPK pathway rescues the NMJ overgrowth phenotype in *unc-104^{bris}* mutants.** (A) and (C), Confocal images of neuromuscular junctions immunostained with HRP antiserum labeling neuronal membrane in larvae of the following four groups for (A): control, *wnd*, *unc-104^{bris}* and *unc-104^{bris};wnd*, and the following six groups for (C): control, UAS-*fos^{DN}*, UAS-*bsk^{DN}*, *unc-104^{bris}*, *unc-104^{bris};UAS-*fos^{DN}** and *unc-104^{bris};UAS-*bsk^{DN}**. Expression was induced by the motor neuron specific driver OK319-Gal4. Bar, 5µm. (B) and (D), Quantification of NMJ length in groups shown in (A) and (C), respectively. Number of NMJs quantified in B and D: N>=8 for all groups. Statistical test: One-way ANOVA followed by Tukey's multiple comparison test. ***, P<0.001; n.s., P>0.05. Error bars indicate the SEM.

negative form of this MAPK (*Bsk^{DN}*) (Adachi-Yamada et al., 1999). A truncated form of Fos with the DNA binding domain and dimerization domain, but lacking the transcriptional activation domain results in a dominant negative form of Fos (*Fos^{DN}*) (Eresh et al., 1997). The motor neuron specific driver OK319-Gal4 was used to induce the expression of *Bsk^{DN}* and *Fos^{DN}* each in an otherwise wildtype or *unc-104^{bris}* mutant background. Expression of *bsk^{DN}* and *Fos^{DN}* both significantly reduced the NMJ length in *unc-104^{bris}* mutant larvae (Fig. 9 C, D). Similar with the effect of *wnd* mutant, disrupting JNK or Fos function in wildtype background also did not result in decreased NMJ length (Fig. 9 C, D).

The above results demonstrated that downregulating the Wnd MAPK pathway had a potent and specific effect of inhibiting the NMJ overgrowth phenotype in *unc-104^{bris}* mutants.

4.2.2 Downregulation of the Wnd MAPK pathway also rescued the AZ assembly phenotype in *unc-104^{bris}* mutant

Observing that the NMJ overgrowth phenotype in the *unc-104^{bris}* mutant can be inhibited by downregulation of the Wnd MAPK pathway, it is interesting to know if the synaptic assembly phenotype in *unc-104^{bris}* mutant can also be rescued by Wnd MAPK pathway downregulation.

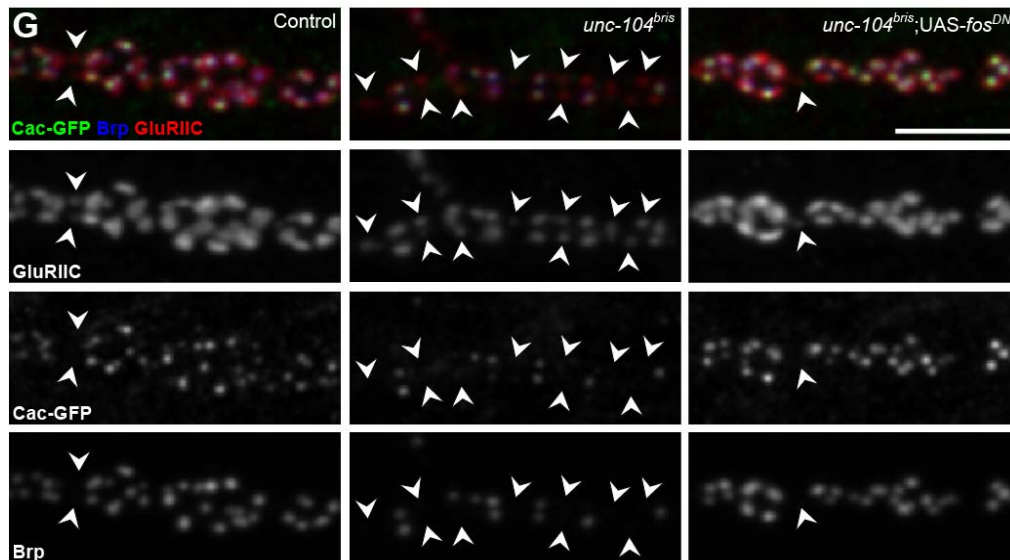
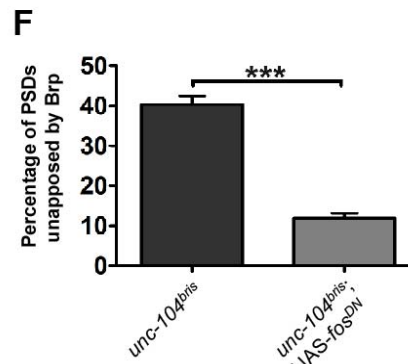
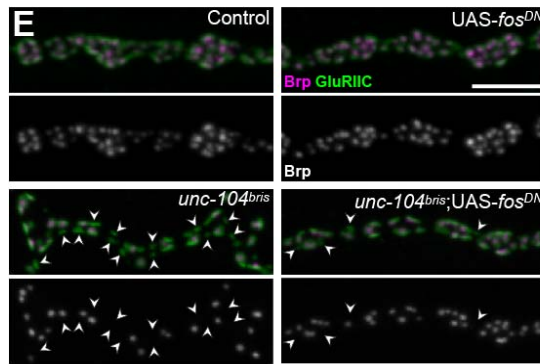
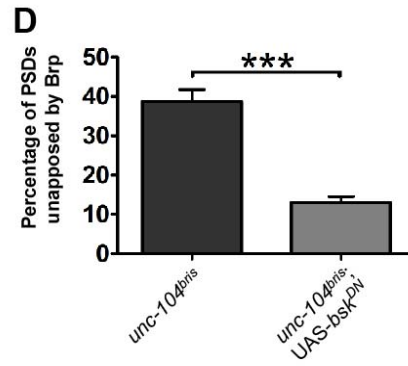
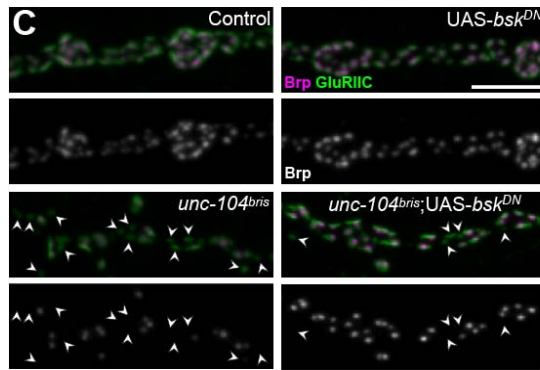
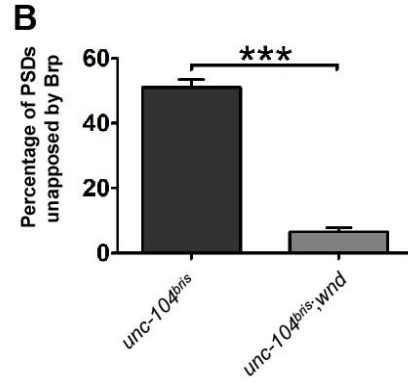
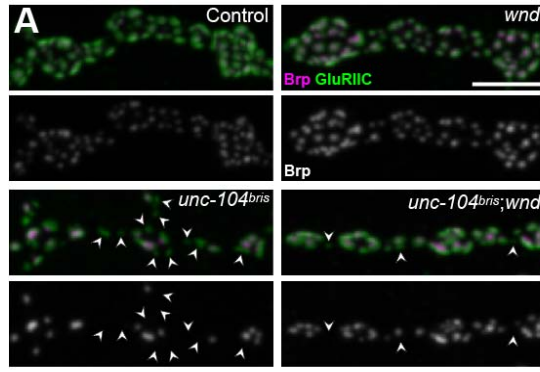


Fig10. Downregulating MAPK pathway inhibits the AZ assembly phenotype in *unc-104^{bris}* mutants. (A), (C) and (E), confocal images of neuromuscular junctions immunostained with the presynaptic active zone protein Brp and PSD marker GluRIIC in larvae of the following four groups for (A): control, *wnd*, *unc-104^{bris}* and *unc-104^{bris};wnd*, and the following four groups for (C): control, UAS-*bsk^{DN}*, *unc-104^{bris}*, and *unc-104^{bris};UAS-*bsk^{DN}**, and following four groups for (E): control, UAS-*fos^{DN}*, *unc-104^{bris}*, *unc-104^{bris};UAS-*fos^{DN}**. Arrowheads indicate PSDs unapposed by Brp. (B), (D) and (F), Quantification of the percentage of PSDs unapposed by Brp in groups shown in (A), (C) and (E), respectively. Loss of function mutation of *wnd*, as well as expression of *Fos^{DN}* and *Bsk^{DN}* can all strongly inhibit the AZ assembly phenotype in *unc-104^{bris}* mutants. (G), *Cac* localization at AZs was rescued by *Fos^{DN}* expression. Confocal images of neuromuscular junctions immunostained with Brp and GluRIIC in control, *unc-104^{bris}* and *unc-104^{bris};UAS-*fos^{DN}** larvae expressing *Cac-GFP*. Arrowheads indicate synapses that are negative for both *Cac-GFP* and Brp. Note the close colocalization of Brp and *Cac-GFP* in all three groups. For larvae in (A), (C), (E) and (G), expression were induced by the motor neuron specific driver OK319-Gal4. Scale bars, 5 μ m. Number of NMJs quantified: N \geq 6 for all groups. Statistical test: Student's t test. ***, P<0.001; **, P<0.01; *, P<0.05. Error bars indicate the SEM.

The percentage of Brp(-) synapses in *unc-104^{bris}* mutant and *unc-104^{bris};wnd* double mutant larvae was first assessed. *Wnd* loss-of-function dramatically reduced the abundance of Brp(-) synapses (Fig. 10 A, B). Similar with *wnd* mutant, expression of *Bsk^{DN}* and *Fos^{DN}* using the motor neuron specific driver OK319-Gal4 also very significantly reduced the percentage of Brp(-) synapses in *unc-104^{bris}* mutant larvae. Notably, *wnd* mutant, *Bsk^{DN}* and *Fos^{DN}* did not have obvious effect on AZ formation in wildtype background (Fig. 10 A, C, E). Thus downregulation of the *Wnd* MAPK cascade also has specific effect of inhibiting the AZ assembly phenotype in *unc-104^{bris}* mutant NMJs.

As shown previously, the Brp(-) synapses in *unc-104^{bris}* mutant NMJs also lacks other essential AZ components, including the Ca²⁺ channel subunit *Cac* (Fig. 3, A). The effect of restoring AZ assembly by downregulating the MAPK pathway could be limited to Brp or common for other AZ components. In order to test this notion, we examined the localization of *Cac* in larvae expressing a GFP tagged *Cac* construct driven by OK319-Gal4. Expression of *Fos^{DN}* in *unc-104^{bris}* mutant larvae also restored localization of *Cac-GFP* (Fig. 10 G). Importantly, the close colocalization of *Cac* with Brp was also preserved in *unc-104^{bris}* larvae with *Fos^{DN}* expression. The above results revealed that downregulation of *Wnd* MAPK pathway has the function of systemically rescuing the AZ assembly phenotype in *unc-104^{bris}* mutant.

4.2.3 No ameliorated axonal transport in *unc-104^{bris}*; *wnd* double mutant larvae

Rescue of the AZ assembly phenotype in *unc-104^{bris}* mutants by MAPK downregulation could be the result of a direct effect of this pathway in regulating active zone assembly, or possibly result of an indirect effect through enhancing the impaired axonal transport. In *unc-104^{bris}* mutants, Brp accumulates in the cell body region of VNC, where normally Brp is scarcely present (fig. 11 A). The abnormal Brp localization is possibly due to disturbed cargo loading caused by the *unc-104^{bris}* mutation. We checked if this ectopic Brp deposit is rescued by *wnd* mutation; surprisingly, Brp deposition in the cell body region of VNC became even more severe in *unc-104^{bris}*; *wnd* double mutant larvae (Fig. 11 A).

Wnd MAPK pathway has been suggested to play a role in motor-cargo binding. Bsk^{DN} expression and loss of function mutation in *wnd* both lead to excessive Brp puncta deposit along the axon (Horiuchi et al., 2007). In our experiments, we found that in *wnd* mutants the excessive Brp deposit is restricted in the axon, but not in neuronal cell bodies at VNC like *unc-104^{bris}* mutants (fig. 11 A, B). *unc-104^{bris}* mutants do not have the phenotype of excessive Brp deposit in the axon, however in *unc-104^{bris}*; *wnd* double mutant larvae there is similar Brp deposit in the axon like *wnd* mutants (fig. 11 A, B). Taken together, *wnd* mutation did not show an effect of rescuing the ectopic Brp deposit in the VNC of *unc-104^{bris}* mutants, and it further led to Brp deposit along the axon, thus it is unlikely that *wnd* mutation rescues through ameliorating axonal transport.

We also compared the quantity of total Brp at the NMJ between *unc-104^{bris}* and in *unc-104^{bris}*; *wnd* double mutants. Brp quantity at the NMJ in the latter group was significantly higher than *unc-104^{bris}* mutants (Fig. 11, C). Because *wnd* mutation did not rescue axonal transport function, the increased synaptic Brp is very likely a due to enhanced Brp stabilization as a result of improved AZ assembly.

It has been shown that *wnd* mutation also leads to increased DVGlut containing deposits in the axon, similar with its effect on Brp (Horiuchi et al., 2007). We also showed that localization of SV associated cargoes, Rab3 and DVGlut, is severely reduced at *unc-104^{bris}* mutant NMJs (fig. 6 A-D). Unlike its effect on Brp, *wnd* mutation

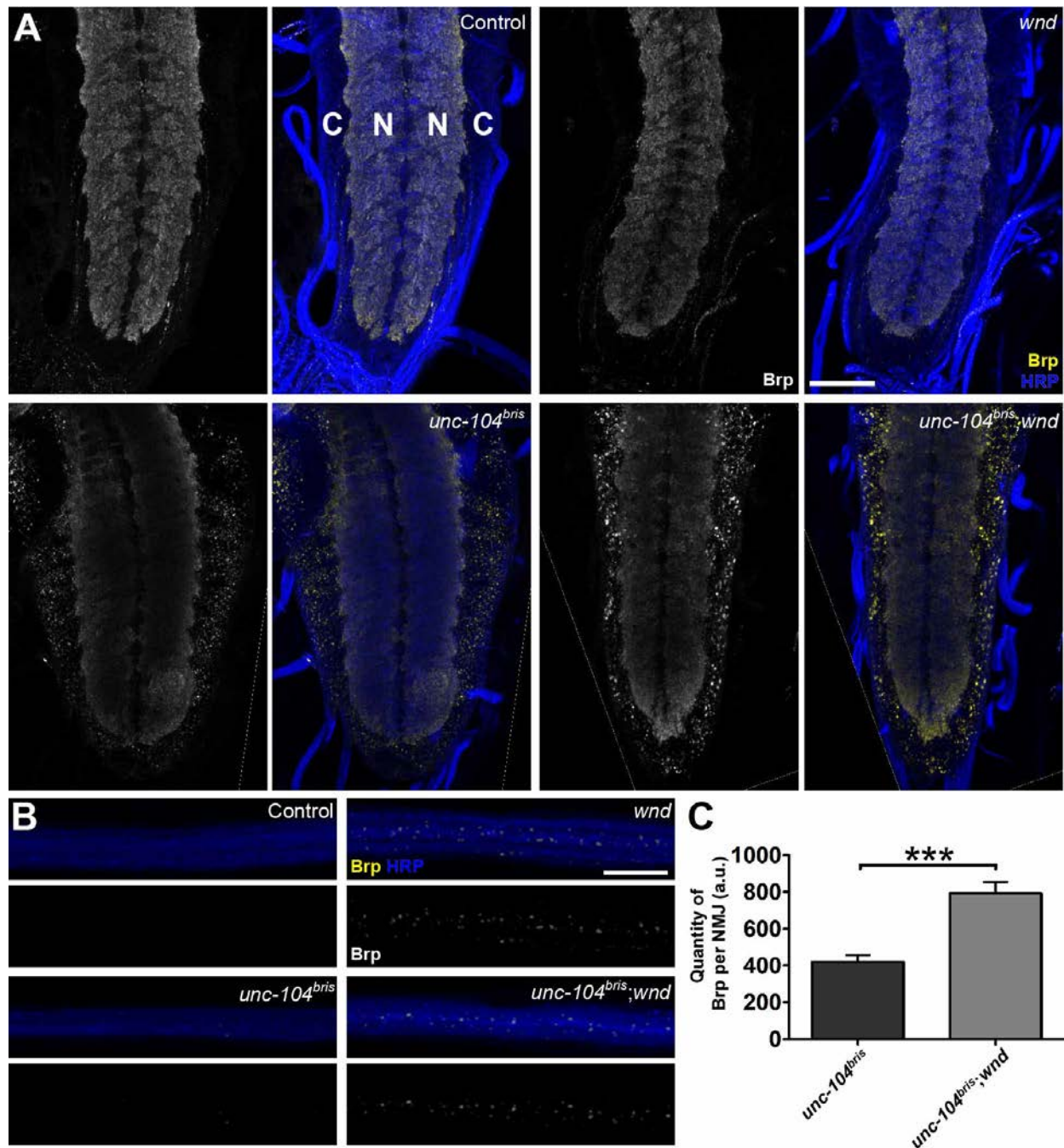


Fig11. Mutations in *wnd* do not ameliorate axonal transport in *unc-104^{bris}* mutants. (A) and (B), confocal images of VNC (A) and segmental nerve (B) in larvae immunostained with Brp and neural membrane marker HRP in control, *wnd*, *unc-104^{bris}* and *unc-104^{bris};wnd* larvae. Note the ectopic deposition of Brp puncta in the cell body region of VNC in *unc-104^{bris}* mutants in (A). Presence of *wnd* mutation in *unc-104^{bris}* mutants worsened this phenotype. (B), presence of *wnd* mutation leads to excessive Brp puncta along the nerve in *unc-104^{bris}* larvae, similar with the phenotype of *wnd* mutants. (C), quantification of total Brp at NMJs in *unc-104^{bris}* and *unc-104^{bris};wnd* larvae (*unc-104^{bris}*: 419.2 ± 38.4 a.u.; *unc-104^{bris};wnd*: 794.0 ± 61.6 a.u. P < 0.001). Presence of *wnd* mutation significantly increased the quantity of Brp at *unc-104^{bris}* NMJs. Scale bars, A, 50 μm; B, 10 μm. Number of NMJs quantified in (C): N ≥ 6 for both groups. Statistical test: Student's t test. *, P < 0.001. Error bars indicate the SEM.**

did not increase the quantity of DVGlut at *unc-104^{bris}* mutant NMJs (fig. 12 A, C), further supporting the notion that *wnd* mutation does not have an effect of ameliorating axonal transport.

4.2.4 The SSR underdevelopment phenotype in *unc-104^{bris}* mutants NMJs is also rescued by downregulation of MAPK pathway

Another striking phenotype at *unc-104^{bris}* mutants NMJs is underdevelopment of the subsynaptic reticulum (SSR), which is an elaborate postsynaptic membranous system surrounding synaptic boutons. Electron microscopy data shows that the SSR in *unc-104^{bris}* mutants NMJs is far simpler, with much fewer layers of membrane structure (Kern et.al, unpublished observations). Localization of the postsynaptic MAGUK protein Dlg at SSR is dramatically reduced in *unc-104^{bris}* mutants NMJs (fig. 12 A, B).

We observed that *wnd* mutant was also able to partially rescue the SSR underdevelopment phenotype in *unc-104^{bris}* mutants. Dlg intensity at *unc-104^{bris}*; *wnd* double mutant larvae were significantly higher than *unc-104^{bris}* mutants. Actually there was also a mild trend that *wnd* mutant leads to higher Dlg intensity at the NMJ compared with wildtype control, but it was not statistically significant (Fig. 12 A, B). Rescue of the SSR underdevelopment phenotype by *wnd* mutation is also not likely a result of general effect of Wnd in inhibiting SSR development.

4.2.5 The locomotion defects in *unc-104^{bris}* mutant larvae is not rescued by downregulation of MAPK pathway

The *unc-104^{bris}* mutant larvae also suffer from severe behavior abnormalities. Locomotion speed of *unc-104^{bris}* mutant larvae dropped to only about 10% of the wildtype larvae (Kern et al., unpublished observations). Observing the above result that downregulating MAPK pathway inhibits the synaptic development phenotypes in *unc-104^{bris}* mutant, it is interesting to know if MAPK downregulation also rescue the behavior abnormalities.

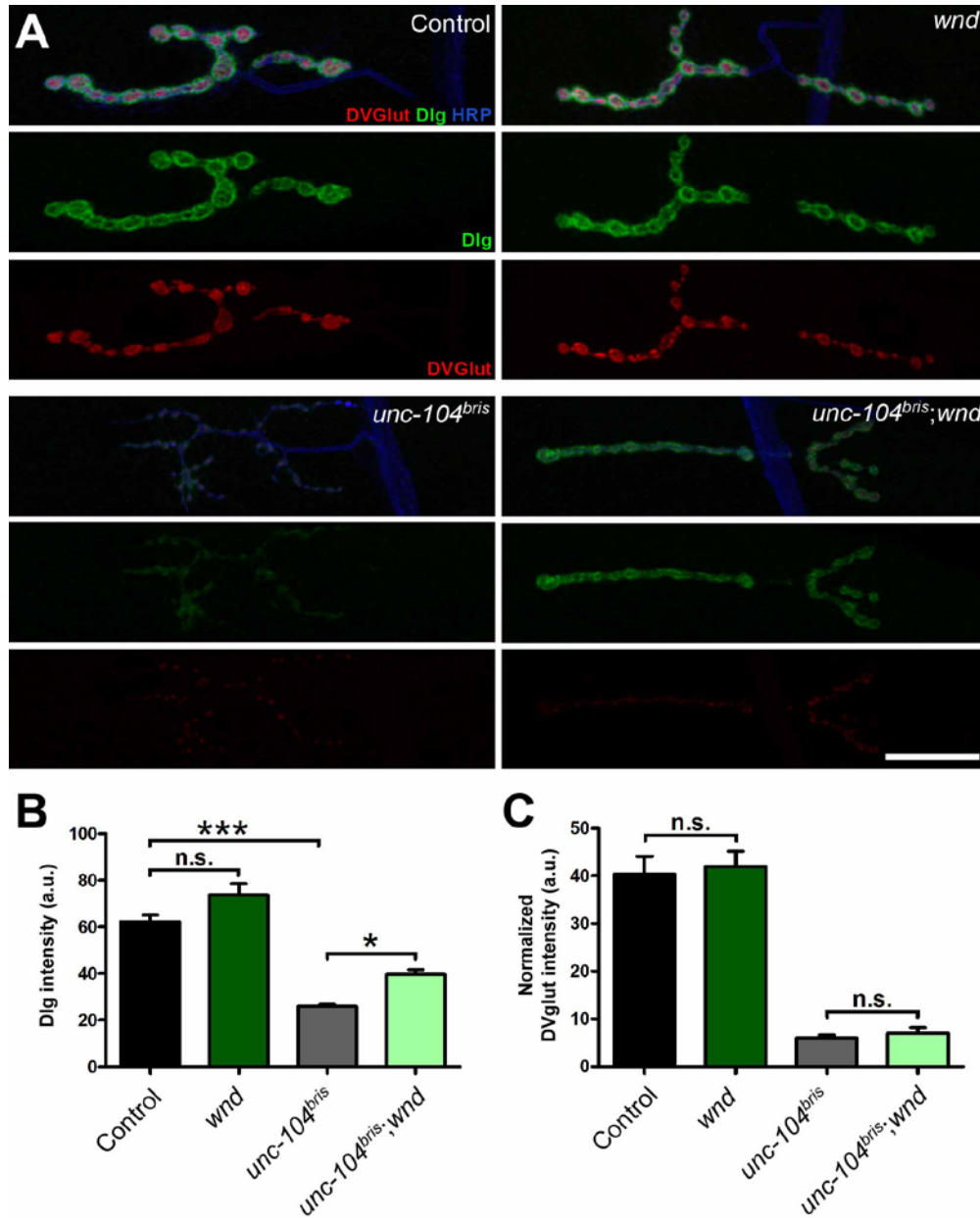


Fig12. Mutations in *wnd* suppress SSR underdevelopment in *unc-104^{bris}* mutants, but do not affect SV localization at NMJ. (A) confocal images of neuromuscular junctions immunostained with the SV associated protein DVGlut (red), the SSR associated protein Dlg (green) and neural membrane marker HRP (blue) in control, *wnd*, *unc-104^{bris}* and *unc-104^{bris};wnd* larvae. (B) and (C), quantifications of Dlg intensity at SSR (B) and DVGlut intensity (C) in groups shown in (A). In (B), Dlg intensity was dramatically reduced compared with control ($P < 0.001$); *wnd* mutation significantly increased Dlg intensity in *unc-104^{bris}* NMJs (*unc-104^{bris}*: 25.84 ± 0.94 a.u.; *unc-104^{bris};wnd*: 39.53 ± 2.15 a.u. $P < 0.05$). There is a mild trend that *wnd* mutation increased Dlg intensity at SSR in wildtype background, but it was not statistically significant (control: 62.26 ± 2.86 a.u.; *wnd*: 73.70 ± 4.92 a.u. $P > 0.05$). In (C), *wnd* mutation did not show an obvious effect on NMJ localization of DVGlut either in wildtype background or *unc-104^{bris}* mutant background (control: 40.35 ± 3.74 a.u.; *wnd*: 41.94 ± 3.26 a.u.; *unc-104^{bris}*: 5.97 ± 0.63 a.u.; *unc-104^{bris};wnd*: 6.96 ± 1.23 a.u.. control vs. *wnd*: $P > 0.05$; *unc-104^{bris}* vs. *unc-104^{bris};wnd*: $P > 0.05$). Scale bars, $20 \mu\text{m}$. Number of NMJs quantified: $N \geq 8$ for all groups. Statistical test: One-way ANOVA followed by Tukey's multiple comparison test. ***, $P < 0.001$; *, $P < 0.05$; n.s., $P > 0.05$. Error bars indicate the SEM.

A larval locomotion assay was performed to assess the effect of loss of function mutation in *wnd* on the locomotion speed of *unc-104^{bris}* mutant larvae. Compared with *unc-104^{bris}* mutant larvae, *unc-104^{bris}; wnd* double mutant larvae did show an enhanced locomotion behavior; although there is a mild trend of increasing locomotion speed, it was not statistically significant (Fig. 13). Interestingly, when comparing the locomotion speed between wildtype and *wnd* mutant larvae, the latter actually had an increased locomotion speed in the 3-4 mm length group (Fig. 13 B). Actually the *wnd* mutant larvae did seem more restless than wildtype larvae when performing the locomotion assay.

Therefore, despite the ameliorated synaptic morphology by downregulating MAPK pathway in *unc-104^{bris}* mutant larvae, the larval locomotion phenotype was not rescued.

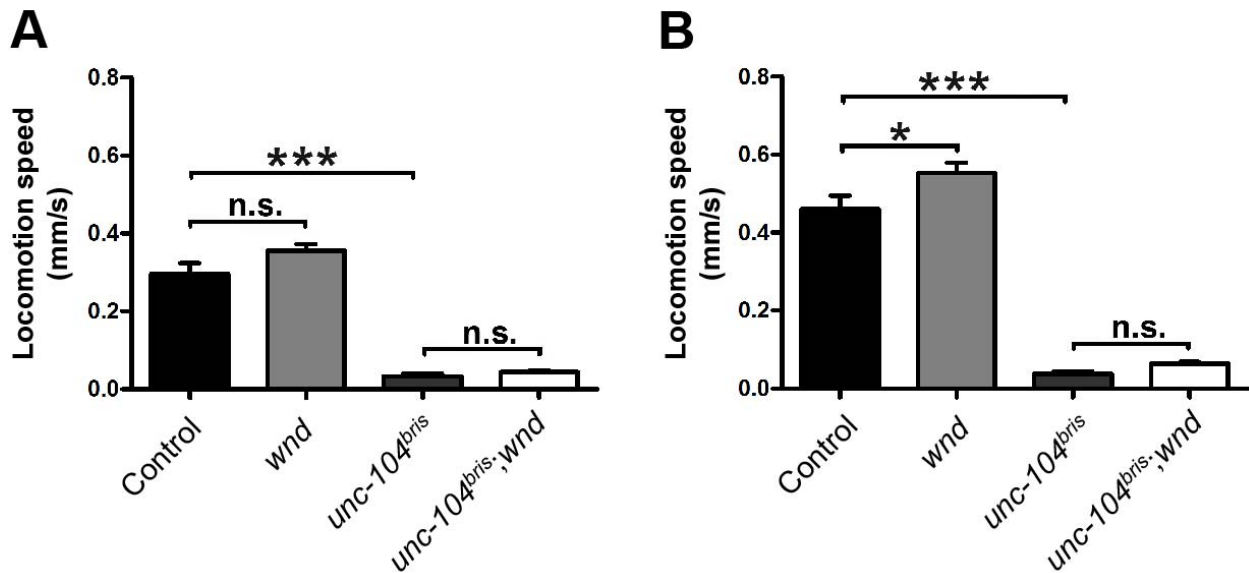


Fig13. Mutations in *wnd* do not rescue the locomotion impairments in *unc-104^{bris}* mutant larvae. (A) and (B), locomotion speed of control, *wnd*, *unc-104^{bris}* and *unc-104^{bris};wnd* larvae which belong to the length group of between 1-3 mm(A) and 3-4 mm(B), respectively. *unc-104^{bris}* mutant larvae have a locomotion speed of about 10% of control ($P < 0.001$). *unc-104^{bris};wnd* double mutant larvae do not have a higher locomotion speed than *unc-104^{bris}* mutant larvae. In (B), *wnd* mutant larvae of the 3-4 mm have higher locomotion speed than control. Number of movies quantified: $N=4$ for all groups, no less than 45 trajectories quantified in each movie. Statistical test: One-way ANOVA followed by Tukey's multiple comparison test. ***, $P < 0.001$; *, $P < 0.05$; n.s., $P > 0.05$. Error bars indicate the SEM.

4.2.6 Overactivation of the Wnd MAPK pathway is sufficient to cause AZ assembly phenotype resembling *unc-104^{bris}* mutants

The data so far support a model that *unc-104^{bris}* mutation leads to MAPK overactivation and causes NMJ overgrowth as well as impaired AZ assembly. It is already known that both *hiw* loss of function mutation and Wnd overexpression causes NMJ overgrowth (Collins et al., 2006). To test if MAPK overactivation also causes impaired AZ assembly independent of Unc-104, we stained Brp and GluRIIC in larvae carrying the *hiw* loss of function allele *hiw^{ΔN}* and in larvae expressing a cDNA construct UAS-*wnd* driven by the pan-neural driver Elav-Gal4 at 25°C. Both *hiw^{ΔN}* mutation and Wnd overexpression led to AZ assembly defect reminiscent of *unc-104^{bris}* mutation (Fig. 14 A, B). Apart from the reported NMJ overgrowth and reduced boutons size, a large amount of GluRIIC clusters in these *hiw^{ΔN}* and Wnd-OE NMJs are unapposed by presynaptic Brp puncta. Notably, the AZ assembly defect in Wnd overexpression larvae is especially pronounced at distal ends of NMJ branches (Fig. 14 B). Hence, overactivation of MAPK pathway caused by either *hiw* loss of function mutation or Wnd overexpression is sufficient to cause AZ assembly defects.

We also examined Brp localization at the VNC of *hiw^{ΔN}* mutant larvae. No ectopic Brp puncta localization in cell body region of VNC was observed (Fig. 14 C). This further confirmed that the ectopic Brp deposition is characteristic of impaired Unc-104 function. Impaired AZ assembly at the NMJ is the consequence of MAPK overactivation in *unc-104^{bris}* mutants, which is genetically separable with ectopic Brp deposition at VNC.

4.2.7 Reduced Hiw level in *unc-104^{bris}* mutants

The data above strongly suggested overactivation of MAPK pathway is mediating the NMJ overgrowth and AZ assembly phenotypes that in *unc-104^{bris}* mutants. We next sought to identify proof of MAPK pathway overactivation in *unc-104^{bris}* mutants.

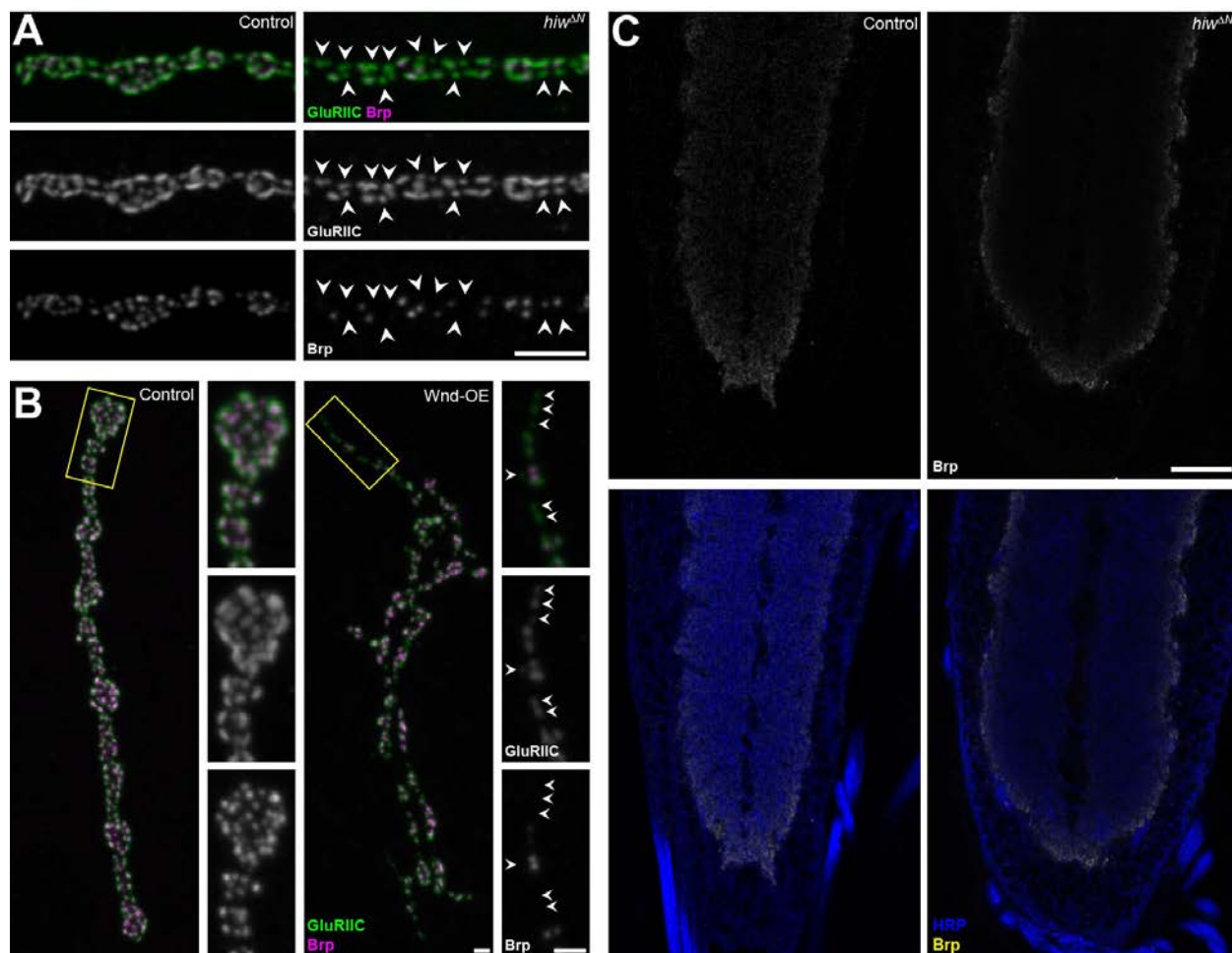


Fig14. Overactivation of MAPK pathway leads to AZ assembly phenotype reminiscent that of *unc-104*^{bris} mutants. (A) and (B), confocal images of neuromuscular junctions immunostained with the presynaptic active zone protein Brp (Magenta) and PSD marker GluRIIC (Green) in control and *hiw*^{ΔN} mutant larvae (A), and control and Wnd overexpression larvae (B). Note the dramatically increased number of PSDs unapposed by Brp (indicated by arrowheads) in *hiw*^{ΔN} mutant as well as Wnd-OE NMJs. In Wnd-OE larvae, this phenotype is especially pronounced in distal ends of NMJs (highlighted by yellow box and insets). (C), single confocal image frame of larval VNC immunostained with Brp and neural membrane marker HRP in control and *hiw*^{ΔN} mutant larvae. Note in *hiw*^{ΔN} mutant larvae there is no ectopic Brp deposition in the cell body region of VNC. For (B), expression was induced by the pan-neural driver *elav-Gal4*. Scale bars, in (A), 5 μm; in (B), 2 μm; in (C), 20 μm.

The E3 Ubiquitin-ligase Hiw has been shown to negatively regulate Wnd protein level in *Drosophila* nervous system. To test if the level of Hiw is altered in *unc-104*^{bris} mutants, a GFP-tagged Hiw construct was expressed in both wildtype control and *unc-104*^{bris} mutant larvae, driven by the pan-neural driver *elav-Gal4*. Compared with controls, Hiw-GFP level in the VNC of *unc-104*^{bris} mutant larvae was reduced by about 50% (fig. 15 A,

B), implying that a posttranscriptional mechanism downregulating Hiw level is probably involved in MAPK overactivation in *unc-104^{bris}* mutants. Directly detecting Wnd level using Wnd anti-serum also has been tried, but so far the Wnd antiserum has not been working in our hands.

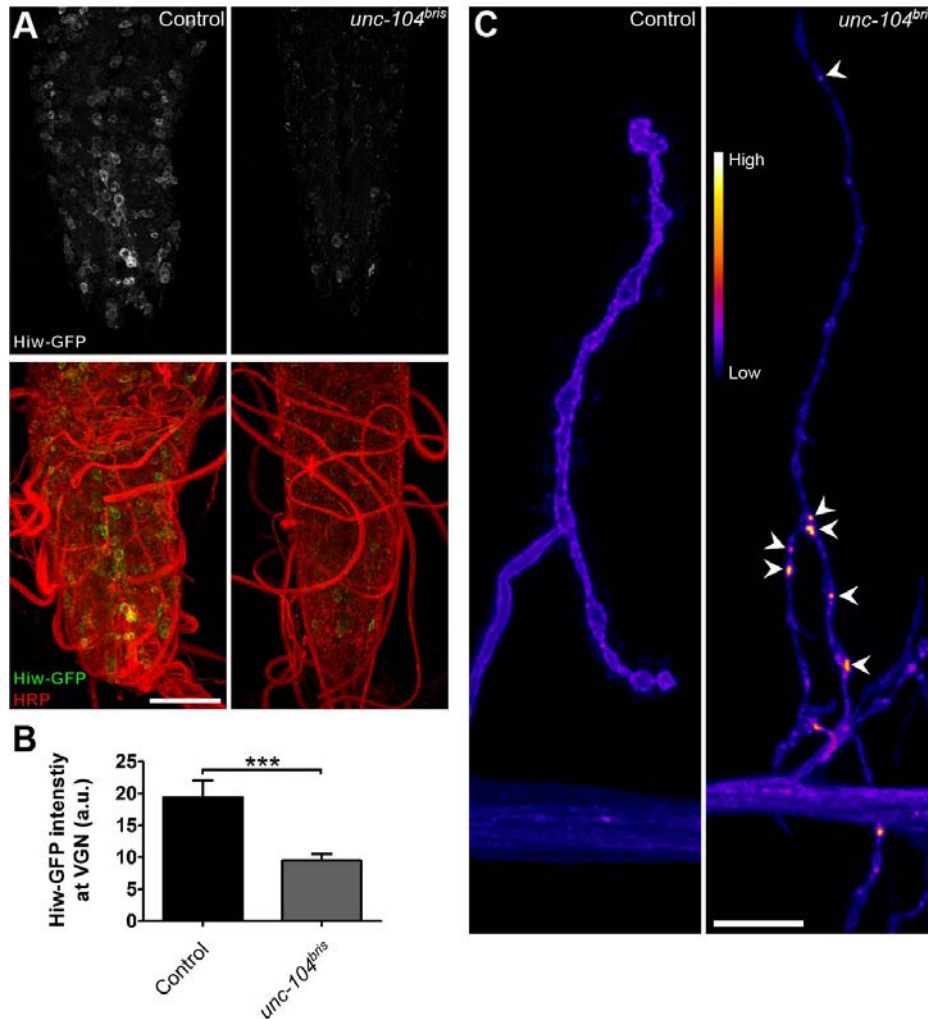


Fig15. Reduced level of Hiw in the CNS of *unc-104^{bris}* mutant larvae. (A), confocal images of VNCs immunostained with membrane marker HRP in control and *unc-104^{bris}* larvae expressing GFP tagged Hiw. (B), quantification of Hiw-GFP intensity at VNC (control: 19.43± 2.57 a.u.; *unc-104^{bris}*:9.55± 0.99 a.u. P<0.001). Expression was induced by the pan-neural driver elav-Gal4. Number of larvae quantified: N=5 for both groups. Statistical test: Student's t test. ***, P<0.001. Error bars indicate the SEM. (C), confocal images of NMJs immunostained with neural membrane marker HRP in control and *unc-104^{bris}* larvae. The lookup table "fire" was used for visualization. Arrowheads indicate vesicle like structure with intense HRP staining. Scale bars, in (A), 50µm; in (C), 10µm.

4.3 larval genotypes in each figure

Fig. 2

elavX-Gal4/+;; (control)

elavX-Gal4/+;unc-104^{bris}/unc-104^{d11024};;

elavX-Gal4/+;unc-104^{bris}/unc-104^{d11024};UAS-brp/+;

Fig. 3 A

elavX-Gal4,UAS-cac-gfp/+;; (control)

elavX-Gal4,UAS-cac-gfp/+; unc-104^{bris}/unc-104^{d11024};;

elavX-Gal4,UAS-cac-gfp/+;; UAS-brp-RNAi/+;

Fig. 3 B

elavX-Gal4/+;;Rab7-lip-gfp/+; (control)

elavX-Gal4/+; unc-104^{bris}/unc-104^{d11024};Rab7-lip-gfp/+;

elavX-Gal4/+;; Rab7-lip-gfp/UAS-brp-RNAi;

Fig. 3 C

elavX-Gal4/+;;UAS-srpk79d-gfp/+ ;(control)

elavX-Gal4/+;unc-104^{bris}/unc-104^{d11024};UAS-srpk79d-gfp/+ ;

elavX-Gal4/+;;UAS-srpk79d-gfp/UAS-brp-RNAi ;

Fig. 3 D-F

elavX-Gal4 UAS-cac-gfp/+;unc-104^{bris}/unc-104^{d11024};;

elavX-Gal4,UAS-cac-gfp/+;unc-104^{bris}/unc-104^{d11024};UAS-brp-RNAi/+;

elavX-Gal4,UAS-cac-gfp/+;unc-104^{bris}/unc-104^{d11024};UAS-brp/+;

Fig. 4

w¹¹¹⁸ (control)

elavX-Gal4/+ ;;UAS-unc-104-mcherry/+;

;unc-104^{bris}/unc-104^{d11024};;

elavX-Gal4/+ ; unc-104^{bris}/unc-104^{d11024};UAS-unc-104-mcherry/+;

Fig. 5

;;glurIIA-mrfp, glurIIB-gfp/+;(control)

;unc-104^{bris}/unc-104^{d11024};glurIIA-mrfp,glurIIB-gfp/+;

Fig. 6 A-B

*w*¹¹¹⁸ (control)
; *unc-104*^{bris} / *unc-104*^{d11024};;

Fig. 6 C-D

*w*¹¹¹⁸ (control)
; *unc-104*^{bris} / *unc-104*^{d11024};;

Fig. 6 E-F

;; *D42-Gal4*, *UAS-anf-gfp*/+; (control)
; *unc-104*^{bris} / *unc-104*^{d11024}; *D42-Gal4*, *UAS-anf-gfp*/+;

Fig. 6 G-H

;; *D42-Gal4*, *UAS-mito-gfp*/+; (control)
; *unc-104*^{bris} / *unc-104*^{d11024}; *D42-Gal4*, *UAS-mito-gfp*/+;

Fig. 7 A-E

elavX-Gal4/+; *unc-104*^{bris} / *unc-104*^{d11024};;
elavX-Gal4/+; *unc-104*^{bris} / *unc-104*^{d11024}; *UAS-rab3*/+;

Fig. 8 A-C

; *OK319-Gal4*/+;; (control)
; *OK319-Gal4*/ *UAS-tnt*;;
; *OK319-Gal4*, *unc-104*^{bris} / *unc-104*^{d11024};;
; *OK319-Gal4*, *unc-104*^{bris} / *UAS-tnt*, *unc-104*^{d11024};;

Fig. 9 A-B

*w*¹¹¹⁸ (control)
;; *wnd1/wnd3*;
; *unc-104*^{bris} / *unc-104*^{d11024};;
; *unc-104*^{bris} / *unc-104*^{d11024}; *wnd1/wnd3*;

Fig. 9 C-D

; *OK319-Gal4*/+;; (control)
; *OK319-Gal4*/+; *UAS-fos*^{DN}/+;
; *OK319-Gal4*/+; *UAS-bsk*^{DN}/+;
; *OK319-Gal4*, *unc-104*^{bris} / *unc-104*^{d11024};;

;OK319-Gal4,unc-104^{bris}/unc-104^{d11024};UAS-fos^{DN}/+;
;OK319-Gal4,unc-104^{bris}/unc-104^{d11024};UAS-bsk^{DN}/+;

Fig. 10 A

w¹¹¹⁸ (control)
;;wnd1/wnd3;
;unc-104^{bris}/unc-104^{d11024};;
;unc-104^{bris}/unc-104^{d11024}; wnd1/wnd3;

Fig. 10 B

;unc-104^{bris}/unc-104^{d11024};;
;unc-104^{bris}/unc-104^{d11024}; wnd1/wnd3;

Fig. 10 C

;OK319-Gal4/+;; (control)
;OK319-Gal4/+;UAS-fos^{DN}/+;
;OK319-Gal4,unc-104^{bris}/unc-104^{d11024};;
;OK319-Gal4,unc-104^{bris}/unc-104^{d11024};UAS-fos^{DN}/+;

Fig. 10 D

;OK319-Gal4,unc-104^{bris}/unc-104^{d11024};;
;OK319-Gal4,unc-104^{bris}/unc-104^{d11024};UAS-fos^{DN}/+;

Fig. 10 E

;OK319-Gal4/+;; (control)
;OK319-Gal4/+;UAS-bsk^{DN}/+;
;OK319-Gal4,unc-104^{bris}/unc-104^{d11024};;
;OK319-Gal4,unc-104^{bris}/unc-104^{d11024};UAS-bsk^{DN}/+;

Fig. 10 F

;OK319-Gal4,unc-104^{bris}/unc-104^{d11024};;
;OK319-Gal4,unc-104^{bris}/unc-104^{d11024};UAS-bsk^{DN}/+;

Fig. 10 G

;OK319-Gal4/+;UAS-cac-gfp/+; (control)
;OK319-Gal4,unc-104^{bris}/unc-104^{d11024};UAS-cac-gfp/+;
;OK319-Gal4,unc-104^{bris}/unc-104^{d11024};UAS-fos^{DN}/UAS-cac-gfp/;

Fig. 11 A-B

w^{1118} (control)

;;*wnd1/wnd3*;

;*unc-104^{bris}/unc-104^{d11024}*;;

;*unc-104^{bris}/unc-104^{d11024}*;*wnd1/wnd3*;

Fig. 11 C

;*unc-104^{bris}/unc-104^{d11024}*;;

;*unc-104^{bris}/unc-104^{d11024}*;*wnd1/wnd3*;

Fig. 12 A-C

w^{1118} (control)

;;*wnd1/wnd3*;

;*unc-104^{bris}/unc-104^{d11024}*;;

;*unc-104^{bris}/unc-104^{d11024}*;*wnd1/wnd3*;

Fig. 13 A-B

w^{1118} (control)

;;*wnd1/wnd3*;

;*unc-104^{bris}/unc-104^{d11024}*;;

;*unc-104^{bris}/unc-104^{d11024}*;*wnd1/wnd3*;

Fig. 14 A, C

w^{1118} (control)

hiw^{4N}

Fig. 14 B

elavX-Gal4/+;; (control)

elavX-Gal4/+;UAS-*wnd/+*;;

Fig. 15 A-B

elavX-Gal4/+;UAS-*hiw-gfp/+*; (control)

elavX-Gal4/+;*unc-104^{bris}/unc-104^{d11024}*;UAS-*hiw-gfp/+*;

Fig. 15 C

w^{1118} (control)

;*unc-104^{bris}/unc-104^{d11024}*;;

5. Discussions

This study shows that a point mutation in the *Drosophila* kinesin-3 homolog *unc-104*, *unc-104^{bris}*, leads to systemic presynaptic active zone assembly defect as well as overgrowth of the neuromuscular junction. Mechanistic study reveals that overactivation of a Wnd MAPK pathway is underlying the synaptic phenotypes in *unc-104^{bris}* mutants.

5.1 A neuronal kinesin regulating AZ assembly

The *unc-104^{bris}* mutation leads to a very distinct AZ assembly phenotype. The AZ organizing protein Brp, along with other major AZ proteins including Cac and Liprin- α are concomitantly absent from a subset of synapses at *unc-104^{bris}* mutant NMJs, implying that AZ assembly is abolished at these synapses.

Morphological studies in Brp-RNAi larvae revealed that Brp is not indispensable for the AZ localization of either Cac or Liprin- α . Consistent with report showing reduced Cac localization in *brp* mutants, Brp(-) synapses in Brp-RNAi larvae have less Cac compared with Brp(+) ones (Fig. 3 A). The C terminus of Cac has been shown to physically interact with the N terminus of Brp (Fouquet et al., 2009). This interaction may be important for the continued incorporation of Cac during synapse maturation, but not its initial localization to the AZ. Actually Cac has been shown to appear at the AZ even slightly earlier than Brp (Fouquet et al., 2009). The Brp(-) synapses in Brp-RNAi larvae also did not show obvious Liprin- α localization abnormality (Fig. 3 B), suggesting that localization of Liprin- α at AZ is also not dependent on Brp. Liprin- α clusters localize at the border of AZ, and Liprin- α has the function of regulating the size and shape of Brp clusters located at the AZ center (Fouquet et al., 2009; Kaufmann et al., 2002). Our result shows that Brp does not have an obvious converse effect on Liprin- α localization. SRPK79D has been shown to colocalize with Brp puncta both at the synapses as well along the segmental nerve (Johnson et al., 2009; Nieratschker et al., 2009). Brp-RNAi experiments showed that localization of SRPK79D to AZ is passively determined by Brp.

Comparison between *unc-104^{bris}* mutants and Brp-RNAi larvae suggests that the AZ assembly phenotype in *unc-104^{bris}* mutants is not secondary of impaired Brp puncta formation at *unc-104^{bris}* mutant synapses. Although Cac and Liprin- α persist in the Brp(-) synapses in Brp-RNAi larvae, they are absent from the Brp(-) synapses in *unc-104^{bris}* mutants (Fig. 3 A-C). Synaptic proteins assemble at the AZ following defined temporal order during synaptogenesis (Fouquet et al., 2009; Oswald et al., 2010). The importance of this order may imply that localization of some components to the AZ at early stage provide the priming unit for other proteins to build upon. If a synapse cannot complete the critical, rate-limiting AZ seeding step, AZ assembly may stop and reverse. The mechanism controlling initial AZ assembly seems to be disrupted in *unc-104^{bris}* mutants.

The fact that Brp overexpression does not effectively rescue Brp assembly at AZ implies that decreased availability of AZ components at the NMJ is not the major cause for the AZ assembly defect in *unc-104^{bris}* mutants. The surplus of Brp provided by overexpression preferably goes to AZs already having Brp, leading to an increase in average Brp puncta size by one fold while leaving more than 10% of all synapses still having none (Fig. 2 A, C). The presynaptic side of Brp(-) synapses in *unc-104^{bris}* mutant appears to have limited ability to form Brp clusters. It is likely that the observed reduction of total Brp at *unc-104^{bris}* mutant NMJs is also predominantly the consequence of decreased ability to stabilize components at the AZ. Conversely, excessive Brp puncta deposition in the neuronal cell body region at the VNCs in *unc-104^{bris}* mutants might be a sign of ectopic AZ formation due to sequestering of certain pro-AZ assembly signaling components in neuronal soma (Fig. 11 A).

5.2 An MAPK pathway regulating synaptic development

This study reveals a novel function of the E3 ubiquitin ligase Hiw and the Wnd MAPK pathway in regulating AZ assembly in *Drosophila*. MAPK pathway overactivation in *hiw^{AN}* mutants and Wnd overexpressing larvae leads to both the NMJ overgrowth and AZ assembly impairments reminiscent of *unc-104^{bris}* mutants (Wan et al., 2000 and Fig. 2, 9 & 14 in this work).

In *C. elegans*, mutation in the *highwire* homolog *rpm-1* is shown to cause abnormal synaptic organization. In *rpm-1* mutant worms, formation of RIM1 positive presynaptic structures is reduced, and spacing between synapses is enlarged (Schaefer et al., 2000). The function of Rpm-1 in regulating presynaptic development is dependent on its function of inhibiting MAPK pathway activity; in *C. elegans*, Rpm-1 downregulates the level of Wallenda homolog DLK-1 (Nakata et al., 2005). Loss of function mutation in MKK4, an MAP2K downstream of DLK-1, suppresses the synaptic phenotype in *rpm-1* mutants; overexpression of MKK4 is sufficient to cause similar synaptic phenotype with *rpm-1* mutants (Nakata et al., 2005).

The synaptic phenotype in *rpm-1* mutant *C. elegans* resembles the AZ assembly phenotype in *hiw*^{ΔN} mutant NMJs in *Drosophila* shown in this study (Fig. 13 A). Hiw also has the function of downregulating Wnd level in flies (Collins et al., 2006), and Wnd overexpression causes similar AZ assembly phenotype with *hiw*^{ΔN} mutants (Fig. 13). Our data shows that the function of Hiw and Wnd MAPK signaling pathway in regulating synaptic development is conserved between worms and flies.

Downstream of Wnd, the *Drosophila* JNK homolog, Bsk, and the transcription factor Fos are required for the NMJ overgrowth and AZ assembly phenotype in *unc-104*^{bris} mutants. Therefore, the function of MAPK pathway in regulating AZ assembly presumably involves modulation of gene expression by Fos. Notably, it is also reported that Fos^{DN}, but not dominant negative form of another JNK regulated transcriptional factor Jun (Jun^{DN}), inhibits the NMJ overgrowth phenotype in *hiw* mutant larvae (Collins et al., 2006). Further work to investigate genes whose expression profiles are altered upon Wnd MAPK pathway overactivation will help to clarify factors directly contributing to the characteristic synaptic phenotype.

One attractive candidate for the direct effector causing MAPK dependent NMJ overgrowth is MSPS/XMAP215, which is a processive microtubule polymerase (Brouhard et al., 2008; Howard and Hyman, 2009). In *Drosophila*, induction of new axon formation after axotomy in the *ddaE* sensory neuron has been shown to be dependent on JNK activity (Stone et al., 2010). After axotomy, enhanced MSPS activity is crucial

for the increased microtubule dynamics as well as inverted microtubule polarity, which is necessary for the conversion of one dendrite into axon (Stone et al., 2010). JNK signaling pathway is necessary for the enhanced MSPS function after axon severing. Observing the similarity between the NMJ overgrowth phenotype in *hiw* mutant larvae and the enhanced growth of some dendrites upon axotomy, it is intriguing to test if in these mutants there is overactivation of MSPS activity and if MSPS is involved in the NMJ overgrowth phenotype.

It is shown that the Wnd MAPKs have the function of inhibiting Brp puncta deposition in the axon (Horiuchi et al., 2007). Loss of function mutation in *wnd* and expression of dominant negative form of JNK leads to formation of Brp deposits along segmental nerve, which resemble Brp puncta at the active zone. In this study, we show that MAPK overactivation leads to decreased Brp puncta formation at the presynaptic active zone. The above phenotypes upon upregulation and downregulation of the MAPK pathway converge on a function of inhibiting AZ assembly by the Wnd MAPKs. The axonal deposits of Brp puncta in *wnd* mutants is probably a result of enhanced AZ assembly, which leads to formation of AZ like structure outside of synaptic region. Further EM studies to show if these Brp containing puncta in *wnd* mutant nerves form “T-bar” like structure, and if synaptic vesicles are associated with them will help further elucidate the nature of these puncta, and confirm the function of Wnd MAPKs in inhibiting AZ assembly.

5.3 MAPK overactivation mediates the synaptic development abnormalities in *unc-104^{bris}* mutants

Impaired Kinesin-3/Unc-104 function leads to MAPK overactivation

Our result shows that the Wnd MAPKs are necessary for the AZ assembly as well as NMJ overgrowth phenotypes in *unc-104^{bris}* mutants. Overactivation of the Wnd MAPK mediates the major synaptic phenotypes in *unc-104^{bris}* mutants.

We found that MAPK overactivation in *unc-104^{bris}* mutants is probably the result of downregulated Hiw level (Fig. 15). One identified mechanism regulating Hiw abundance is the autophagy related pathway (Shen and Ganetzky, 2009; Tian et al., 2011). Overexpression of Atg1, one of the core components of autophagy machinery has been shown to cause NMJ overgrowth in *Drosophila* (Shen and Ganetzky, 2009). Notably, the role of Atg1 in regulating NMJ growth depends on its autophagy-promoting function to downregulate Hiw level and thus to cause overactivation of the MAPK pathway. Atg1 dependent NMJ overgrowth is abolished by loss of function mutations in *wnd* and expression of Bsk^{DN} (Shen and Ganetzky, 2009). Indeed, vesicular structures with intense HRP staining which resemble autophagosomes are frequently observed at *unc-104^{bris}* mutant NMJs (Fig. 14 C), supplying a sign of possibly enhanced autophagy activity. Further studies are yet needed to elucidate if these vesicles contain autophagy markers as well to identify how impaired Kinesin-3/Unc-104 function leads to increased autophagy.

In *C. elegans*, Unc-104 is shown to undergo ubiquitin based proteolysis upon reaching axonal terminal and not transported back to neuronal soma (Kumar et al., 2010). My colleague found that in *unc-104^{bris}* mutants, Unc-104 forms aggregates both in the ventral nerve cord of larval CNS as well at the tips of NMJs, whereas in wildtype larvae Unc-104 does not form aggregates (Kern et al., unpublished observations). This implies that the *unc-104^{bris}* mutation leads to a pro-aggregation and proteolysis-resistant form of Unc-104. These Unc-104 aggregates may disrupt proteasome function or compete with Wnd for degradation, which leads to higher Wnd level and MAPK pathway overactivation.

It cannot be totally excluded that Hiw independent mechanisms may also contribute to the MAPK overactivation upon impaired Kinesin-3/Unc-104 function. Wnd is associated with membranes, transported along the axon and located at the NMJ in *Drosophila* (Collins et al., 2006; Xiong et al., 2010). Axonal transport of Wnd may be perturbed in *unc-104^{bris}* mutants, which in turn leads to ectopic MAPK overactivation.

JNK interacting proteins (JIPs) may also be involved in the MAPK activation in *unc-104* mutants. In *C. elegans*, JIP3/Unc-16 has been identified as an Unc-104 binding partner (Hsu et al., 2011). JIP3-associated Unc-104 localizes predominantly in neuronal soma, whereas binding to other partners like Liprin- α and DNC-1/Glued directs Unc-104 to axonal and axon terminal specific localization (Hsu et al., 2011). On the other hand, JIP3 shows specific interaction with JNKs in mammalian cells (Ito et al., 1999). JIP3 also interacts directly with the MAP3K MKK1 and MAP2K MEK with different regions, and works as a scaffold to enable the association of MAPK components and facilitate their function; overexpression of JIP3 leads to enhanced JNK activity (Ito et al., 1999). The *unc-104^{bris}* mutation may disrupt the interaction between Unc-104 and JIP3, which in turn enhances JIP3-MAPKs association and leads to MAPK overactivation.

MAPK overactivation is one of the consequences of impaired Kinesin-3/Unc-104 function

It is noteworthy that although *Wnd* is necessary for the NMJ overgrowth and AZ assembly phenotype in *unc-104^{bris}* mutants, Brp deposition in the cell body region of VNC is not rescued by loss of function mutations in *wnd* (Fig. 11 A). Mutations in *hiw* lead to similar NMJ overgrowth and AZ assembly phenotype with *unc-104^{bris}* mutants without showing obvious impairment of AZ protein transport (Fig.13 C). Therefore, Brp deposition in the cell body region of VNC is probably caused by disrupting certain aspect of Unc-104 function, which contributes little, if any, to the impaired AZ assembly in *unc-104^{bris}* mutants (Fig. 16). Possibly reduced transport of AZ proteins may exacerbate, but is not a major cause, of the AZ assembly phenotype in *unc-104^{bris}* mutants.

Neither loss of function mutation in *wnd*, nor expression of Bsk^{DN} or Fos^{DN} in motor neurons rescued the larval lethality and locomotion defects in *unc-104^{bris}* mutants (Fig. 13). What is more, *hiw^{AN}* mutant flies which also show MAPK overactivation are viable and fertile, with grossly normal behavior, despite the electrophysiological impairments as well as synaptic abnormalities (Wan et al., 2000). Therefore, MAPK overactivation is

one of the consequences of impaired Unc-104 function, which causes the NMJ overgrowth, and synaptic assembly phenotype. MAPK overactivation is not likely the cause for locomotion defects or larval lethality in *unc-104* mutants. Other MAPK independent functions of Unc-104 are required for normal behavior and survival.

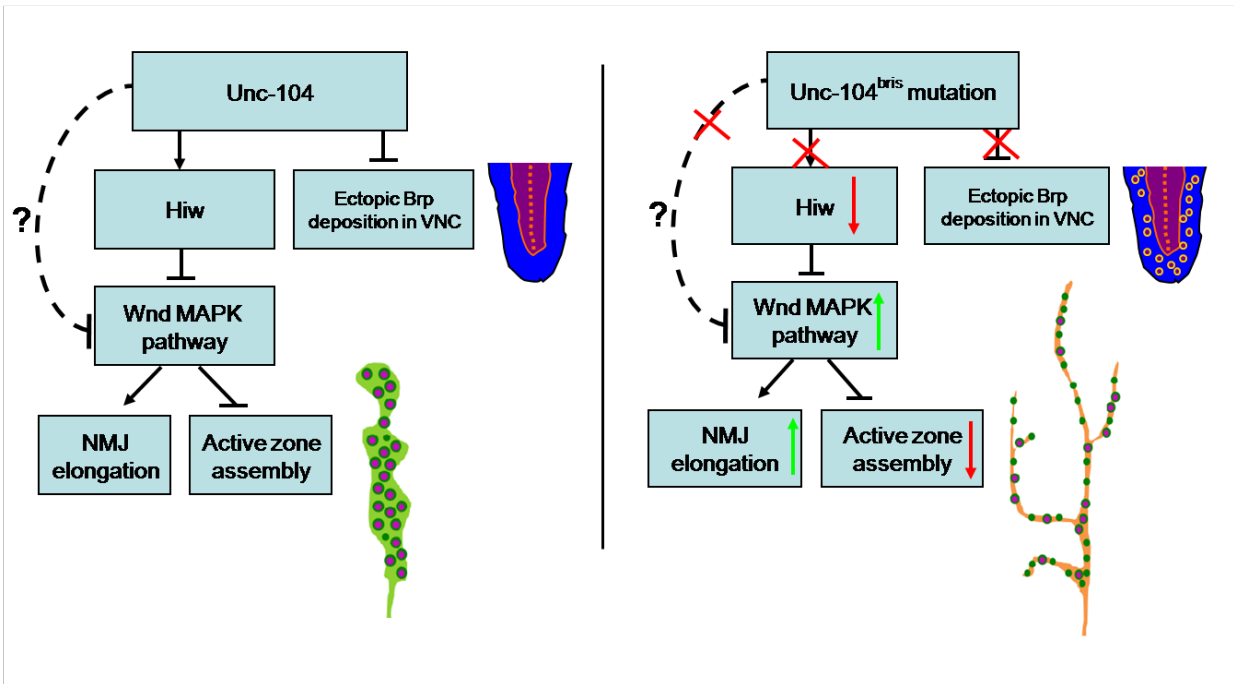


Fig16. A schematic illustration of the functions of Unc-104 and the Wnd MAPK pathway. Unc-104 inhibits the activity of the Wnd MAPK pathway through promoting Highwire function and also possibly through Highwire-independent mechanism. Mutation in *unc-104* leads to MAPK overactivation and causes the NMJ overgrowth, as well as AZ assembly phenotype. The Function of inhibiting ectopic Brp deposition in the cell body region of ventral nerve cord is an Unc-104 function which is genetically separable with MAPK pathway activity.

Other possible factors contributing to the morphological changes in *unc-104^{bris}* mutants

The AZ assembly phenotype in *unc-104^{bris}* mutants shows certain similarity with *Drosophila rab3* mutants, where AZs appear to be absent from two thirds of the synapses at NMJ, while the rest are with enlarged presynaptic Brp puncta as well as bigger Cac cluster. Based on this phenotype, Rab3 has been proposed to facilitate AZ assembly in *Drosophila*. (Graf et al., 2009). The reduced AZ formation in *unc-104^{bris}*

mutant may involve insufficient Rab3 at the NMJ (Fig. 6 C, D), observing the ameliorated AZ assembly phenotype by Rab3 overexpression (Fig. 7). The result that Rab3 overexpression increased the quantity of Brp at *unc-104^{bris}* mutant NMJs is a bit surprising, as Rab3 has been suggested to have the function of regulating AZ components distribution among synapses but not of changing their overall abundance at the NMJ.

One possibility is that apart from regulating the distribution of AZ components, Rab3 may have the function of maintaining the normal quantity of AZ components at NMJ, which overlaps with other proteins. In *unc-104^{bris}* mutants, mechanisms maintaining the quantity of AZ components at the synapse were severely impaired (Fig. 2 & Fig. 3), thus the function of Rab3 to increase Brp quantity at the NMJ is uncovered. Rab3 overexpression only mildly rescues the AZ assembly phenotype in *unc-104^{bris}* mutants, which is probably also due to the reduced function of transporting SV associated proteins including Rab3 to the NMJ (Fig. 6). Actually Rab3 may even function as an indirect downstream effector of the Wnd MAPK pathway. In *hiw^{AN}* mutant larvae, which show MAPK overactivation and similar AZ assembly phenotype with *unc-104^{bris}* mutants, the level of Rab3 at the NMJ is also reduced (unpublished observations).

It remains elusive to what extent the defect in Neuropeptide signaling contributes to the observed morphological change in *unc-104^{bris}* mutants. As shown by others (Barkus et al., 2008; Lo et al., 2011; Pack-Chung et al., 2007) and in our study, Kinesin-3 family members are the major transporters for peptide containing large DCV. A neuropeptide signaling pathway has been reported recently to regulate NMJ growth through the cAMP-PKA-CREB cascade (Chen and Ganetzky, 2012). Mutation in gene encoding the neuropeptide drosulfakinin (DSK) or its presynaptic receptor, the cholecystokinin-like receptor (CCKLR) which is a G-protein coupled receptor (GPCR), leads to NMJ undergrowth, decreased bouton number and apparently larger bouton size. Excessive activation of this pathway by overexpressing CCKLR or CREB leads to NMJ overgrowth, resembling the NMJ phenotype in *unc-104^{bris}* mutants (Chen and Ganetzky, 2012). Whether there is change in synapse morphology in case of overactivation of this DSK-CCKLR pathway is not yet known, although fewer synapses form in *dsk* or *ccklr* mutants

without obvious abnormality in AZ morphology (Chen and Ganetzky, 2012). It is interesting to investigate the synapse morphological change caused by DSK-CCKLR pathway overactivation, and compare with that in *unc-104^{bris}* mutants. So far we still only have limited understanding about the role of neuropeptide signaling pathway in regulating synaptic development. It is very intriguing to identify other neuropeptides or DCV associated signaling molecules and figure out their synaptic development related functions.

Comparison between different alleles of *unc-104*

Two published hypomorphic alleles of *unc-104*, *unc-104^{O1.2}* and *unc-103^{O3.1}*, lead to reduction in NMJ length, in contrast to NMJ overgrowth which occurs in *unc-104^{bris}* mutants; numbers of synaptic boutons at the NMJ in *unc-104^{O1.2}* and *unc-103^{O3.1}* mutants drop to only half of that in wildtype (Barkus et al., 2008). However, *unc-104^{O1.2}* and *unc-103^{O3.1}* mutants share important similarity in NMJ morphology with *unc-104^{bris}* mutants that the size of synaptic boutons is dramatically reduced (Barkus et al., 2008 and Fig. 9 in this study), whereas the axonal terminals in null mutants of *unc-104* is totally incapable of transforming to synaptic boutons (Pack-Chung et al., 2007). The phenotype of reduced NMJ size in *unc-104^{O1.2}* and *unc-103^{O3.1}* mutants rather than NMJ overgrowth is probably a sign of being stronger alleles than *unc-104^{bris}*. Actually, depending on the strength of expression, an *Unc-104* RNAi construct can either lead to an NMJ atrophy or NMJ overgrowth phenotype (unpublished observations).

5.4 Kinesin-3/Unc-104 and synaptic function

This study provides new insight in understanding the role of *Unc-104* in maintaining synaptic function.

The published null alleles of *Drosophila unc-104* was initially screened out using the EGUF-*hid* method which creates homozygous mutant eyes in a heterozygous fly.

Mutant eyes lack the “on-off-transients” of the electroretinograms, indicating impaired synaptic transmission from photo receptors to second order neurons (Pack-Chung et al., 2007). *unc-104^{bris}* mutants seem to have preserved some basic function in facilitation synaptic function. Null mutants can go through embryo development but are paralyzed and unable to hatch; homozygous *unc-104^{bris}* mutant can however survive till late larval/pupal stage; although showing reduced locomotion speed than wildtype larvae, they still obviously behave better than the transheterozygous *unc-104^{bris}/unc-104^{d11024}* larvae (Kern et al., unpublished observations).

Structural basis for the impaired synaptic activity *unc-104^{bris}* mutants

The vast morphological changes in *unc-104^{bris}* mutants are well consistent with the drastic reduction in electrophysiological parameters including reduced mEJP amplitude and EJP amplitude, decreased mEJP frequency as well as smaller quantal content (Fig. 4).

A conspicuous reduction in GluRIIA clustering and consequent increase in the ratio of GluRIIB/GluRIIA was observed in *unc-104^{bris}* mutants (Fig. 5). The conductivity of IIA-type glutamate receptors are much larger and IIB-type receptors, and change in the ratio between these two receptor has been shown to modulate quantal size (DiAntonio et al., 1999). Therefore, the observed reduction in GluRIIA clustering is very likely the cause of decreased mEJP amplitude and in turn contributes to the impaired EJP. Change in SV size also has been reported to influence quantal size (Daniels et al., 2004), however EM results do not show different SV size in *unc-104^{bris}* mutants (Kern et al., unpublished observations).

Apart from reduced quantum size caused by the change in postsynaptic receptor composition, smaller quantal content is another factor contributing to the reduction in evoked release in *unc-104^{bris}* and *hiw^{ΔN}* mutants. The 90% reduction in SV localization at the NMJ is probably the major cause of reduced neurotransmitter release at evoked event, which may have been further worsened by fewer release sites as a result of

impaired AZ formation. Reduced SV localization at the NMJ is also well likely responsible for the abruptly reduced spontaneous release in *unc-104^{bris}* mutants (Fig. 4 F).

Reduction in Rab3 at the NMJ likely contributes little to the severely compromised synaptic function in *unc-104^{bris}* mutants, as *rab3* mutant larvae have grossly normal synaptic activities (Graf et al., 2009). However, insufficient delivery of other SV associated proteins regulating neurotransmitter release might contribute to some aspects of the synaptic transmission impairments in *unc-104^{bris}* mutants (Rizo and Rosenmund, 2008; Santos et al., 2009).

Importantly, the severely impaired synaptic activity in *unc-104^{bris}* mutants is the result of synaptic morphology alterations and not vice versa. Blocking synaptic transmission by TNT in wildtype background does not lead to similar synaptic development effect with *unc-104^{bris}* mutants, nor does TNT expression in the *unc-104^{bris}* mutant background exacerbate the major morphological alterations (Fig. 7).

Common structural alteration cause impairment in synaptic activity

The phenotype of impaired synaptic activity in *hiw* mutants is strikingly similar with that in *unc-104^{bris}* mutants (Wan et al., 2000). In this study, we proved that *hiw^{ΔN}* mutant NMJs have very similar synaptic development phenotype with *unc-104^{bris}* mutants including reduced active zone assembly and NMJ overgrowth (Fig. 13), speaking for a common structural alteration responsible for the impaired synaptic activity in both mutants. Importantly, the characteristic morphological changes in both *hiw* and *unc-104* mutants are mediated by Wnd MAPK pathway overactivation, pinning down an important role of this pathway in regulating synaptic activity.

However *hiw^{ΔN}* and *unc-104^{bris}* mutants have important difference that locomotion behavior of *hiw^{ΔN}* mutant larvae is grossly normal despite of reduced synaptic activity (Wan et al., 2000), but the locomotion speed of *unc-104^{bris}* mutant larvae are severely

reduced, dropping to only 10% of wildtype control (Fig. 13). This can possibly be explained by the functional redundancy of the synaptic structure (Peled and Isacoff, 2011). Under physiological conditions, the still preserved synaptic function in *Wnd* MAPK pathway overactivating NMJ is sufficiency to convey muscle contraction for larvae normal locomotion. However, due to the important function of Kinesin-3/Unc-104 throughout the nervous system, functional impairment may occur to high-order neurons which control motor neurons, and causes the locomotion impairments in *unc-104^{bris}* mutants.

Role of Kinesin-3/Unc-104 in regulating synaptic homeostasis

In the nervous system, homeostatic signaling is an essential feedback mechanism to enable stable synaptic activity in a high variable environment. Homeostatic signaling has been shown to compensate for perturbation of synaptic excitability through multiple mechanisms including changing the efficacy of synaptic vesicle release, ion channel density, neurotransmitter receptor composition, etc. (Frank et al., 2006; Murthy et al., 2001; Thiagarajan et al., 2005; Thiagarajan et al., 2002).

Change in neurotransmitter composition is an important postsynaptic compensation mechanisms involved in synaptic homeostasis regulation. Mutation in the presynaptic AZ protein *DSyd-1* causes reduction in evoked synaptic reaction. Postsynaptic GluRIIA composition increases at *dsyd-1* mutant synapses which may be a compensation effect (Owald et al., 2010). Another study showed that synaptic transmission blockage via presynaptic expression of tetanus toxin leads to higher amount of the GluRIIA at the PSD (Schmid et al., 2008).

Increase in synaptic size also has been shown to be a compensatory effect for reduced synaptic activity (Murthy et al., 2001). Consistently, in this study we showed that blocking synaptic vesicle release via presynaptic tetanus toxin expression increases PSD size when expressed in an otherwise wildtype background. Because tetanus toxin expression also increases GluRIIA clustering at PSD, and high GluRIIA composition is

characteristic for immature synapses (Schmid et al., 2008), blocking synaptic vesicle release may cause prolonged synaptic development, which leads to excessive glutamate receptor incorporation and increased PSD size. Similar mechanism may be conserved in vertebrates and involved in synaptic activity dependent regulation of receptor recruitment during synaptic development and plasticity (Bredt and Nicoll, 2003; Malinow and Malenka, 2002).

Synaptic homeostatic mechanism coordinating pre- and postsynaptic function seems disrupted in *unc-104^{bris}* mutants. Despite the severely impaired presynaptic active zone assembly (Fig. 3), no sign of postsynaptic compensation is observed *unc-104^{bris}* mutants; actually there is a dramatic reduction of GluRIIA clustering at the PSD (Fig. 5). Unlike the increased PSD size in TNT expressing larvae, the severely impaired synaptic activity in *unc-104^{bris}* mutants is not accompanied with any change in average PSD size (Fig. 8 C). These results imply that Kinesin-3/Unc-104 dependent transsynaptic signaling is probably an essential component of a homeostasis mechanism at *Drosophila* NMJ. This notion is further supported by the result that whereas TNT expression in wildtype background increases PSD size, in *unc-104^{bris}* mutants TNT expression leads to decreased PSD size (Fig. 8 C).

It is still not clear if the same disturbance in homeostasis regulation is present in other models with increased Wnd MAPK signaling activity, e.g. in *hiw* mutants and Wnd overexpression larvae. However, observing that MAPK overactivation is responsible for the synaptic morphology in both *unc-104^{bris}* as well as *hiw* mutants, it is very likely that MAPK signaling is part of the synaptic homeostasis pathway regulated by Unc-104/Kinesin-3.

5.5 No sign of synaptic retraction in *unc-104^{bris}* mutants

In *unc-104^{bris}* mutants, despite vast perturbation in synaptic development and severely impaired synaptic activity, synapses continue to exist without obvious sign of synaptic degeneration. The subpopulation of synapses without presynaptic active zone seem to

persist rather than disassemble or degenerate, as the average PSD size of Brp(-) synapses at *unc-104^{bris}* mutant NMJ is larger than that of Brp(-) synapses in wildtype (Fig. 3 E). In contrast, mutation in the *Drosophila* kinesin-1 gene, *khc*, has been shown to cause synaptic retraction at the NMJ (Hurd and Saxton, 1996).

Enhanced MAPK signaling has been shown to promote synaptic stability (Massaro et al., 2009). Loss of presynaptic α -spectrin disrupts microtubule skeleton and leads to synaptic retraction at *Drosophila* NMJ (Pielage et al., 2005). Increasing the Wnd MAPK pathway activity by Fos overexpression or *hiw* mutation similarly suppresses the synaptic retraction in α -spectrin knockdown larvae (Massaro et al., 2009). Therefore, overactivation of MAPK pathway may have the physiological significance of inhibiting synaptic retraction in *unc-104^{bris}* mutants, despite causing the defects in synaptic development.

6. Summary

In this study the synaptic development defect caused by an allele of the *Drosophila* kinesin-3 homolog *unc-104* was investigated. The pre- and postsynaptic development phenotypes caused by a point mutation in the FHA domain of *unc-104* was systematically characterized. Notably, AZ formation in a subset of neuromuscular synapses in the *unc-104^{bris}* mutant larvae were total abolished; major AZ components including Brp, Cac, Liprin- α , etc. are absent from the presynaptic side of these synapses. The interdependence of AZ proteins for their AZ localization was also analyzed and the absence of other AZ components is proved not to be secondary of impaired Brp assembly.

Next the signaling pathway involved in the observed phenotype in the *unc-104^{bris}* mutant was indentified. Downregulation of a Wnd MAPK pathway rescued both the NMJ overgrowth and AZ assembly phenotype in *unc-104^{bris}* mutants. Notably, rescue of these two phenotypes is not achieved via ameliorating axonal transport defect. I found that overactivation of the Wnd MAPK pathway is sufficient to cause the AZ assembly defects resembling that of *unc-104^{bris}* mutants. A major inhibitor of the Wnd MAPK pathway, Hiw, is downregulated in *unc-104^{bris}* mutants, which may be responsible for the Wnd MAPK pathway overactivation.

This study reveals a new function of Kinesin-3/Unc-104 in regulating synaptic assembly, which involves regulation of a Wnd MAPK pathway. These efforts bring new insight to the understanding of mechanisms regulating synaptic development and plasticity.

7. References

- Aberle, H., A.P. Haghghi, R.D. Fetter, B.D. McCabe, T.R. Magalhaes, and C.S. Goodman. 2002. wishful thinking encodes a BMP type II receptor that regulates synaptic growth in *Drosophila*. *Neuron*. 33:545–558.
- Adachi–Yamada, T., M. Nakamura, K. Irie, Y. Tomoyasu, Y. Sano, E. Mori, S. Goto, N. Ueno, Y. Nishida, and K. Matsumoto. 1999. p38 mitogen-activated protein kinase can be involved in transforming growth factor beta superfamily signal transduction in *Drosophila* wing morphogenesis. *Mol Cell Biol*. 19:2322–2329.
- Adams, M.D., S.E. Celniker, R.A. Holt, C.A. Evans, J.D. Gocayne, P.G. Amanatides, S.E. Scherer, P.W. Li, R.A. Hoskins, R.F. Galle, R.A. George, S.E. Lewis, S. Richards, M. Ashburner, S.N. Henderson, G.G. Sutton, J.R. Wortman, M.D. Yandell, Q. Zhang, L.X. Chen, R.C. Brandon, Y.H. Rogers, R.G. Blazej, M. Champe, B.D. Pfeiffer, K.H. Wan, C. Doyle, E.G. Baxter, G. Helt, C.R. Nelson, G.L. Gabor, J.F. Abril, A. Agbayani, H.J. An, C. Andrews–Pfannkoch, D. Baldwin, R.M. Ballew, A. Basu, J. Baxendale, L. Bayraktaroglu, E.M. Beasley, K.Y. Beeson, P.V. Benos, B.P. Berman, D. Bhandari, S. Bolshakov, D. Borkova, M.R. Botchan, J. Bouck, P. Brokstein, P. Brottier, K.C. Burtis, D.A. Busam, H. Butler, E. Cadieu, A. Center, I. Chandra, J.M. Cherry, S. Cawley, C. Dahlke, L.B. Davenport, P. Davies, B. de Pablos, A. Delcher, Z. Deng, A.D. Mays, I. Dew, S.M. Dietz, K. Dodson, L.E. Doup, M. Downes, S. Dugan–Rocha, B.C. Dunkov, P. Dunn, K.J. Durbin, C.C. Evangelista, C. Ferraz, S. Ferriera, W. Fleischmann, C. Fosler, A.E. Gabrielian, N.S. Garg, W.M. Gelbart, K. Glasser, A. Glodek, F. Gong, J.H. Gorrell, Z. Gu, P. Guan, M. Harris, N.L. Harris, D. Harvey, T.J. Heiman, J.R. Hernandez, J. Houck, D. Hostin, K.A. Houston, T.J. Howland, M.H. Wei, C. Ibegwam, et al. 2000. The genome sequence of *Drosophila melanogaster*. *Science*. 287:2185–2195.
- Ahmad–Annuar, A., L. Ciani, I. Simeonidis, J. Herreros, N.B. Fredj, S.B. Rosso, A. Hall, S. Brickley, and P.C. Salinas. 2006. Signaling across the synapse: a role for Wnt and Dishevelled in presynaptic assembly and neurotransmitter release. *J Cell Biol*. 174:127–139.

- Akins, M.R., and T. Biederer. 2006. Cell–cell interactions in synaptogenesis. *Curr Opin Neurobiol.* 16:83–89.
- Ataman, B., J. Ashley, M. Gorczyca, P. Ramachandran, W. Fouquet, S.J. Sigrist, and V. Budnik. 2008. Rapid activity–dependent modifications in synaptic structure and function require bidirectional Wnt signaling. *Neuron.* 57:705–718.
- Bagrodia, S., and R.A. Cerione. 1999. Pak to the future. *Trends Cell Biol.* 9:350–355.
- Bagrodia, S., S.J. Taylor, K.A. Jordon, L. Van Aelst, and R.A. Cerione. 1998. A novel regulator of p21–activated kinases. *J Biol Chem.* 273:23633–23636.
- Banovic, D., O. Khorramshahi, D. Oswald, C. Wichmann, T. Riedt, W. Fouquet, R. Tian, S.J. Sigrist, and H. Aberle. 2010. Drosophila neuroligin 1 promotes growth and postsynaptic differentiation at glutamatergic neuromuscular junctions. *Neuron.* 66:724–738.
- Barkus, R.V., O. Klyachko, D. Horiuchi, B.J. Dickson, and W.M. Saxton. 2008. Identification of an axonal kinesin–3 motor for fast anterograde vesicle transport that facilitates retrograde transport of neuropeptides. *Mol Biol Cell.* 19:274–283.
- Bayat, V., M. Jaiswal, and H.J. Bellen. 2011. The BMP signaling pathway at the Drosophila neuromuscular junction and its links to neurodegenerative diseases. *Curr Opin Neurobiol.* 21:182–188.
- Bellen, H.J., R.W. Levis, G. Liao, Y. He, J.W. Carlson, G. Tsang, M. Evans–Holm, P.R. Hiesinger, K.L. Schulze, G.M. Rubin, R.A. Hoskins, and A.C. Spradling. 2004. The BDGP gene disruption project: single transposon insertions associated with 40% of Drosophila genes. *Genetics.* 167:761–781.
- Benson, D.L., and H. Tanaka. 1998. N–cadherin redistribution during synaptogenesis in hippocampal neurons. *J Neurosci.* 18:6892–6904.
- Biederer, T., and T.C. Sudhof. 2001. CASK and protein 4.1 support F–actin nucleation on neuroligins. *J Biol Chem.* 276:47869–47876.
- Bozdagi, O., M. Valcin, K. Poskanzer, H. Tanaka, and D.L. Benson. 2004. Temporally distinct demands for classic cadherins in synapse formation and maturation. *Mol Cell Neurosci.* 27:509–521.
- Brand, A.H., and N. Perrimon. 1993. Targeted gene expression as a means of altering cell fates and generating dominant phenotypes. *Development.* 118:401–415.

- Bredt, D.S., and R.A. Nicoll. 2003. AMPA receptor trafficking at excitatory synapses. *Neuron*. 40:361–379.
- Bresler, T., M. Shapira, T. Boeckers, T. Dresbach, M. Futter, C.C. Garner, K. Rosenblum, E.D. Gundelfinger, and N.E. Ziv. 2004. Postsynaptic density assembly is fundamentally different from presynaptic active zone assembly. *J Neurosci*. 24:1507–1520.
- Bridgman, P.C. 2004. Myosin-dependent transport in neurons. *J Neurobiol*. 58:164–174.
- Brock, L.G., J.S. Coombs, and J.C. Eccles. 1952. The nature of the monosynaptic excitatory and inhibitory processes in the spinal cord. *Proc R Soc Lond B Biol Sci*. 140:170–176.
- Brouhard, G.J., J.H. Stear, T.L. Noetzel, J. Al-Bassam, K. Kinoshita, S.C. Harrison, J. Howard, and A.A. Hyman. 2008. XMAP215 is a processive microtubule polymerase. *Cell*. 132:79–88.
- Budnik, V., and P.C. Salinas. 2011. Wnt signaling during synaptic development and plasticity. *Curr Opin Neurobiol*. 21:151–159.
- Budreck, E.C., and P. Scheiffele. 2007. Neuroligin-3 is a neuronal adhesion protein at GABAergic and glutamatergic synapses. *Eur J Neurosci*. 26:1738–1748.
- Cai, Q., C. Gerwin, and Z.H. Sheng. 2005. Syntabulin-mediated anterograde transport of mitochondria along neuronal processes. *J Cell Biol*. 170:959–969.
- Cai, Q., P.Y. Pan, and Z.H. Sheng. 2007. Syntabulin-kinesin-1 family member 5B-mediated axonal transport contributes to activity-dependent presynaptic assembly. *J Neurosci*. 27:7284–7296.
- Cai, Q., and Z.H. Sheng. 2009. Molecular motors and synaptic assembly. *Neuroscientist*. 15:78–89.
- Casadio, A., K.C. Martin, M. Giustetto, H. Zhu, M. Chen, D. Bartsch, C.H. Bailey, and E.R. Kandel. 1999. A transient, neuron-wide form of CREB-mediated long-term facilitation can be stabilized at specific synapses by local protein synthesis. *Cell*. 99:221–237.
- Chang, L., and M. Karin. 2001. Mammalian MAP kinase signalling cascades. *Nature*. 410:37–40.
- Chavis, P., and G. Westbrook. 2001. Integrins mediate functional pre- and postsynaptic maturation at a hippocampal synapse. *Nature*. 411:317–321.

- Chen, K., H.Z. Li, N. Ye, J. Zhang, and J.J. Wang. 2005. Role of GABAB receptors in GABA and baclofen-induced inhibition of adult rat cerebellar interpositus nucleus neurons in vitro. *Brain Res Bull.* 67:310–318.
- Chen, X., and B. Ganetzky. 2012. A neuropeptide signaling pathway regulates synaptic growth in *Drosophila*. *J Cell Biol.*
- Chia, P.H., M.R. Patel, and K. Shen. 2012. NAB-1 instructs synapse assembly by linking adhesion molecules and F-actin to active zone proteins. *Nat Neurosci.* 15:234–242.
- Chubykin, A.A., D. Atasoy, M.R. Etherton, N. Brose, E.T. Kavalali, J.R. Gibson, and T.C. Sudhof. 2007. Activity-dependent validation of excitatory versus inhibitory synapses by neuroligin-1 versus neuroligin-2. *Neuron.* 54:919–931.
- Collingridge, G.L., R.W. Olsen, J. Peters, and M. Spedding. 2009. A nomenclature for ligand-gated ion channels. *Neuropharmacology.* 56:2–5.
- Collins, C.A., Y.P. Wairkar, S.L. Johnson, and A. DiAntonio. 2006. Highwire restrains synaptic growth by attenuating a MAP kinase signal. *Neuron.* 51:57–69.
- Coppola, T., S. Magnin-Luthi, V. Perret-Menoud, S. Gattesco, G. Schiavo, and R. Regazzi. 2001. Direct interaction of the Rab3 effector RIM with Ca²⁺ channels, SNAP-25, and synaptotagmin. *J Biol Chem.* 276:32756–32762.
- Couteaux, R., and M. Pecot-Dechavassine. 1970. [Synaptic vesicles and pouches at the level of "active zones" of the neuromuscular junction]. *C R Acad Sci Hebd Seances Acad Sci D.* 271:2346–2349.
- Dai, Y., H. Taru, S.L. Deken, B. Grill, B. Ackley, M.L. Nonet, and Y. Jin. 2006. SYD-2 Liprin- α organizes presynaptic active zone formation through ELKS. *Nat Neurosci.* 9:1479–1487.
- Dalva, M.B., M.A. Takasu, M.Z. Lin, S.M. Shamah, L. Hu, N.W. Gale, and M.E. Greenberg. 2000. EphB receptors interact with NMDA receptors and regulate excitatory synapse formation. *Cell.* 103:945–956.
- Daniels, R.W., C.A. Collins, M.V. Gelfand, J. Dant, E.S. Brooks, D.E. Krantz, and A. DiAntonio. 2004. Increased expression of the *Drosophila* vesicular glutamate transporter leads to excess glutamate release and a compensatory decrease in quantal content. *J Neurosci.* 24:10466–10474.

- Davis, G.W., C.M. Schuster, and C.S. Goodman. 1997. Genetic analysis of the mechanisms controlling target selection: target-derived Fasciclin II regulates the pattern of synapse formation. *Neuron*. 19:561–573.
- Dent, E.W., J.L. Callaway, G. Szebenyi, P.W. Baas, and K. Kalil. 1999. Reorganization and movement of microtubules in axonal growth cones and developing interstitial branches. *J Neurosci*. 19:8894–8908.
- Derynck, R., R.J. Akhurst, and A. Balmain. 2001. TGF- β signaling in tumor suppression and cancer progression. *Nat Genet*. 29:117–129.
- DiAntonio, A., S.A. Petersen, M. Heckmann, and C.S. Goodman. 1999. Glutamate receptor expression regulates quantal size and quantal content at the *Drosophila* neuromuscular junction. *J Neurosci*. 19:3023–3032.
- Dick, O., S. tom Dieck, W.D. Altmann, J. Ammermüller, R. Weiler, C.C. Garner, E.D. Gundelfinger, and J.H. Brandstätter. 2003. The presynaptic active zone protein bassoon is essential for photoreceptor ribbon synapse formation in the retina. *Neuron*. 37:775–786.
- Diefenbach, R.J., E. Diefenbach, M.W. Douglas, and A.L. Cunningham. 2002. The heavy chain of conventional kinesin interacts with the SNARE proteins SNAP25 and SNAP23. *Biochemistry*. 41:14906–14915.
- Eaton, B.A., and G.W. Davis. 2005. LIM Kinase1 controls synaptic stability downstream of the type II BMP receptor. *Neuron*. 47:695–708.
- Eglen, R.M. 2006. Muscarinic receptor subtypes in neuronal and non-neuronal cholinergic function. *Auton Autacoid Pharmacol*. 26:219–233.
- Eresh, S., J. Riese, D.B. Jackson, D. Bohmann, and M. Bienz. 1997. A CREB-binding site as a target for decapentaplegic signalling during *Drosophila* endoderm induction. *EMBO J*. 16:2014–2022.
- Fannon, A.M., and D.R. Colman. 1996. A model for central synaptic junctional complex formation based on the differential adhesive specificities of the cadherins. *Neuron*. 17:423–434.
- Farias, G.G., I.E. Alfaro, W. Cerpa, C.P. Grabowski, J.A. Godoy, C. Bonansco, and N.C. Inestrosa. 2009. Wnt-5a/JNK signaling promotes the clustering of PSD-95 in hippocampal neurons. *J Biol Chem*. 284:15857–15866.
- Fenster, S.D., W.J. Chung, R. Zhai, C. Cases-Langhoff, B. Voss, A.M. Garner, U. Kaempfer, S. Kindler, E.D. Gundelfinger, and C.C. Garner. 2000. Piccolo, a

- presynaptic zinc finger protein structurally related to bassoon. *Neuron*. 25:203–214.
- Ferreira, A., and S. Paganoni. 2002. The formation of synapses in the central nervous system. *Mol Neurobiol*. 26:69–79.
- Fischer, M., T. Raabe, M. Heisenberg, and M. Sendtner. 2009. Drosophila RSK negatively regulates bouton number at the neuromuscular junction. *Dev Neurobiol*. 69:212–220.
- Fogel, A.I., M.R. Akins, A.J. Krupp, M. Stagi, V. Stein, and T. Biederer. 2007. SynCAMs organize synapses through heterophilic adhesion. *J Neurosci*. 27:12516–12530.
- Fouquet, W., D. Oswald, C. Wichmann, S. Mertel, H. Depner, M. Dyba, S. Hallermann, R.J. Kittel, S. Eimer, and S.J. Sigrist. 2009. Maturation of active zone assembly by Drosophila Bruchpilot. *J Cell Biol*. 186:129–145.
- Frank, C.A., M.J. Kennedy, C.P. Goold, K.W. Marek, and G.W. Davis. 2006. Mechanisms underlying the rapid induction and sustained expression of synaptic homeostasis. *Neuron*. 52:663–677.
- Fransson, A., A. Ruusala, and P. Aspenstrom. 2003. Atypical Rho GTPases have roles in mitochondrial homeostasis and apoptosis. *J Biol Chem*. 278:6495–6502.
- Fuger, P., L.B. Behrends, S. Mertel, S.J. Sigrist, and T.M. Rasse. 2007. Live imaging of synapse development and measuring protein dynamics using two-color fluorescence recovery after photo-bleaching at Drosophila synapses. *Nat Protoc*. 2:3285–3298.
- Gardoni, F., L.H. Schrama, A. Kamal, W.H. Gispen, F. Cattabeni, and M. Di Luca. 2001. Hippocampal synaptic plasticity involves competition between Ca²⁺/calmodulin-dependent protein kinase II and postsynaptic density 95 for binding to the NR2A subunit of the NMDA receptor. *J Neurosci*. 21:1501–1509.
- Giustetto, M., A.N. Hegde, K. Si, A. Casadio, K. Inokuchi, W. Pei, E.R. Kandel, and J.H. Schwartz. 2003. Axonal transport of eukaryotic translation elongation factor 1alpha mRNA couples transcription in the nucleus to long-term facilitation at the synapse. *Proc Natl Acad Sci U S A*. 100:13680–13685.
- Glater, E.E., L.J. Megeath, R.S. Stowers, and T.L. Schwarz. 2006. Axonal transport of mitochondria requires milton to recruit kinesin heavy chain and is light chain independent. *J Cell Biol*. 173:545–557.

- Gong, Y., and C.F. Lippa. 2010. Review: disruption of the postsynaptic density in Alzheimer's disease and other neurodegenerative dementias. *Am J Alzheimers Dis Other Demen.* 25:547–555.
- Graf, E.R., R.W. Daniels, R.W. Burgess, T.L. Schwarz, and A. DiAntonio. 2009. Rab3 dynamically controls protein composition at active zones. *Neuron.* 64:663–677.
- Graf, E.R., X. Zhang, S.X. Jin, M.W. Linhoff, and A.M. Craig. 2004. Neurexins induce differentiation of GABA and glutamate postsynaptic specializations via neuroligins. *Cell.* 119:1013–1026.
- Guillaud, L., M. Setou, and N. Hirokawa. 2003. KIF17 dynamics and regulation of NR2B trafficking in hippocampal neurons. *J Neurosci.* 23:131–140.
- Gyoeva, F.K., D.V. Sarkisov, A.L. Khodjakov, and A.A. Minin. 2004. The tetrameric molecule of conventional kinesin contains identical light chains. *Biochemistry.* 43:13525–13531.
- Hakimi, M.A., D.W. Speicher, and R. Shiekhatar. 2002. The motor protein kinesin-1 links neurofibromin and merlin in a common cellular pathway of neurofibromatosis. *J Biol Chem.* 277:36909–36912.
- Hall, A.C., F.R. Lucas, and P.C. Salinas. 2000. Axonal remodeling and synaptic differentiation in the cerebellum is regulated by WNT-7a signaling. *Cell.* 100:525–535.
- Hall, D.H., and E.M. Hedgecock. 1991. Kinesin-related gene unc-104 is required for axonal transport of synaptic vesicles in *C. elegans*. *Cell.* 65:837–847.
- Hallam, S.J., A. Goncharov, J. McEwen, R. Baran, and Y. Jin. 2002. SYD-1, a presynaptic protein with PDZ, C2 and rhoGAP-like domains, specifies axon identity in *C. elegans*. *Nat Neurosci.* 5:1137–1146.
- Hallermann, S., R.J. Kittel, C. Wichmann, A. Weyhersmuller, W. Fouquet, S. Mertel, D. Oswald, S. Eimer, H. Depner, M. Schwarzel, S.J. Sigrist, and M. Heckmann. 2010. Naked dense bodies provoke depression. *J Neurosci.* 30:14340–14345.
- Han, Y., P.S. Kaeser, T.C. Sudhof, and R. Schneggenburger. 2011. RIM determines Ca²⁺ channel density and vesicle docking at the presynaptic active zone. *Neuron.* 69:304–316.

- Harlow, M.L., D. Ress, A. Stoschek, R.M. Marshall, and U.J. McMahan. 2001. The architecture of active zone material at the frog's neuromuscular junction. *Nature*. 409:479–484.
- Hata, Y., S. Butz, and T.C. Sudhof. 1996. CASK: a novel dlg/PSD95 homolog with an N-terminal calmodulin-dependent protein kinase domain identified by interaction with neurexins. *J Neurosci*. 16:2488–2494.
- Henriquez, J.P., A. Webb, M. Bence, H. Bildsoe, M. Sahores, S.M. Hughes, and P.C. Salinas. 2008. Wnt signaling promotes AChR aggregation at the neuromuscular synapse in collaboration with agrin. *Proc Natl Acad Sci U S A*. 105:18812–18817.
- Hibino, H., R. Pironkova, O. Onwumere, M. Vologodskaja, A.J. Hudspeth, and F. Lesage. 2002. RIM binding proteins (RBPs) couple Rab3-interacting molecules (RIMs) to voltage-gated Ca(2+) channels. *Neuron*. 34:411–423.
- Hirokawa, N., and Y. Noda. 2008. Intracellular transport and kinesin superfamily proteins, KIFs: structure, function, and dynamics. *Physiol Rev*. 88:1089–1118.
- Horiuchi, D., C.A. Collins, P. Bhat, R.V. Barkus, A. Diantonio, and W.M. Saxton. 2007. Control of a kinesin-cargo linkage mechanism by JNK pathway kinases. *Curr Biol*. 17:1313–1317.
- Howard, J., and A.A. Hyman. 2009. Growth, fluctuation and switching at microtubule plus ends. *Nat Rev Mol Cell Biol*. 10:569–574.
- Hsu, C.C., J.D. Moncaleano, and O.I. Wagner. 2011. Sub-cellular distribution of UNC-104(KIF1A) upon binding to adaptors as UNC-16(JIP3), DNC-1(DCTN1/Glued) and SYD-2(Liprin-alpha) in *C. elegans* neurons. *Neuroscience*. 176:39–52.
- Hurd, D.D., and W.M. Saxton. 1996. Kinesin mutations cause motor neuron disease phenotypes by disrupting fast axonal transport in *Drosophila*. *Genetics*. 144:1075–1085.
- Impey, S., K. Obrietan, and D.R. Storm. 1999. Making new connections: role of ERK/MAP kinase signaling in neuronal plasticity. *Neuron*. 23:11–14.
- Inoue, A., and J.R. Sanes. 1997. Lamina-specific connectivity in the brain: regulation by N-cadherin, neurotrophins, and glycoconjugates. *Science*. 276:1428–1431.

- Irie, M., Y. Hata, M. Takeuchi, K. Ichtchenko, A. Toyoda, K. Hirao, Y. Takai, T.W. Rosahl, and T.C. Sudhof. 1997. Binding of neuroligins to PSD-95. *Science*. 277:1511-1515.
- Ito, M., K. Yoshioka, M. Akechi, S. Yamashita, N. Takamatsu, K. Sugiyama, M. Hibi, Y. Nakabeppu, T. Shiba, and K.I. Yamamoto. 1999. JSAP1, a novel jun N-terminal protein kinase (JNK)-binding protein that functions as a Scaffold factor in the JNK signaling pathway. *Mol Cell Biol*. 19:7539-7548.
- Jahn, R., T. Lang, and T.C. Sudhof. 2003. Membrane fusion. *Cell*. 112:519-533.
- Jin, Y. 2005. Synaptogenesis. *WormBook*:1-11.
- Jing, L., J.L. Lefebvre, L.R. Gordon, and M. Granato. 2009. Wnt signals organize synaptic prepatterning and axon guidance through the zebrafish unplugged/MuSK receptor. *Neuron*. 61:721-733.
- Johnson, E.L., 3rd, R.D. Fetter, and G.W. Davis. 2009. Negative regulation of active zone assembly by a newly identified SR protein kinase. *PLoS Biol*. 7:e1000193.
- Jover-Mengual, T., R.S. Zukin, and A.M. Etgen. 2007. MAPK signaling is critical to estradiol protection of CA1 neurons in global ischemia. *Endocrinology*. 148:1131-1143.
- Kaesler, P.S., L. Deng, Y. Wang, I. Dulubova, X. Liu, J. Rizo, and T.C. Sudhof. 2011. RIM proteins tether Ca²⁺ channels to presynaptic active zones via a direct PDZ-domain interaction. *Cell*. 144:282-295.
- Kamm, C., H. Boston, J. Hewett, J. Wilbur, D.P. Corey, P.I. Hanson, V. Ramesh, and X.O. Breakefield. 2004. The early onset dystonia protein torsinA interacts with kinesin light chain 1. *J Biol Chem*. 279:19882-19892.
- Kaufmann, N., J. DeProto, R. Ranjan, H. Wan, and D. Van Vactor. 2002. Drosophila liprin-alpha and the receptor phosphatase Dlar control synapse morphogenesis. *Neuron*. 34:27-38.
- Kawasaki, F., and R.W. Ordway. 2009. Molecular mechanisms determining conserved properties of short-term synaptic depression revealed in NSF and SNAP-25 conditional mutants. *Proc Natl Acad Sci U S A*. 106:14658-14663.
- Kawasaki, F., B. Zou, X. Xu, and R.W. Ordway. 2004. Active zone localization of presynaptic calcium channels encoded by the cacophony locus of Drosophila. *J Neurosci*. 24:282-285.

- Kim, E., M. Niethammer, A. Rothschild, Y.N. Jan, and M. Sheng. 1995. Clustering of Shaker-type K⁺ channels by interaction with a family of membrane-associated guanylate kinases. *Nature*. 378:85–88.
- Kim, E., and M. Sheng. 2004. PDZ domain proteins of synapses. *Nat Rev Neurosci*. 5:771–781.
- Kim, S.M., V. Kumar, Y.Q. Lin, S. Karunanithi, and M. Ramaswami. 2009. Fos and Jun potentiate individual release sites and mobilize the reserve synaptic vesicle pool at the *Drosophila* larval motor synapse. *Proc Natl Acad Sci U S A*. 106:4000–4005.
- Kittel, R.J., C. Wichmann, T.M. Rasse, W. Fouquet, M. Schmidt, A. Schmid, D.A. Wagh, C. Pawlu, R.R. Kellner, K.I. Willig, S.W. Hell, E. Buchner, M. Heckmann, and S.J. Sigrist. 2006. Bruchpilot promotes active zone assembly, Ca²⁺ channel clustering, and vesicle release. *Science*. 312:1051–1054.
- Klassen, M.P., and K. Shen. 2007. Wnt signaling positions neuromuscular connectivity by inhibiting synapse formation in *C. elegans*. *Cell*. 130:704–716.
- Ko, J., M. Na, S. Kim, J.R. Lee, and E. Kim. 2003. Interaction of the ERC family of RIM-binding proteins with the liprin- α family of multidomain proteins. *J Biol Chem*. 278:42377–42385.
- Koh, Y.H., C. Ruiz-Canada, M. Gorczyca, and V. Budnik. 2002. The Ras1-mitogen-activated protein kinase signal transduction pathway regulates synaptic plasticity through fasciclin II-mediated cell adhesion. *J Neurosci*. 22:2496–2504.
- Kohsaka, H., E. Takasu, and A. Nose. 2007. In vivo induction of postsynaptic molecular assembly by the cell adhesion molecule Fasciclin2. *J Cell Biol*. 179:1289–1300.
- Kumar, J., B.C. Choudhary, R. Metpally, Q. Zheng, M.L. Nonet, S. Ramanathan, D.R. Klopfenstein, and S.P. Koushika. 2010. The *Caenorhabditis elegans* Kinesin-3 motor UNC-104/KIF1A is degraded upon loss of specific binding to cargo. *PLoS Genet*. 6:e1001200.
- Lardi-Studler, B., and J.M. Fritschy. 2007. Matching of pre- and postsynaptic specializations during synaptogenesis. *Neuroscientist*. 13:115–126.

- Lee, C.H., T. Herman, T.R. Clandinin, R. Lee, and S.L. Zipursky. 2001. N-cadherin regulates target specificity in the *Drosophila* visual system. *Neuron*. 30:437–450.
- Lee, J.R., H. Shin, J. Choi, J. Ko, S. Kim, H.W. Lee, K. Kim, S.H. Rho, J.H. Lee, H.E. Song, S.H. Eom, and E. Kim. 2004. An intramolecular interaction between the FHA domain and a coiled coil negatively regulates the kinesin motor KIF1A. *EMBO J*. 23:1506–1515.
- Lee, R.C., T.R. Clandinin, C.H. Lee, P.L. Chen, I.A. Meinertzhagen, and S.L. Zipursky. 2003. The protocadherin Flamingo is required for axon target selection in the *Drosophila* visual system. *Nat Neurosci*. 6:557–563.
- Lenzi, D., and H. von Gersdorff. 2001. Structure suggests function: the case for synaptic ribbons as exocytotic nanomachines. *Bioessays*. 23:831–840.
- Li, J., J. Ashley, V. Budnik, and M.A. Bhat. 2007. Crucial role of *Drosophila* neurexin in proper active zone apposition to postsynaptic densities, synaptic growth, and synaptic transmission. *Neuron*. 55:741–755.
- Liu, K.S., M. Siebert, S. Mertel, E. Knoche, S. Wegener, C. Wichmann, T. Matkovic, K. Muhammad, H. Depner, C. Mettke, J. Buckers, S.W. Hell, M. Muller, G.W. Davis, D. Schmitz, and S.J. Sigrist. 2011. RIM-binding protein, a central part of the active zone, is essential for neurotransmitter release. *Science*. 334:1565–1569.
- Lo, K.Y., A. Kuzmin, S.M. Unger, J.D. Petersen, and M.A. Silverman. 2011. KIF1A is the primary anterograde motor protein required for the axonal transport of dense-core vesicles in cultured hippocampal neurons. *Neurosci Lett*. 491:168–173.
- Lucas, F.R., R.G. Goold, P.R. Gordon-Weeks, and P.C. Salinas. 1998. Inhibition of GSK-3 β leading to the loss of phosphorylated MAP-1B is an early event in axonal remodelling induced by WNT-7a or lithium. *J Cell Sci*. 111 (Pt 10):1351–1361.
- Luo, Z.G., Q. Wang, J.Z. Zhou, J. Wang, Z. Luo, M. Liu, X. He, A. Wynshaw-Boris, W.C. Xiong, B. Lu, and L. Mei. 2002. Regulation of AChR clustering by Dishevelled interacting with MuSK and PAK1. *Neuron*. 35:489–505.
- MacAskill, A.F., K. Brickley, F.A. Stephenson, and J.T. Kittler. 2009. GTPase dependent recruitment of Grif-1 by Miro1 regulates mitochondrial trafficking in hippocampal neurons. *Mol Cell Neurosci*. 40:301–312.

- Malinow, R., and R.C. Malenka. 2002. AMPA receptor trafficking and synaptic plasticity. *Annu Rev Neurosci.* 25:103–126.
- Manser, E., T.H. Loo, C.G. Koh, Z.S. Zhao, X.Q. Chen, L. Tan, I. Tan, T. Leung, and L. Lim. 1998. PAK kinases are directly coupled to the PIX family of nucleotide exchange factors. *Mol Cell.* 1:183–192.
- Marques, G., H. Bao, T.E. Haerry, M.J. Shimell, P. Duchek, B. Zhang, and M.B. O'Connor. 2002. The Drosophila BMP type II receptor Wishful Thinking regulates neuromuscular synapse morphology and function. *Neuron.* 33:529–543.
- Marrus, S.B., S.L. Portman, M.J. Allen, K.G. Moffat, and A. DiAntonio. 2004. Differential localization of glutamate receptor subunits at the Drosophila neuromuscular junction. *J Neurosci.* 24:1406–1415.
- Massague, J., and D. Wotton. 2000. Transcriptional control by the TGF-beta/Smad signaling system. *EMBO J.* 19:1745–1754.
- Massaro, C.M., J. Pielage, and G.W. Davis. 2009. Molecular mechanisms that enhance synapse stability despite persistent disruption of the spectrin/ankyrin/microtubule cytoskeleton. *J Cell Biol.* 187:101–117.
- McCabe, B.D., S. Hom, H. Aberle, R.D. Fetter, G. Marques, T.E. Haerry, H. Wan, M.B. O'Connor, C.S. Goodman, and A.P. Haghghi. 2004. Highwire regulates presynaptic BMP signaling essential for synaptic growth. *Neuron.* 41:891–905.
- McCabe, B.D., G. Marques, A.P. Haghghi, R.D. Fetter, M.L. Crotty, T.E. Haerry, C.S. Goodman, and M.B. O'Connor. 2003. The BMP homolog Gbb provides a retrograde signal that regulates synaptic growth at the Drosophila neuromuscular junction. *Neuron.* 39:241–254.
- McGuire, J.R., J. Rong, S.H. Li, and X.J. Li. 2006. Interaction of Huntingtin-associated protein-1 with kinesin light chain: implications in intracellular trafficking in neurons. *J Biol Chem.* 281:3552–3559.
- McLachlan, E.M., and A.R. Martin. 1981. Non-linear summation of end-plate potentials in the frog and mouse. *J Physiol.* 311:307–324.
- Medina, P.M., L.L. Swick, R. Andersen, Z. Blalock, and J.E. Brenman. 2006. A novel forward genetic screen for identifying mutations affecting larval neuronal dendrite development in *Drosophila melanogaster*. *Genetics.* 172:2325–2335.

- Miki, H., M. Setou, K. Kaneshiro, and N. Hirokawa. 2001. All kinesin superfamily protein, KIF, genes in mouse and human. *Proc Natl Acad Sci U S A*. 98:7004–7011.
- Miller, B.R., C. Press, R.W. Daniels, Y. Sasaki, J. Milbrandt, and A. DiAntonio. 2009. A dual leucine kinase-dependent axon self-destruction program promotes Wallerian degeneration. *Nat Neurosci*. 12:387–389.
- Miller, K.E., J. DeProto, N. Kaufmann, B.N. Patel, A. Duckworth, and D. Van Vactor. 2005. Direct observation demonstrates that Liprin-alpha is required for trafficking of synaptic vesicles. *Curr Biol*. 15:684–689.
- Morris, R.L., and P.J. Hollenbeck. 1993. The regulation of bidirectional mitochondrial transport is coordinated with axonal outgrowth. *J Cell Sci*. 104 (Pt 3):917–927.
- Moustakas, A., S. Souchelnytskyi, and C.H. Heldin. 2001. Smad regulation in TGF-beta signal transduction. *J Cell Sci*. 114:4359–4369.
- Murthy, V.N., T. Schikorski, C.F. Stevens, and Y. Zhu. 2001. Inactivity produces increases in neurotransmitter release and synapse size. *Neuron*. 32:673–682.
- Naisbitt, S., E. Kim, J.C. Tu, B. Xiao, C. Sala, J. Valtschanoff, R.J. Weinberg, P.F. Worley, and M. Sheng. 1999. Shank, a novel family of postsynaptic density proteins that binds to the NMDA receptor/PSD-95/GKAP complex and cortactin. *Neuron*. 23:569–582.
- Nakata, K., B. Abrams, B. Grill, A. Goncharov, X. Huang, A.D. Chisholm, and Y. Jin. 2005. Regulation of a DLK-1 and p38 MAP kinase pathway by the ubiquitin ligase RPM-1 is required for presynaptic development. *Cell*. 120:407–420.
- Nam, C.I., and L. Chen. 2005. Postsynaptic assembly induced by neurexin-neurologin interaction and neurotransmitter. *Proc Natl Acad Sci U S A*. 102:6137–6142.
- Nieratschker, V., A. Schubert, M. Jauch, N. Bock, D. Bucher, S. Dippacher, G. Krohne, E. Asan, S. Buchner, and E. Buchner. 2009. Bruchpilot in ribbon-like axonal agglomerates, behavioral defects, and early death in SRPK79D kinase mutants of *Drosophila*. *PLoS Genet*. 5:e1000700.
- Niethammer, M., E. Kim, and M. Sheng. 1996. Interaction between the C terminus of NMDA receptor subunits and multiple members of the PSD-

- 95 family of membrane-associated guanylate kinases. *J Neurosci.* 16:2157–2163.
- Ohtsuka, T., E. Takao-Rikitsu, E. Inoue, M. Inoue, M. Takeuchi, K. Matsubara, M. Deguchi-Tawarada, K. Satoh, K. Morimoto, H. Nakanishi, and Y. Takai. 2002. Cast: a novel protein of the cytomatrix at the active zone of synapses that forms a ternary complex with RIM1 and munc13-1. *J Cell Biol.* 158:577–590.
- Owald, D., W. Fouquet, M. Schmidt, C. Wichmann, S. Mertel, H. Depner, F. Christiansen, C. Zube, C. Quentin, J. Korner, H. Urlaub, K. Mechtler, and S.J. Sigrist. 2010. A Syd-1 homologue regulates pre- and postsynaptic maturation in *Drosophila*. *J Cell Biol.* 188:565–579.
- Owald, D., and S.J. Sigrist. 2009. Assembling the presynaptic active zone. *Curr Opin Neurobiol.* 19:311–318.
- Pack-Chung, E., P.T. Kurshan, D.K. Dickman, and T.L. Schwarz. 2007. A *Drosophila* kinesin required for synaptic bouton formation and synaptic vesicle transport. *Nat Neurosci.* 10:980–989.
- Packard, M., E.S. Koo, M. Gorczyca, J. Sharpe, S. Cumberledge, and V. Budnik. 2002. The *Drosophila* Wnt, wingless, provides an essential signal for pre- and postsynaptic differentiation. *Cell.* 111:319–330.
- Packard, M., D. Mathew, and V. Budnik. 2003. FAST remodeling of synapses in *Drosophila*. *Curr Opin Neurobiol.* 13:527–534.
- Park, E., M. Na, J. Choi, S. Kim, J.R. Lee, J. Yoon, D. Park, M. Sheng, and E. Kim. 2003. The Shank family of postsynaptic density proteins interacts with and promotes synaptic accumulation of the beta PIX guanine nucleotide exchange factor for Rac1 and Cdc42. *J Biol Chem.* 278:19220–19229.
- Patel, M.R., E.K. Lehrman, V.Y. Poon, J.G. Crump, M. Zhen, C.I. Bargmann, and K. Shen. 2006. Hierarchical assembly of presynaptic components in defined *C. elegans* synapses. *Nat Neurosci.* 9:1488–1498.
- Patel, M.R., and K. Shen. 2009. RSY-1 is a local inhibitor of presynaptic assembly in *C. elegans*. *Science.* 323:1500–1503.
- Peled, E.S., and E.Y. Isacoff. 2011. Optical quantal analysis of synaptic transmission in wild-type and rab3-mutant *Drosophila* motor axons. *Nat Neurosci.* 14:519–526.
- Petersen, S.A., R.D. Fetter, J.N. Noordermeer, C.S. Goodman, and A. DiAntonio. 1997. Genetic analysis of glutamate receptors in *Drosophila* reveals a

- retrograde signal regulating presynaptic transmitter release. *Neuron*. 19:1237–1248.
- Phillips, G.R., H. Tanaka, M. Frank, A. Elste, L. Fidler, D.L. Benson, and D.R. Colman. 2003. Gamma-protocadherins are targeted to subsets of synapses and intracellular organelles in neurons. *J Neurosci*. 23:5096–5104.
- Pielage, J., R.D. Fetter, and G.W. Davis. 2005. Presynaptic spectrin is essential for synapse stabilization. *Curr Biol*. 15:918–928.
- Pin, J.P., and F. Acher. 2002. The metabotropic glutamate receptors: structure, activation mechanism and pharmacology. *Curr Drug Targets CNS Neurol Disord*. 1:297–317.
- Qin, G., T. Schwarz, R.J. Kittel, A. Schmid, T.M. Rasse, D. Kappei, E. Ponimaskin, M. Heckmann, and S.J. Sigrist. 2005. Four different subunits are essential for expressing the synaptic glutamate receptor at neuromuscular junctions of *Drosophila*. *J Neurosci*. 25:3209–3218.
- Rao, S., C. Lang, E.S. Levitan, and D.L. Deitcher. 2001. Visualization of neuropeptide expression, transport, and exocytosis in *Drosophila melanogaster*. *J Neurobiol*. 49:159–172.
- Rasse, T.M., W. Fouquet, A. Schmid, R.J. Kittel, S. Mertel, C.B. Sigrist, M. Schmidt, A. Guzman, C. Merino, G. Qin, C. Quentin, F.F. Madeo, M. Heckmann, and S.J. Sigrist. 2005. Glutamate receptor dynamics organizing synapse formation in vivo. *Nat Neurosci*. 8:898–905.
- Rawson, J.M., M. Lee, E.L. Kennedy, and S.B. Selleck. 2003. *Drosophila* neuromuscular synapse assembly and function require the TGF- β type I receptor saxophone and the transcription factor Mad. *J Neurobiol*. 55:134–150.
- Rebola, N., B.N. Srikumar, and C. Mulle. 2010. Activity-dependent synaptic plasticity of NMDA receptors. *J Physiol*. 588:93–99.
- Rizo, J. 2003. SNARE function revisited. *Nat Struct Biol*. 10:417–419.
- Rizo, J., and C. Rosenmund. 2008. Synaptic vesicle fusion. *Nat Struct Mol Biol*. 15:665–674.
- Robitaille, R., E.M. Adler, and M.P. Charlton. 1990. Strategic location of calcium channels at transmitter release sites of frog neuromuscular synapses. *Neuron*. 5:773–779.

- Roos, J., T. Hummel, N. Ng, C. Klambt, and G.W. Davis. 2000. Drosophila Futsch regulates synaptic microtubule organization and is necessary for synaptic growth. *Neuron*. 26:371–382.
- Rougon, G., and O. Hobert. 2003. New insights into the diversity and function of neuronal immunoglobulin superfamily molecules. *Annu Rev Neurosci*. 26:207–238.
- Rumbaugh, G., J.P. Adams, J.H. Kim, and R.L. Huganir. 2006. SynGAP regulates synaptic strength and mitogen-activated protein kinases in cultured neurons. *Proc Natl Acad Sci U S A*. 103:4344–4351.
- Sahores, M., A. Gibb, and P.C. Salinas. 2010. Frizzled-5, a receptor for the synaptic organizer Wnt7a, regulates activity-mediated synaptogenesis. *Development*. 137:2215–2225.
- Sala, C., V. Piech, N.R. Wilson, M. Passafaro, G. Liu, and M. Sheng. 2001. Regulation of dendritic spine morphology and synaptic function by Shank and Homer. *Neuron*. 31:115–130.
- Samson, R.D., and D. Pare. 2005. Activity-dependent synaptic plasticity in the central nucleus of the amygdala. *J Neurosci*. 25:1847–1855.
- Santos, M.S., H. Li, and S.M. Voglmaier. 2009. Synaptic vesicle protein trafficking at the glutamate synapse. *Neuroscience*. 158:189–203.
- Schaefer, A.M., G.D. Hadwiger, and M.L. Nonet. 2000. rpm-1, a conserved neuronal gene that regulates targeting and synaptogenesis in *C. elegans*. *Neuron*. 26:345–356.
- Scheiffele, P. 2003. Cell-cell signaling during synapse formation in the CNS. *Annu Rev Neurosci*. 26:485–508.
- Scheiffele, P., J. Fan, J. Choih, R. Fetter, and T. Serafini. 2000. Neuroligin expressed in nonneuronal cells triggers presynaptic development in contacting axons. *Cell*. 101:657–669.
- Schmid, A., S. Hallermann, R.J. Kittel, O. Khorramshahi, A.M. Frolich, C. Quentin, T.M. Rasse, S. Mertel, M. Heckmann, and S.J. Sigrist. 2008. Activity-dependent site-specific changes of glutamate receptor composition in vivo. *Nat Neurosci*. 11:659–666.
- Schulze, K.L., K. Broadie, M.S. Perin, and H.J. Bellen. 1995. Genetic and electrophysiological studies of Drosophila syntaxin-1A demonstrate its role in nonneuronal secretion and neurotransmission. *Cell*. 80:311–320.

- Setou, M., T. Nakagawa, D.H. Seog, and N. Hirokawa. 2000. Kinesin superfamily motor protein KIF17 and mLin-10 in NMDA receptor-containing vesicle transport. *Science*. 288:1796–1802.
- Setou, M., D.H. Seog, Y. Tanaka, Y. Kanai, Y. Takei, M. Kawagishi, and N. Hirokawa. 2002. Glutamate-receptor-interacting protein GRIP1 directly steers kinesin to dendrites. *Nature*. 417:83–87.
- Shapira, M., R.G. Zhai, T. Dresbach, T. Bresler, V.I. Torres, E.D. Gundelfinger, N.E. Ziv, and C.C. Garner. 2003. Unitary assembly of presynaptic active zones from Piccolo-Bassoon transport vesicles. *Neuron*. 38:237–252.
- Shapiro, L., and D.R. Colman. 1999. The diversity of cadherins and implications for a synaptic adhesive code in the CNS. *Neuron*. 23:427–430.
- Shen, K., and C.I. Bargmann. 2003. The immunoglobulin superfamily protein SYG-1 determines the location of specific synapses in *C. elegans*. *Cell*. 112:619–630.
- Shen, K., R.D. Fetter, and C.I. Bargmann. 2004. Synaptic specificity is generated by the synaptic guidepost protein SYG-2 and its receptor, SYG-1. *Cell*. 116:869–881.
- Shen, W., and B. Ganetzky. 2009. Autophagy promotes synapse development in *Drosophila*. *J Cell Biol*. 187:71–79.
- Shepherd, G.M., and K.M. Harris. 1998. Three-dimensional structure and composition of CA3→CA1 axons in rat hippocampal slices: implications for presynaptic connectivity and compartmentalization. *J Neurosci*. 18:8300–8310.
- Song, J.Y., K. Ichtchenko, T.C. Sudhof, and N. Brose. 1999. Neuroligin 1 is a postsynaptic cell-adhesion molecule of excitatory synapses. *Proc Natl Acad Sci U S A*. 96:1100–1105.
- Sorra, K.E., A. Mishra, S.A. Kirov, and K.M. Harris. 2006. Dense core vesicles resemble active-zone transport vesicles and are diminished following synaptogenesis in mature hippocampal slices. *Neuroscience*. 141:2097–2106.
- Stewart, B.A., H.L. Atwood, J.J. Renger, J. Wang, and C.F. Wu. 1994. Improved stability of *Drosophila* larval neuromuscular preparations in haemolymph-like physiological solutions. *J Comp Physiol A*. 175:179–191.

- Stigloher, C., H. Zhan, M. Zhen, J. Richmond, and J.L. Bessereau. 2011. The presynaptic dense projection of the *Caenorhabditis elegans* cholinergic neuromuscular junction localizes synaptic vesicles at the active zone through SYD-2/liprin and UNC-10/RIM-dependent interactions. *J Neurosci.* 31:4388–4396.
- Stone, M.C., M.M. Nguyen, J. Tao, D.L. Allender, and M.M. Rolls. 2010. Global up-regulation of microtubule dynamics and polarity reversal during regeneration of an axon from a dendrite. *Mol Biol Cell.* 21:767–777.
- Stowers, R.S., L.J. Megeath, J. Gorska-Andrzejak, I.A. Meinertzhagen, and T.L. Schwarz. 2002. Axonal transport of mitochondria to synapses depends on Milton, a novel *Drosophila* protein. *Neuron.* 36:1063–1077.
- Strack, S., S. Choi, D.M. Lovinger, and R.J. Colbran. 1997. Translocation of autophosphorylated calcium/calmodulin-dependent protein kinase II to the postsynaptic density. *J Biol Chem.* 272:13467–13470.
- Su, Q., Q. Cai, C. Gerwin, C.L. Smith, and Z.H. Sheng. 2004. Syntabulin is a microtubule-associated protein implicated in syntaxin transport in neurons. *Nat Cell Biol.* 6:941–953.
- Sudhof, T.C. 2008. Neuroligins and neurexins link synaptic function to cognitive disease. *Nature.* 455:903–911.
- Takao-Rikitsu, E., S. Mochida, E. Inoue, M. Deguchi-Tawarada, M. Inoue, T. Ohtsuka, and Y. Takai. 2004. Physical and functional interaction of the active zone proteins, CAST, RIM1, and Bassoon, in neurotransmitter release. *J Cell Biol.* 164:301–311.
- Tanaka, Y., Y. Kanai, Y. Okada, S. Nonaka, S. Takeda, A. Harada, and N. Hirokawa. 1998. Targeted disruption of mouse conventional kinesin heavy chain, kif5B, results in abnormal perinuclear clustering of mitochondria. *Cell.* 93:1147–1158.
- Tang, Y., and R.S. Zucker. 1997. Mitochondrial involvement in post-tetanic potentiation of synaptic transmission. *Neuron.* 18:483–491.
- Taru, H., and Y. Jin. 2011. The Liprin homology domain is essential for the homomeric interaction of SYD-2/Liprin- α protein in presynaptic assembly. *J Neurosci.* 31:16261–16268.
- ten Dijke, P., K. Miyazono, and C.H. Heldin. 2000. Signaling inputs converge on nuclear effectors in TGF- β signaling. *Trends Biochem Sci.* 25:64–70.

- Thiagarajan, T.C., M. Lindskog, and R.W. Tsien. 2005. Adaptation to synaptic inactivity in hippocampal neurons. *Neuron*. 47:725–737.
- Thiagarajan, T.C., E.S. Piedras–Renteria, and R.W. Tsien. 2002. alpha- and betaCaMKII. Inverse regulation by neuronal activity and opposing effects on synaptic strength. *Neuron*. 36:1103–1114.
- Tian, X., J. Li, V. Valakh, A. DiAntonio, and C. Wu. 2011. Drosophila Rael controls the abundance of the ubiquitin ligase Highwire in post-mitotic neurons. *Nat Neurosci*. 14:1267–1275.
- tom Dieck, S., L. Sanmarti–Vila, K. Langnaese, K. Richter, S. Kindler, A. Soyke, H. Wex, K.H. Smalla, U. Kampf, J.T. Franzer, M. Stumm, C.C. Garner, and E.D. Gundelfinger. 1998. Bassoon, a novel zinc–finger CAG/glutamine–repeat protein selectively localized at the active zone of presynaptic nerve terminals. *J Cell Biol*. 142:499–509.
- Tu, J.C., B. Xiao, S. Naisbitt, J.P. Yuan, R.S. Petralia, P. Brakeman, A. Doan, V.K. Aakalu, A.A. Lanahan, M. Sheng, and P.F. Worley. 1999. Coupling of mGluR/Homer and PSD–95 complexes by the Shank family of postsynaptic density proteins. *Neuron*. 23:583–592.
- Tu, J.C., B. Xiao, J.P. Yuan, A.A. Lanahan, K. Leoffert, M. Li, D.J. Linden, and P.F. Worley. 1998. Homer binds a novel proline–rich motif and links group 1 metabotropic glutamate receptors with IP3 receptors. *Neuron*. 21:717–726.
- Ushkaryov, Y.A., A.G. Petrenko, M. Geppert, and T.C. Sudhof. 1992. Neurexins: synaptic cell surface proteins related to the alpha–latrotoxin receptor and laminin. *Science*. 257:50–56.
- Vale, R.D. 2003. The molecular motor toolbox for intracellular transport. *Cell*. 112:467–480.
- van Amerongen, R., and R. Nusse. 2009. Towards an integrated view of Wnt signaling in development. *Development*. 136:3205–3214.
- Varoqueaux, F., S. Jamain, and N. Brose. 2004. Neuroligin 2 is exclusively localized to inhibitory synapses. *Eur J Cell Biol*. 83:449–456.
- Wagh, D.A., T.M. Rasse, E. Asan, A. Hofbauer, I. Schwenkert, H. Durrbeck, S. Buchner, M.C. Dabauvalle, M. Schmidt, G. Qin, C. Wichmann, R. Kittel, S.J. Sigrist, and E. Buchner. 2006. Bruchpilot, a protein with homology to ELKS/CAST, is required for structural integrity and function of synaptic active zones in Drosophila. *Neuron*. 49:833–844.

- Wagner, O.I., A. Esposito, B. Kohler, C.W. Chen, C.P. Shen, G.H. Wu, E. Butkevich, S. Mandalapu, D. Wenzel, F.S. Wouters, and D.R. Klopfenstein. 2009. Synaptic scaffolding protein SYD-2 clusters and activates kinesin-3 UNC-104 in *C. elegans*. *Proc Natl Acad Sci U S A*. 106:19605–19610.
- Wairkar, Y.P., H. Toda, H. Mochizuki, K. Furukubo-Tokunaga, T. Tomoda, and A. Diantonio. 2009. Unc-51 controls active zone density and protein composition by downregulating ERK signaling. *J Neurosci*. 29:517–528.
- Waites, C.L., A.M. Craig, and C.C. Garner. 2005. Mechanisms of vertebrate synaptogenesis. *Annu Rev Neurosci*. 28:251–274.
- Wan, H.I., A. DiAntonio, R.D. Fetter, K. Bergstrom, R. Strauss, and C.S. Goodman. 2000. Highwire regulates synaptic growth in *Drosophila*. *Neuron*. 26:313–329.
- Wang, X., and T.L. Schwarz. 2009. The mechanism of Ca²⁺-dependent regulation of kinesin-mediated mitochondrial motility. *Cell*. 136:163–174.
- Wang, X., W.R. Shaw, H.T. Tsang, E. Reid, and C.J. O'Kane. 2007. *Drosophila* spichthyn inhibits BMP signaling and regulates synaptic growth and axonal microtubules. *Nat Neurosci*. 10:177–185.
- Wang, X., J.A. Weiner, S. Levi, A.M. Craig, A. Bradley, and J.R. Sanes. 2002. Gamma protocadherins are required for survival of spinal interneurons. *Neuron*. 36:843–854.
- Wang, Y., M. Okamoto, F. Schmitz, K. Hofmann, and T.C. Sudhof. 1997. Rim is a putative Rab3 effector in regulating synaptic-vesicle fusion. *Nature*. 388:593–598.
- Weimer, R.M., E.O. Gracheva, O. Meyrignac, K.G. Miller, J.E. Richmond, and J.L. Bessereau. 2006. UNC-13 and UNC-10/rim localize synaptic vesicles to specific membrane domains. *J Neurosci*. 26:8040–8047.
- Wu, H., W.C. Xiong, and L. Mei. 2010. To build a synapse: signaling pathways in neuromuscular junction assembly. *Development*. 137:1017–1033.
- Xiao, B., J.C. Tu, R.S. Petralia, J.P. Yuan, A. Doan, C.D. Breder, A. Ruggiero, A.A. Lanahan, R.J. Wenthold, and P.F. Worley. 1998. Homer regulates the association of group 1 metabotropic glutamate receptors with multivalent complexes of homer-related, synaptic proteins. *Neuron*. 21:707–716.
- Xiong, X., X. Wang, R. Ewanek, P. Bhat, A. Diantonio, and C.A. Collins. 2010. Protein turnover of the Wallenda/DLK kinase regulates a retrograde response to axonal injury. *J Cell Biol*. 191:211–223.

- Yagi, T., and M. Takeichi. 2000. Cadherin superfamily genes: functions, genomic organization, and neurologic diversity. *Genes Dev.* 14:1169–1180.
- Yamagata, M., J.A. Weiner, and J.R. Sanes. 2002. Sidekicks: synaptic adhesion molecules that promote lamina-specific connectivity in the retina. *Cell.* 110:649–660.
- Yan, D., Z. Wu, A.D. Chisholm, and Y. Jin. 2009. The DLK-1 kinase promotes mRNA stability and local translation in *C. elegans* synapses and axon regeneration. *Cell.* 138:1005–1018.
- Yasuyama, K., I.A. Meinertzhagen, and F.W. Schurmann. 2002. Synaptic organization of the mushroom body calyx in *Drosophila melanogaster*. *J Comp Neurol.* 445:211–226.
- Yonekawa, Y., A. Harada, Y. Okada, T. Funakoshi, Y. Kanai, Y. Takei, S. Terada, T. Noda, and N. Hirokawa. 1998. Defect in synaptic vesicle precursor transport and neuronal cell death in KIF1A motor protein-deficient mice. *J Cell Biol.* 141:431–441.
- Zhai, R.G., and H.J. Bellen. 2004. The architecture of the active zone in the presynaptic nerve terminal. *Physiology (Bethesda).* 19:262–270.
- Zhai, R.G., H. Vardinon-Friedman, C. Cases-Langhoff, B. Becker, E.D. Gundelfinger, N.E. Ziv, and C.C. Garner. 2001. Assembling the presynaptic active zone: a characterization of an active zone precursor vesicle. *Neuron.* 29:131–143.
- Zhao, C., J. Takita, Y. Tanaka, M. Setou, T. Nakagawa, S. Takeda, H.W. Yang, S. Terada, T. Nakata, Y. Takei, M. Saito, S. Tsuji, Y. Hayashi, and N. Hirokawa. 2001. Charcot-Marie-Tooth disease type 2A caused by mutation in a microtubule motor KIF1Bbeta. *Cell.* 105:587–597.
- Zhen, M., X. Huang, B. Bamber, and Y. Jin. 2000. Regulation of presynaptic terminal organization by *C. elegans* RPM-1, a putative guanine nucleotide exchanger with a RING-H2 finger domain. *Neuron.* 26:331–343.
- Zhen, M., and Y. Jin. 1999. The liprin protein SYD-2 regulates the differentiation of presynaptic termini in *C. elegans*. *Nature.* 401:371–375.

8. Curriculum Vitae

Personal Details

Yao Zhang

Ph.D Candidate
Junior Research Group Synaptic Plasticity
Hertie Institute for Clinical Brain Research
University of Tübingen
Paul-Ehrlich-Str. 15, 72076 Tübingen, Germany

Phone: +49-7071-29-89191

Email: yao.zhang@uni-tuebingen.de

Date/Place of Birth: 25.06.1984 in Cangzhou, P. R. China

Nationality: Chinese

Marital Status: Single

Education

Oct. 2008-Present: Ph.D student in Hertie Institute for Clinical Brain Research, Graduate School of **Cellular and Molecular Neuroscience**, University of Tübingen, Tübingen, Germany (planned graduation in **July 2012**)

Oct. 2005-May. 2008: M.Sc. in **Neuropathophysiology**, at Tongji Medical College, Huazhong University of Science and Technology, Wuhan, China

Sep. 2002-May. 2006: B.Sc in **Biopharmaceutics**, at Tongji Medical College, Huazhong University of Science and Technology, Wuhan, China

Sep. 1996-Jul. 2002: No.2 Middle school, Cangzhou, China

Research Experience

Oct. 2008-Present:

Investigating mechanisms controlling synaptic development in *Drosophila* neuromuscular synapses
Junior Research Group Synaptic plasticity, Hertie-Institute for Clinical Brain Research, University of Tübingen, Tübingen, Germany

Oct. 2006-May.2008:

Reproduction of Alzheimer like rat model using Adeno-Associated Virus mediated overexpression of GSK-3 β

Department of Pathophysiology, Tongji Medical College, Huazhong University of Science and Technology, Wuhan, China

Jan. 2006-Nov.2006:

Investigation of the mechanism of GSK3 β activation induced PP2A inhibition and its implication in Alzheimer's disease

Department of Pathophysiology, Tongji Medical College, Huazhong University of Science and Technology, Wuhan, China

Language Skills

English Very good in speaking, writing, reading and listening
German Everyday communications
Chinese Native speaker

Experimental Skills

Very extensive experience in working with confocal microscopy
Very experienced with immunohistochemistry, western blotting, molecular biology, quantitative realtime PCR, cell culture& transfection, brain stereotaxic injection and animal handling

Computer Skills

Very familiar with the Image processing and analysis software: **Imagej** and **Adobe Photoshop**
Very familiar with Windows **Office Word, Excel, PowerPoint**
Very familiar with data analysis and plotting software: **Graphpad Prism 5**
National Certificate in programming language: Level II of **C programming language**

Trainings and Internships

Mar. 25-Apr. 4, 2009 EMBO practical course of advanced optical imaging in Plymouth, UK

Topics covered in lectures, practicals and demonstrations included:
Conventional Brightfield Microscopy, Confocal Microscopy, Digital Cameras,
Total Internal Reflection Fluorescence Microscopy, Multiphoton Microscopy,
Laser Traps, etc.

Jul. 7-Jul. 19, 2008 International health summer school in Wuhan and Xi'an, China

Topics include: Tropical Medicine, Epidemiology, Disease Control and Travel
Medicine, HIV/AIDS, Tropical Laboratory, Health Promotion and
Empowerment, and other public topics related to public health

Soft skill courses leadership skills, conflict management, scientific writing, grant writing

Conference Attendance

2011 Society for Neuroscience 41st annual meeting, Washington DC, USA

2010 Horizons in Molecular Biology, International PhD Student Symposium in Molecular Biology,
Göttingen, Germany

Honors and Awards

2007 Prize for Outstanding Publication, Huazhong University of Science and Technology

2005 Tongji Medical College Scholarship, Huazhong University of Science and Technology

2004 B grade Scholarship, Tongji Medical College, Huazhong University of Science and
Technology

2004 Honorary member of the Volunteer Association of Tongji Medical College

2003 Tongji Medical College Scholarship, Huazhong University of Science and Technology

Social Work

- 2002-2006** Student representative of the class Biopharmaceutics
- 2002-2006** Member and Later the vice Principle Organizer of the Volunteer Association of Tongji Medical College, Huazhong University of Science and Technology
- 2002-2008** Member of the HIV/AIDS Prevention and Education Association of Tongji Medical College, Huazhong University of Science and Technology

Teaching Experience

Supervising master students for journal club in the graduate school
Teaching new members in our lab: Imagej and image processing, in vivo imaging& fly genetics

Publications

Zhang Y, et. al. Role of Kinesin-3 homolog Unc-104 in regulating synaptic development and function in *Drosophila*. **(In revision)**

Lehner J, **Zhang Y**, Berendt S, Rasse TM, Forchhammer K, Maldener I. The morphogene AmiC2 is pivotal for multicellular development in the cyanobacterium *Nostoc punctiforme*. ***Molecular Microbiology*** (2011)

Zhang Y, Fuger P, Hannan S, Kern J, Lasky B, Rasse T. *In vivo* imaging of intact *Drosophila* larvae at sub-cellular resolution. ***Journal of Visualized Experiments*** (2010)

Liu GP, Wei W, Zhou X, **Zhang Y**, Shi HH, Yin J, Yao XQ, Peng CX, Hu J, Wang Q, Li HL, Wang JZ. I2PP2A regulates p53 and Akt correlatively and leads the neurons to abort apoptosis. ***Neurobiology of Aging*** (2010)

Wang HH, Li HL, Liu R, **Zhang Y**, Liao K, Wang Q, Wang JZ, Liu SJ. Tau overexpression inhibits cell apoptosis with the mechanisms involving multiple viability-related factors. ***Journal of Alzheimer's Disease*** (2010)

Zhang CE, Wei W, Liu YH, Peng JH, Tian Q, Liu GP, **Zhang Y**, Wang JZ. Hyperhomocysteinemia increases β -amyloid through enhancing expression of γ -secretase and phosphorylation of amyloid precursor protein in rat brain. ***The American Journal of Pathology*** (2009)

Liu GP, **Zhang Y**, Yao XQ, Zhang CE, Fang J, Wang Q, Wang JZ. Activation of glycogen synthase kinase-3 inhibits protein phosphatase-2A and the underlying mechanisms. ***Neurobiology of Aging*** (2008)

Hobbies and Interests

Very interested in gardening, especially in orchids and rhododendron